WHITE PAPER

ASBESTOS, HEALTH RISK AND TREMOLITIC TALC

Prepared By:

John W. Kelse, Corporate Industrial Hygienist
Manager, Corporate Risk Management Department

R. T. Vanderbilt Company, Inc.
30 Winfield Street
Norwalk, Connecticut 06855

Telephone: 203-853-1400
Fax: 203-831-0648
Email: jkelse@rtvanderbilt.com

Most Recent Update:
April 2007
(Prior update: January 2005)

TALC AND MIXED TALC/AMPHIBOLE FIBER

With the above mineral and biological background in mind (especially the understanding that Vanderbilt talc cancer health studies do not support a "same as" asbestos health risk), a minor component in Vanderbilt talc that is far more complicated than amphibole cleavage fragments can be addressed. This component is the minor talc fiber and mixed fiber mentioned earlier.

The following reflects the actual composition (by weight %) of Vanderbilt tremolitic talc. These ranges are inclusive of all grades.

VANDERBILT TALC COMPOSITION [85]
(Weight %)

Talc:	**20 to 40%**
(Talc & Talc/amphibole fiber = 0.5 to 5.6% in whole product)*	
Tremolite (nonasbestiform):	**40 to 60%**
Serpentine (antigorite-lizardite):	**15 to 30%**
Anthophyllite (nonasbestiform):	**1 to 5%**
Quartz:	**<1% (when detected at all)**

*** Of combined fiber (<0.05 to 1.8 in the whole product is asbestiform (Avg. all grades <0.50)**

The nonasbestiform amphibole component in this talc is obvious. Note also that there is a minor but measurable amount of talc fiber and mixed fiber in this talc. The mixed or "transitional" fiber is part talc and part amphibole (most probably anthophyllite), intimately mixed at the lattice level [86-98]. These are true fibers which are very long and thin. Some, but not all of these fibers do exhibit an asbestiform growth habit. These fibers have been described as academic curiosities and are relatively unrecognized outside the mineral science community. The combined weight % for those fibers that do exhibit an asbestiform growth habit typically falls around 0.5%. These fibers are not cleavage fragments, nor are they asbestos.

There are analytical laboratories that would contradict this statement. A few laboratories believe that some of these fibers are anthophyllite asbestos (though typically at an extremely trace level) [99, 100]. There is debate over whether some or all of the mixed fiber is asbestiform, and whether it should be called anthophyllite asbestos when amphibole is the dominant phase (assuming it can be determined which phase is dominant) [94]. Mineral scientists argue against this last proposition because the physical properties of these mixed fibers differ from those of either constituent, while impurities in asbestos fibers do not, in contrast, reflect significant alteration in their physical properties [101, 102].

Beyond some of these more detailed issues, it is admittedly confusing to most to hear that a fiber may be "asbestiform" but not "asbestos". It does sound like a contradiction. However, it must be remembered that asbestos is a commercial term that is applied to the six minerals earlier discussed. The term "asbestiform" merely means "like asbestos". Asbestiform fibers grow like

asbestos, they look like asbestos, they exhibit parallel crystal growth, they are flexible, they appear as fiber bundles with splayed terminations, they are very long and thin. However, these characteristics do not make them asbestos merely because they exhibit morphological similarities [8].

As mentioned earlier, it has been reported that upwards of 100 minerals may grow in an asbestiform habit, and the mineral talc is one of them. The following photomicrographs reflect the minor fiber content of Vanderbilt talc. The reader may wish to compare these photomicrographs with those earlier presented of asbestos fibers (last two pages).

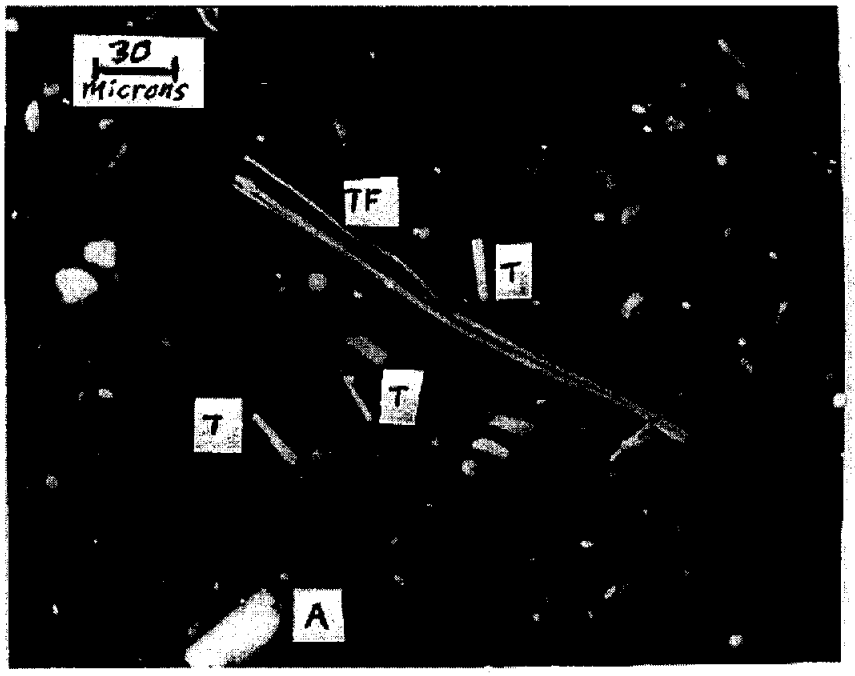

The large fiber in the center of the photomicrograph labeled "TF" is an asbestiform talc fiber. There is evidence of bundling, some curvature suggesting flexibility and it's very long and thin. The particle at the lower left labeled "A" is a prismatic anthophyllite cleavage fragment. The particles labeled "T" are elongated tremolite cleavage fragments [93]. Some laboratories fail to recognize that there are anthophyllite cleavage fragments in this talc and may misinterpret SAED patterns of these fragments as anthophyllite asbestos.

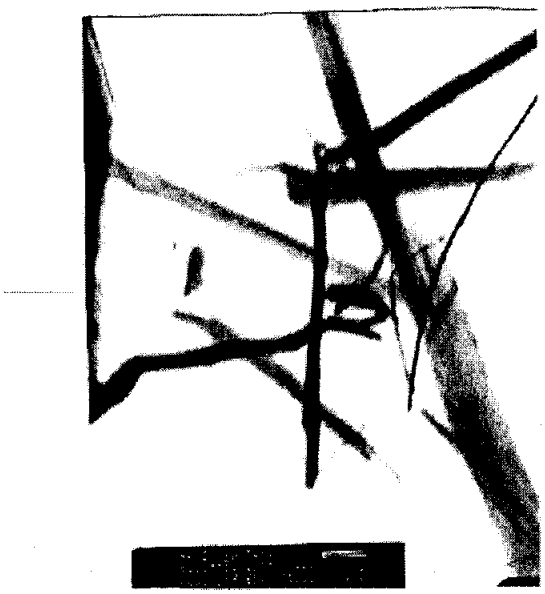

The above photomicrograph shows a more typical talc fiber found in Vanderbilt talc [94]. This fiber tends to be ribbon-like, and some feel it would not properly be called asbestiform. This is pure talc – not an amphibole or a mixed fiber.

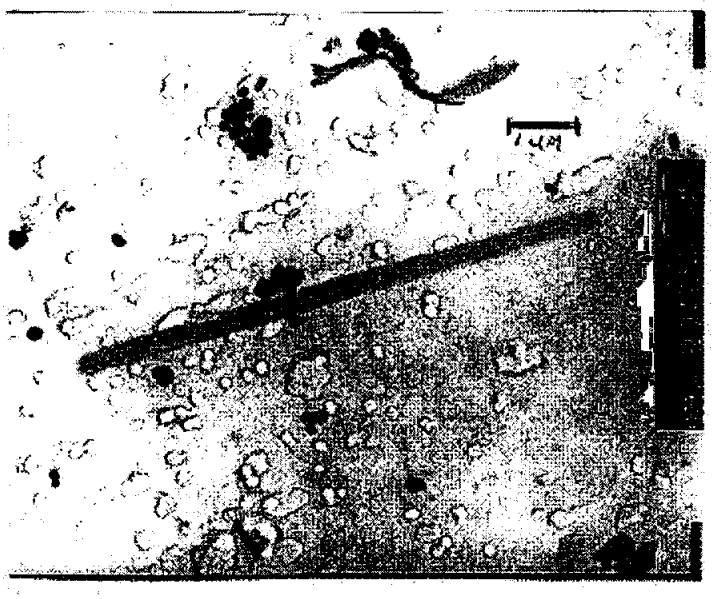

The above photomicrograph is a typical mixed fiber found in Vanderbilt talc. It is part talc and part amphibole [92]. These fibers tend to be rod-like and are also subject to controversy as to whether they are or are not truly "asbestiform".

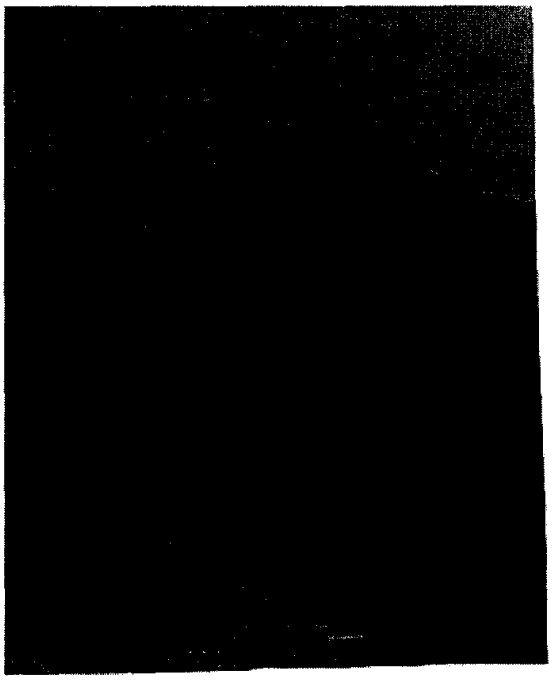

This photomicrograph shows the termination of one of these rods [94]. Some of the mixed fiber rods exhibit flat terminations while others (pictured) suggest the pulling apart of fibrils – though this is less pronounced then that typically seen in asbestos fibers.

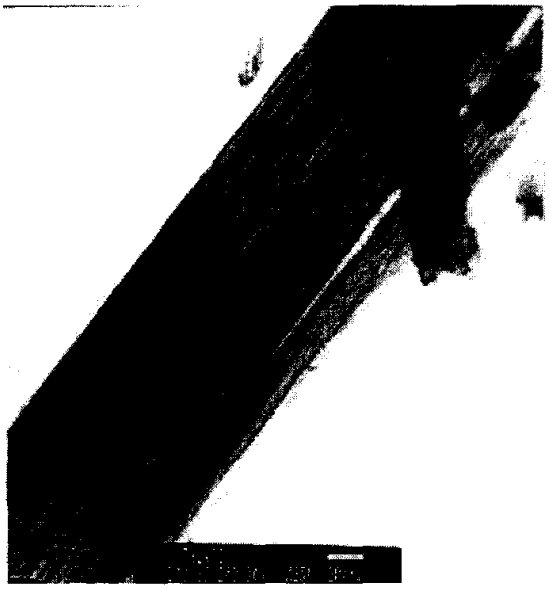

The above photomicrograph shows light and dark areas on a transitional fiber [94]. These areas are said to be different mineral domains – areas of talc, areas of amphibole (likely anthophyllite). If one directs an electron diffraction beam against different portions of this fiber, a different mineral fingerprint or pattern will emerge depending on where the beam strikes the fiber. This is another common area of analytical confusion.

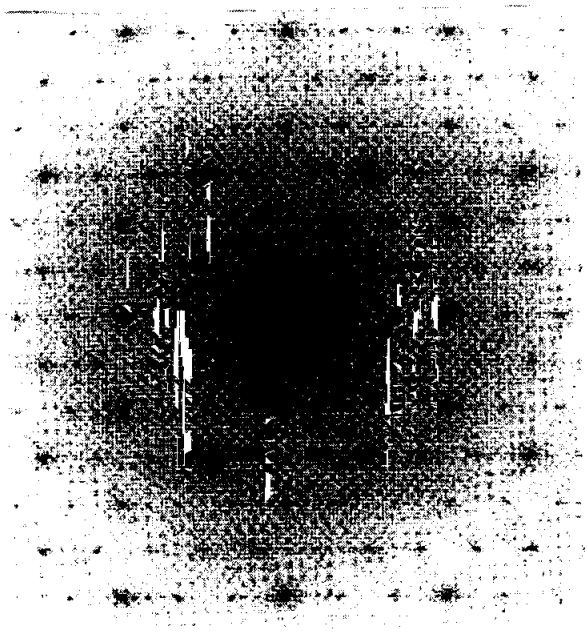

The above diffraction pattern is common for talc/anthophyllite intergrowth [94]. Note the "triplet" spots. The center spot is linked to a talc pattern – a forbidden reflection for pure anthophyllite.

Other ways exist to distinguished the mixed fibers. For example, Polarized Light Microscopy and index oils can be used to identify the mineral with a refractive index [85]. Mixed fibers will give an index above pure talc but below the lower limit of an amphibole. Commonly applied index criteria appear below.

Mineral	α, RI	γ, RI
Talc	< 1.598	≤ 1.598
Transitional	< 1.598	> 1.598
Amphibole	≥ 1.598	> 1.598

Given the level of attention these fibers receive, it is easy to lose sight of the fact that they make up a very small component of this talc, especially on a weight basis. It is common, however, to find widely divergent percent content data for these fibers. Percentages must be interpreted with caution. Often, percents refer to particle counts and not weight. To further complicate matters, many of these fiber prevalence percents relate only to subsets and not the whole product. Widely divergent fiber content levels have also been reported based upon broad "approximations" or extrapolation from very small fractions of the material (such as those seen by TEM). Improper mineral identification and sample preparation can play a role in quantification error as well. Mineral scientists often refer to these fibers as "mineral curiosities." General public exposure to these fibers is extremely limited to nonexistent.

Still, as interesting as these fibers may be mineralogically, the key concern is always risk. It is known that the six regulated asbestos minerals (particularly amphibole asbestos) are associated with significant health risks. However, it appears that other minerals that form in an asbestiform habit show various levels of risk. Some mineral fibers like fibrous erionite (a zeolite), richterite and winchite (amphiboles) suggest a risk every bit as strong as that of asbestos. On the other end of the spectrum are talc fibers and water-soluble fibers (i.e. xonotilite) that do not pose an asbestos risk [7].

Besides morphology, different minerals have different biodurability, surface chemistry, friability once in the lung, harshness scores, etc. These differences do appear to influence their biological activity in whole or in part [7, 8, 50, 103]. This is one of the reasons it is important to recognize the physical properties of minerals and call them by their proper names. Further, the critical role of dose should not be ignored. Risk is not simply a matter of good and bad but rather a matter of degree. The common saying in toxicology that "the dose makes the poison" is no less true for asbestos than any other material.

Despite the minor fibers present in Vanderbilt tremolitic talc, it clearly does not act like an asbestos-containing material in people or in test animals. Proponents of "morphology is everything" thinking, or those who incorrectly believe the term "asbestiform" is or should be a synonym for "asbestos", argue that the reason Vanderbilt talc does not act like an asbestos-containing material is because these fibers are too few. "Well, if there were more of them, then the talc would act like asbestos", is a common refrain. The correct response to this is "Well, there aren't". This is important to note because Vanderbilt talc may well contain more of these fibers than any other talc.

Although there is no known higher exposure to these rare fibers, it would be of interest to test this dose-linked assertion because it would speak to the "morphology is everything" proposition. Accordingly, a test was undertaken to test this hypothesis. In this test a concentrate of talc (predominantly) and mixed fiber from Vanderbilt talc was tested against an equal weight of asbestos fiber in a rodent tracheal epithelial and mesothelial cell study. The findings of this study are reflected below.

Wylie, A. G., Mossman, B. T., et al – 1997 [50]

Mineralogical Features Associated with Cytotoxic and Proliferative Effects of Fibrous Talc and Asbestos on Rodent Tracheal Epithelial and Pleural Mesothelial Cells

"fibrous talc does not cause proliferation of HTE cells or cytotoxicity equivalent to asbestos in either cell type despite the fact that talc samples contain durable mineral fibers with dimensions similar to asbestos. These results are consistent with the findings of Stanton, et al (1981) who found no significant increases in pleural sarcomas in rats after implantation of minerals containing fibrous talc."

The talc fiber concentrate acted differently than the asbestos fibers, again suggesting that more than simple fiber morphology is involved in asbestos pathogenicity. This study also suggests that the demonstrated absence of an asbestos risk in Vanderbilt tremolitic talc is not simply dose related.

As desirable as it would be to find one simple, easy to recognize characteristic that predicts "fiber" risk, studies like this, as well as the entire nonasbestiform amphibole experience, suggest that we need to proceed with caution. Finding one variable linked to fiber risk (i.e. morphology) does not automatically mean that other variables can or should be ignored. At least not until scientifically discounted.

CONCLUSION - LESSONS LEARNED

It is important that we call substances by their proper names and that we control them based on demonstrated risk. When health studies characterize exposures in broad brush terms and ignore proper nomenclature, researchers are less likely to understand risk. Less discrimination in the name of prudence is a "slippery slope," one more likely to lead to the presumption of risks that do not exist rather than the avoidance of those that do. This is certainly one of the lessons of the tremolitic talc saga.

There are many reasons why Vanderbilt talc has been the source of debate and confusion for decades. Imprecise asbestos definitions [5, 15, 86-103] over zealous federal agencies inclined to champion excessive prudence over good science [2, 24, 27, 31, 32, 35, 104] imprecise asbestos analytical protocols [7, 10, 11, 13, 15, 19, 84-98, 105-108], bias/experience factors leading to possible error in difficult medical evaluations (i.e., chest x-ray interpretations, mesothelioma diagnosis and attribution), the relationship of past exposure risk to current exposure risk and irresponsible media involvement [3] are key among these reasons. The tremolitic talc story may well be one of the very best examples of a confluence of serious ongoing lapses.

Certainly there are serious risks in this world, we must be cautious and act prudently. But even prudence can be excessively stretched. While we must not ignore adverse health effects when

TOXICOLOGY AND APPLIED PHARMACOLOGY 147, 000–000 (1997)
ARTICLE NO. TO978276

Mineralogical Features Associated with Cytotoxic and Proliferative Effects of Fibrous Talc and Asbestos on Rodent Tracheal Epithelial and Pleural Mesothelial Cells

Ann G. Wylie,* H. Catherine W. Skinner,† Joanne Marsh,‡ Howard Snyder,† Carmala Garzione,* Damian Hodkinson,* Roberta Winters,* and Brooke T. Mossman,‡

*Laboratory for Mineral Deposits Research, Department of Geology, University of Maryland, College Park, Maryland 20742; †Department of Geology and Geophysics, Yale University, New Haven, Connecticut 06511-8130; and ‡Department of Pathology, University of Vermont College of Medicine, Burlington, Vermont 05405

Received May 12, 1997; accepted August 11, 1997

Mineralogical Features Associated with Cytotoxic and Proliferative Effects of Fibrous Talc and Asbestos on Rodent Tracheal Epithelial and Pleural Mesothelial Cells. Wylie, A. G., Skinner, H. C. W., Marsh, J., Snyder, H., Garzione, C., Hodkinson, D., Winters, R. and Mossman, B. T. (1997). *Toxicol. Appl. Pharmacol.* 147, 000–000.

Inhalation of asbestos fibers causes cell damage and increases in cell proliferation in various cell types of the lung and pleura *in vivo*. By using a colony-forming efficiency (CFE) assay, the cytotoxicity and proliferative potential of three mineral samples containing various proportions of fibrous talc were compared to NIEHS samples of crocidolite and chrysotile asbestos in cell types giving rise to tracheobronchial carcinomas, i.e., hamster tracheal epithelial (HTE) cells, and mesotheliomas, i.e., rat pleural mesothelial (RPM) cells. Characterization of mineralogical composition, surface area, and size distributions as well as proportions of fibers in all mineral samples allowed examination of data by various dose parameters including equal weight concentrations, numbers of fibers >5 μm in length, and equivalent surface areas. Exposure to samples of asbestos caused increased numbers of colonies of HTE cells, an indication of proliferative potential, but fibrous talc did not. RPMs did not exhibit increased CFE in response to either asbestos or talc samples. Decreased numbers of colonies, an indication of cytotoxicity, were observed in both cell types and were more striking at lower weight concentrations of asbestos in comparison to talc samples. However, all samples of fibrous minerals produced comparable dose–response effects when dose was measured as numbers of fibers greater than 5 μm or surface area. The unique proliferative response of HTE cells to asbestos could not be explained by differences in fiber dimensions or surface areas, indicating an important role of mineralogical composition rather than size of fibers. © 1997 Academic Press

Occupational exposures to mineral fibers such as asbestos are associated with the development of pulmonary and pleural disease (Mossman and Gee, 1989; Mossman *et al.*, 1990; Guthrie and Mossman, 1993). Although various types of asbestos are biologically active in a number of *in vivo* and *in vitro* bioassays, the properties of fibers important in reactivity with cells and tissues are unclear (Guthrie and Mossman, 1993; Mossman and Begin, 1989). It is generally agreed that length and width or aspect ratio are important variables for predicting the carcinogenicity and fibrogenicity of durable fibers (Davis *et al.*, 1986; Stanton *et al.*, 1981). However, the mineralogical composition and structural features of fibers and particles may also play a role in pathogenicity (Oehlert, 1991; Wylie *et al.*, 1987; Skinner *et al.*, 1988; Wylie *et al.*, 1993). These properties govern surface properties as well as durability of fibers in the lungs and pleura, factors that may be critical in the development of lung cancer and mesothelioma. (Mossman and Gee, 1989; Mossman *et al.*, 1990; Guthrie and Mossman, 1993; Health Effects Institute, 1991).

Asbestos types, in contrast to a number of other fibrous and nonfibrous nonpathogenic materials, cause both cell proliferation and cytotoxicity in a dose-related fashion in several cell types (reviewed in Health Effects Institute, 1991). These biological responses may reflect the disease potential of various fiber types, as cell injury and hyperplasia are early events in rodent inhalation models of asbestosis and carcinogenesis (Mossman and Gee, 1989; Mossman *et al.*, 1990; Guthrie and Mossman, 1993; Health Effects Institute, 1991). In this study, we compared the cytotoxicity and proliferative potential of three New York talc samples to crocidolite and chrysotile asbestos in cell types affected in asbestos-induced tumors, i.e., hamster tracheal epithelial (HTE) cells, which can give rise to tracheobronchial neoplasms, and rat pleural mesothelial (RPM) cells, cells affected in the development of mesothelioma. In studies here, we used an established colony-forming efficiency (CFE) assay that documents both increases in cell proliferation and cell survival, as measured by increases in numbers of colonies, at low concentrations of minerals, and growth inhibition, as indicated by decreases in colony formation or size at high concentration of minerals, to compare responses to well-characterized samples of asbestos and fibrous talc in HTE and RPM cells. An additional advantage of this bioassay is that it employs cells from the lung and pleura and measures responses

0041-008X/97 $25.00

to minerals over a 7-day time period of exposure as opposed to shorter time frames used (<24 hr) in most other *in vitro* assays in the literature (reviewed in Health Effects Institute, 1991. In the CFE assay, nonfibrous particles such as glass beads are proliferative or cytotoxic to HTE cells at ≥100-fold concentrations when compared to asbestos at equal weight concentrations (Mossman and Sesko, 1990; Marsh *et al.*, 1994; Timblin *et al.*, 1995).

The three talc samples used here differ somewhat in their mineralogy, both in the types of minerals and in their relative abundances. However, all three contain varying proportions of fibrous talc which is similar dimensionally and morphologically to asbestos. We thus hypothesized that factors other than length and width of fibers would govern the reactivity of minerals in the *in vitro* assays used here. The experiments were undertaken to explore the questions: (1) Do fibrous talc and asbestos fibers cause similar biological responses in epithelial and mesothelial cells? (2) Is reactivity to mineral samples dose related? and (3) Are responses in various cell types related only to numbers and sizes of fibers in each preparation or does mineralogy, including chemical composition, surface properties, and mineral structure, play a role?

METHODS

Sources of Mineral Samples

Three samples from the New York State Gouverneur Mining District, FD14, S157, and CPS183, and two asbestos samples, NIEHS chrysotile (Plastibest 20) and NIEHS crocidolite, were used in this study. The asbestos samples are essentially monomineralic and have been studied in detail (Campbell *et al.*, 1980). The general geology and mineralogy of the Gouverneur District are described by Engle (1962) and Ross *et al.* (1968). FD14 is a commercial talc, S157 was once produced from this district as a fiber talc product, and CPS183 is a laboratory separated concentrate of fibrous talc. Fibrous talc is a general term that includes fibers composed entirely of the mineral talc as well as fibers that are composed of both talc and amphibole (probably anthophyllite) intergrown on a submicrometer scale (Stemple and Brindley, 1960; Virta, 1985). The index of refraction of the fibers increases as the amphibole component increases (Veblen and Wylie, 1993). Fibrous talc is present in trace amounts in many commercial talc deposits, but it is a major component of most talc products from the Gouverneur Talc District. All samples were characterized by scanning electron microscopy (SEM), optical microscopy (OM), and x-ray diffraction (XRD); CPS183 and NIEHS crocidolite were also studied by TEM as this technique is more sensitive for the detection of smaller, thinner particles.

Characterization of Minerals

The samples were studied by XRD and SEM at Yale University in order to establish the overall mineralogy, mineral abundances, and the number of fibers per microgram. They were examined by OM at the Laboratory for Mineral Deposits Research, University of Maryland, in order to determine the mineralogy, mineral abundances, and number of fibers per microgram of the samples, and by transmission electron microscopy (TEM) at AMA Laboratories, Beltsville, Maryland (under the direction of the Laboratory for Mineral Deposits Research) for the purpose of determining the detailed size distribution of fibrous talc and especially to examine the content of fibers 0.1 μm in width and smaller. The protocols followed in each laboratory are described below. For purposes of this paper, "particles" refers to particles of all aspect ratios. "Fiber" refers to particles that have an aspect ratio (length/width) of at least five and to bundles of such fibers. "Fibers" (unless otherwise specified) include true mineral fibers (very high aspect ratio particles whose shapes were attained during mineral formation) as well as elongated cleavage fragments (shape produced during comminution).

X-ray diffraction. Samples mixed with an internal standard and spun to minimize preferred orientation were analyzed by using a SCITAG Pad V automated diffractometer. Identification of minerals was based on comparison of the X-ray pattern with standard patterns.

Optical microscopy. A known weight of sample was dispersed in water and then passed through a 22-gauge needle 8× and sonicated 4 min before mounting on slides. A drop of immersion oil $n_D = 1.598$ was placed over the dried sample. For all samples except chrysotile ($N = 2$ mixtures), at least five separate mixtures were prepared from each sample and at least two slides were made from each mixture. One-hundred fibers were counted from each slide. All fibers longer than 5 μm and all particles that appeared to be composed of bundles of fibers were categorized by length and width and by index of refraction according to the following characteristics: all indices of refraction greater than 1.598 (amphibole), index of refraction parallel to elongation greater than 1.598 and index of refraction perpendicular to elongation less than 1.598 (fibers composed of talc and a significant amount of amphibole, and referred to as talc/amphibole), or all indices of refraction less than 1.598 (fibers dominated by the mineral talc). The number of fiber per microgram was calculated by assuming that particle distributions were representative and directly proportional to the area of the filter.

Scanning electron microscopy. A known weight of sample was dispersed in water, passed through a 22-gauge syringe needle 8×, and deposited onto a 0.45-μm cellulose filter. Replicate preparations were made for each sample and analyzed independently to test for homogeneity. The filters were examined with a JEOL JXA 8600 SEM equipped with EDXA. Particles that were at least 1 μm in length and 0.12 μm in width could be detected. Mineral identification was automated by predetermining the relative percentages of Na, Ca, K, Mg, Al, Si, Mn, and Fe in mineral standards and comparing them to the elemental compositions determined on the sample particles (Petruk and Skinner, 1997). The number of particles per microgram of sample was calculated by assuming that the particle distributions were representative and directly proportional to the area of the filter.

Transmission electron microscopy. A known weight of sample was dispersed in water, flushed with a 22-gauge syringe needle 8×, and then sonicated for 4 min. The solutions were then diluted and filtered through a 0.22-μm cellulose acetate filter. The samples were analyzed on a JEOL 100 CX II electron microscope at 19,000× magnification. Over 300 fibers from each sample were measured.

Surface area measurements. All five samples were tested for single point N_2-BET surface areas by J. W. Anderson of R. T. Vanderbilt Corporation. The tests were repeated 4× for each sample. Data were expressed as square millimeters per gram of sample.

Cell culture and addition of fibers to bioassay. A HTE cell line previously isolated and characterized by Mossman *et al.* (1980) was maintained at passages from 38 to 50 and cultured routinely in Ham's F12 medium (Gibco, Grand Island, NY) containing penicillin and streptomycin (both at 100 U/ml) and 10% newborn calf serum (Gibco). This cell line is diploid and possesses features, i.e., mucin secretion and cilia, of differentiated epithelial cells. Primary cultures of RPM cells were isolated by scraping the parietal pleural of two weanling male Fischer 344 rats (Janssen *et al.*, 1994) and were maintained for up to eight passages in Ham's F12–DMEM containing antibiotics (as above), 10% fetal calf serum (Gibco), hydrocortisone (100 ng/ml), insulin (2.5 μg/ml), transferrin (2.5 μg/ml), and selenium (2.5 ng/ml).

Mineral samples presterilized in a dry oven overnight at 130°C were added to Hanks' balanced salt solution (HBSS) before titration 8× through a 22-gauge syringe needle and addition to cultures in 2% serum-containing medium.

A CFE assay was also used as a sensitive test for cytotoxicity and cell proliferation (Mossman and Sesko, 1990; Marsh *et al.*, 1994; Timblin *et al.*, 1995). HTE (400 cells/60 mm dish) and RPM (2000/60 mm dish) were plated for 24 hr before addition of dusts to medium containing 2% serum as described

TABLE 1
Characterization of Talc and Asbestos Samples

Sample	Mineralogy (% of sample)
	Mineral composition
FD14	Talc (37), tremolite (35), serpentine (15), other (<2), unknown (12)[a]
S157	Talc (60), tremolite (12), unknown (21), other (4), anthophyllite (3), quartz (1)
CPS183	Talc (50), quartz (12), unknown (28), tremolite (4), other (4), anthophyllite (3)
NIEHS crocidolite	Riebeckite (100)
NIEHS chrysotile	Chrysotile (100)
	Mineralogy of fibers >5 μm
FD14	Talc (62), amphibole (24),[b] talc/amphibole (14)
S157	Talc (84), amphibole (11), talc/amphibole (5)
CPS183	Talc (99), amphibole (1), talc/amphibole (<1)
NIEHS crocidolite	Crocidolite (100)
NIEHS chrysotile	Chrysotile (100)

Sample	Surface area (mm^2/gm)	Fibers/μg	Fibers ≥ 5 μm/μg
	Surface area and fibers/μg[c]		
FD14	6.2 ± 0.2[d]	2.5×10^3	0.8×10^3
S157	4.9 ± 0.2	1.1×10^4	4.8×10^3
CPS183	4.9 ± 0.4	1.1×10^4	9.2×10^3
NIEHS crocidolite	10.3 ± 1.3	5.3×10^5	3.8×10^5
NIEHS chrysotile	25.4 ± 0.5	5.3×10^4	3.4×10^4

[a] Primarily magnesium silicates (talc and talc/amphibole) with SEM/EDXA spectra too low for conclusive identification.

[b] The most abundant amphibole is tremolite. A very small amount of anthophyllite may be included.

[c] Data are based on SEM measurements. Chrysotile values are low due to its poor visibility on the SEM. Standard error of measurement is estimated to be 20%.

[d] Mean ± standard error of measurement of four individual measurements per group.

above. Minerals were then added, and untreated and mineral-exposed cultures were maintained for 7 days before examination. At this time, plates were rinsed in HBSS and fixed in methanol and stained with 10% Giemsa stain, and total colonies greater than 50 cells per plate were counted by using a blind code (Mossman and Sesko, 1990; Marsh *et al.*, 1994; Timblin *et al.*, 1995). Duplicate experiments were performed for each bioassay with $N = 3$–4 dishes per group per experiment. Statistical analyses of all data were performed by using analysis of variance and trend analysis.

RESULTS

Mineralogy

The overall mineralogical composition, the mineral composition of the fibers, the number of fibers per microgram, and the surface area measurement of the samples used in our studies are given in Table 1. FD14 is composed of platy talc, true mineral fibers of talc and talc/amphibole, cleavage fragments of tremolite, platy serpentine (chrysotile absent), and trace amounts of other minerals. Fibers make up approximately 11% of the particles identified by SEM. They are mostly talc followed by amphibole cleavage fragments and talc/amphibole. S157 is composed of platy talc, true mineral fibers of talc and talc/amphibole, tremolite and anthophyllite cleavage fragments, and quartz. Fibers make up about 37% of the particles, and they are mostly talc with smaller amounts of amphibole cleavage fragments and talc/amphibole. CPS183 is composed of true mineral fibers of talc and a very small amount of talc/amphibole, cleavage fragments of tremolite and anthophyllite, and quartz. Fifty-nine percent of the particles are fibers, and they are almost all fibers of talc. The three talc samples represent a range in the amount of fiber present (both in portion of sample and in number of fibers/μg) and in the mineralogy of the fibrous portion, primarily in the content of amphibole both as a separate phase and as a component of fibrous talc. NIEHS crocidolite and NIEHS chrysotile are essentially monomineralic populations of true mineral fibers of riebeckite and chrysotile, respectively. The very small widths result in many more fibers per microgram than are found in the talc samples.

Surface Area

The specific surface areas (mm^2/g) of talc samples are smaller than asbestos samples and roughly comparable to each other. The larger surface area of FD14 compared to the other talc samples is probably due to the presence of more abundant small platy talc particles that have two almost equivalent dimensions and one that is very much smaller, producing a large surface area/mass ratio. The greater surface area of chrysotile with respect to crocidolite can be attributed to its lower density and small fibril width and perhaps in part to the straw-like structure of the chrysotile fibers if N_2 penetrates the hollow center of the chrysotile tubes. Since the surface reactivity of different minerals affects the surface adsorption of N_2, some of the variation among samples may be related to mineralogy as well.

Size Distributions of Fibers in Mineral Preparations

Figure 1 shows the frequency of length and width for all fibers in units of fibers/microgram and the frequency of width for only those fibers greater than or equal to 5 μm in length as established by SEM and OM. The abundance of narrow crocidolite fibers accounts for the fact that the NIEHS crocidolite contains more fibers per microgram than any other sample (Table 1). CPS183 and S157 are very similar in many respects. They are composed of similar numbers of fibers per microgram, but there are slightly more longer fibers and fewer long, wide fibers in CPS183. FD14 contains the smallest number of fibers per microgram and the highest proportion of the widest fibers. In general, talc fibers are narrower than amphibole cleavage fragments and the differences in the sizes of the fibers among the talc samples in part reflect the differences in the abundance of amphibole cleavage fragments vs fibrous talc. As

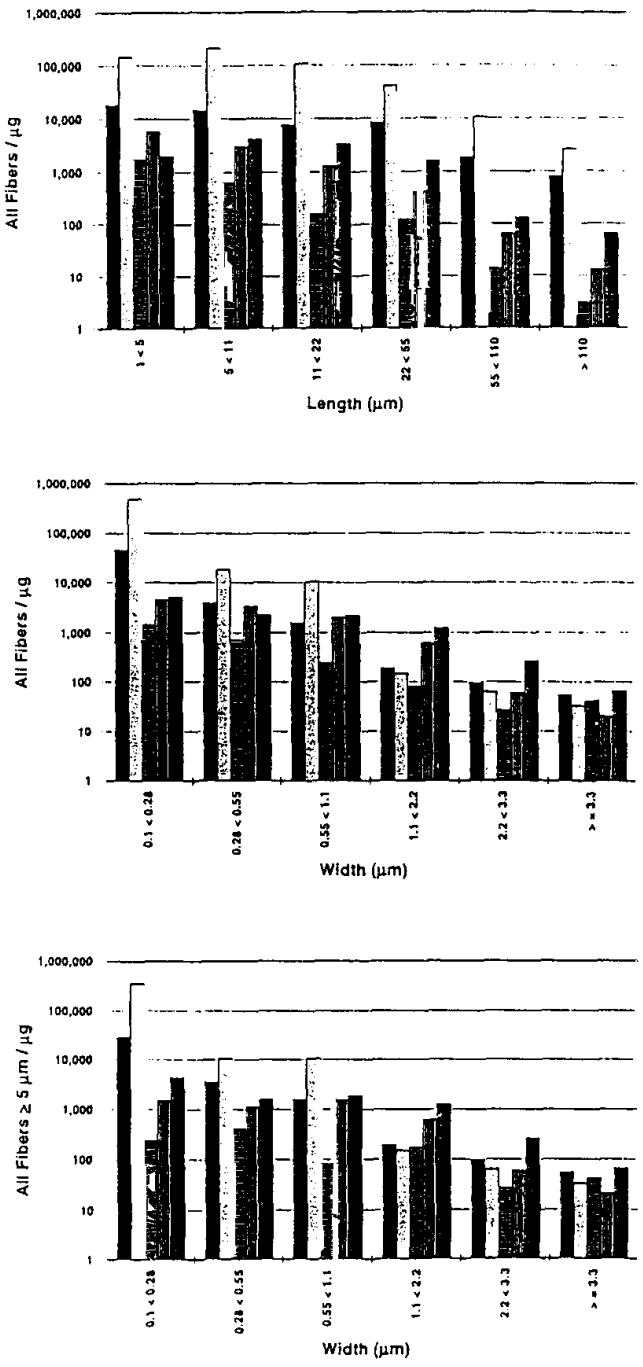

FIG. 1. The frequencies of length and width in units of fibers per microgram are shown for the three talc samples and two NIEHS asbestos samples. Also shown is the frequency of width (fibers/µg) for those fibers longer than 5 µm. (■) Chrysotile; (▨) crocidolite; (▤) FD14; (▥) S157; (▧) CPS183.

the amphibole content increases from CPS183 to S157 to FD14, the total fiber content goes down, and, on average, the fibers decrease in length and increase in width. No distinction between the size distributions of talc and talc/amphibole fibers were documented.

T2 Table 2 gives the percentage of fibers in length–width categories for CPS183 and NIEHS crocidolite asbestos as measured by TEM. These data enable a direct comparison between the dimensions of fibrous talc and crocidolite that is not restricted by the 0.1-µm width limit in the SEM data. These two true mineral fiber populations are quite similar, differing most notably in the higher proportion of wide (>0.5 µm) fibers and slightly lower proportion of long (>20 µm) fibers in fibrous talc.

CFE Assays

Combined data from duplicate experiments with HTE and RPM cells are presented in Figs. 2 and 3, respectively. CFE data F3 are expressed as a ratio of the number of colonies in mineral-exposed cultures in comparison to control colonies × 100 at various concentrations of minerals on a weight basis ($\mu g/cm^2$) as is typically found in the literature (Mossman *et al.*, 1990; Health Effects Institute, 1991). In HTE cells, both asbestos types showed an elevated number of colonies ($p < 0.05$) at lowest concentrations indicating increased cell proliferation and/or survival in response to asbestos fibers and confirming earlier studies (Mossman and Sesko, 1990; Marsh *et al.*, 1994). Significant decreases ($P < 0.05$) in CFE, an indication of toxicity or growth inhibition, were observed at concentrations of asbestos of 0.5 $\mu g/cm^2$ and greater. In contrast, RPM cells did not exhibit proliferative effects in response to either asbestos type, but statistically significant ($p < 0.05$) decreases in CFE were observed at concentrations of asbestos fibers greater than 0.05 $\mu g/cm^2$. In both cell types, the talc samples were less cytotoxic than asbestos. CPS183 was the most toxic talc sample, followed by S157 and FD14. In contrast to the other mineral samples, S157 and FD14 did not exhibit significant linear trends in cytotoxicity with increasing dosages in HTE cells.

Figures 4 and 5 show the same cellular response data as F4-F5 Figs. 2 and 3, but dose is calculated based on the number of

TABLE 2
Percentage of Fibers by Length and Width (µm) as Determined by Transmission Electron Microscopy

Length	Width: 0.01–0.1	>0.1–0.25	>0.25–0.5	>0.5–1.0	>1.0
CPS183					
<1	2.9	1.6	—	—	—
>1–2	4.1	14.1	0.5	—	—
>2–5	2.5	22.0	6.8	1.6	—
>5–10	0.9	9.8	4.3	4.5	0.5
>10–20	0.5	7.3	3.2	2.3	2.5
>20–50	0.2	1.8	2.7	1.4	2.0
>50–100	—	—	—	—	0.2
		NIEHS crocidolite			
<1	0.3	0.3	—	—	—
>1–2	1.1	9.5	0.3	—	—
>2–5	4.6	31.6	2.9	—	—
>5–10	1.4	18.1	3.7	0.6	—
>10–20	1.7	10.7	3.2	0.3	—
>20–50	0.6	2.9	1.4	1.1	—
>50–100	—	1.7	1.4	0.6	—

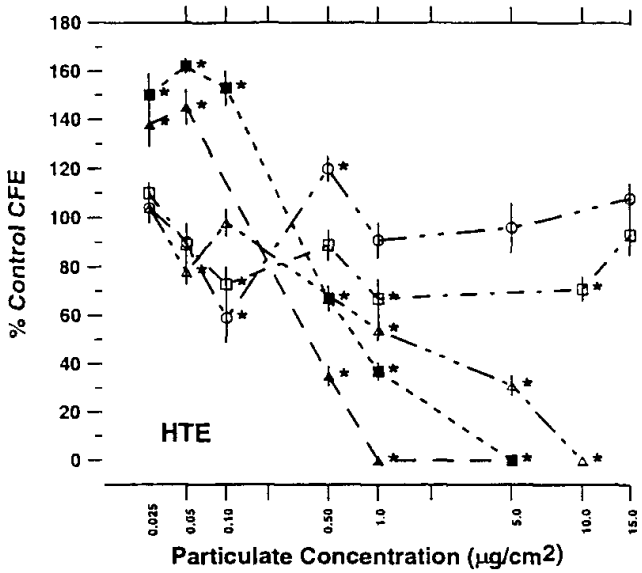

FIG. 2. Colony-forming efficiency (CFE) of HTE cells at various weight concentrations of samples. Standard error in CFE is indicated on symbol. *$p <$ 0.05 in comparison to untreated controls. (▲) Chrysotile; (■) crocidolite; (○) FD14; (□) S157; (△) CPS183.

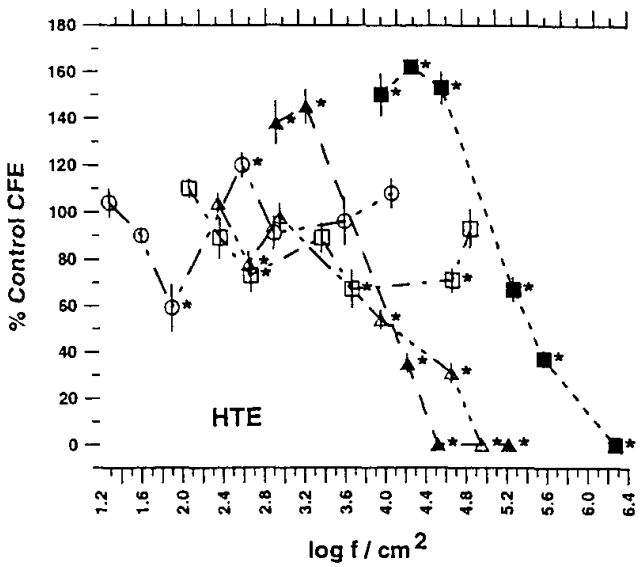

FIG. 4. Colony-forming efficiency (CFE) assays in HTE cells expressed as a function of fibers ≥5 μm in length per cm^2 (f/cm^2). The symbol width is equal to or greater than estimated error. The standard error in CFE is indicated on the symbols. *$p < 0.05$ in comparison to untreated controls. (▲) Chrysotile; (■) crocidolite; (○) FD14; (□) S157; (△) CPS183.

fibers greater than or equal to 5 μm/cm^2 (fibers/cm^2) rather than total sample weight per square centimeter. The data are taken from the SEM characterizations, but the comparisons would be the same if OM or TEM data were used. Doses of total sample per square centimeter administered to the cultures covered such a wide range that there were equivalent doses of fibers per square centimeter in almost all length/width categories for all samples. Therefore, even though crocidolite and chrysotile contained many more fibers per microgram than the talc samples, the same number of fibers per centimeter were administered in low doses of asbestos and high doses of talc (μg/cm^2).

As shown in Fig. 4, the enhanced responses of HTE cells to asbestos appear to be a function of mineralogy and not fiber

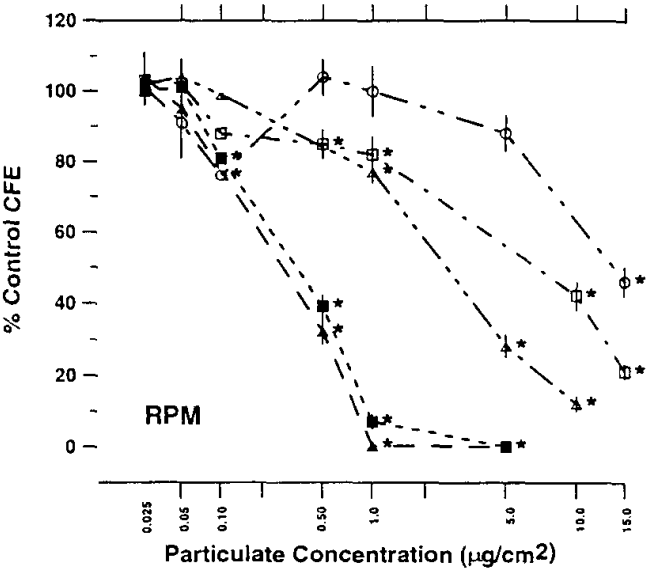

FIG. 3. Colony-forming efficiency (CFE) of RPM cells at various weight concentrations of samples. The standard error in CFE is indicated on the symbols. *$p < 0.05$ in comparison to untreated controls. (▲) Chrysotile; (■) crocidolite; (○) FD14; (□) S157; (△) CPS183.

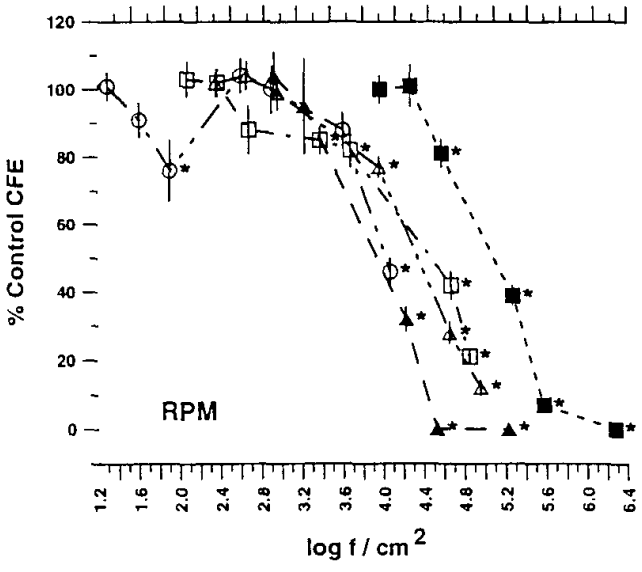

FIG. 5. Colony-forming efficiency (CFE) assays in RPM cells expressed as a function of fibers ≥5 μm in length and length:width ≥ 5:1 per cm^2 (f/cm^2). The symbol width is equal to or greater than estimated error. The standard error in CFE is indicated on the symbols. *$p < 0.05$ in comparison to untreated controls. (▲) Chrysotile; (■) crocidolite; (○) FD14; (□) S157; (△) CPS183.

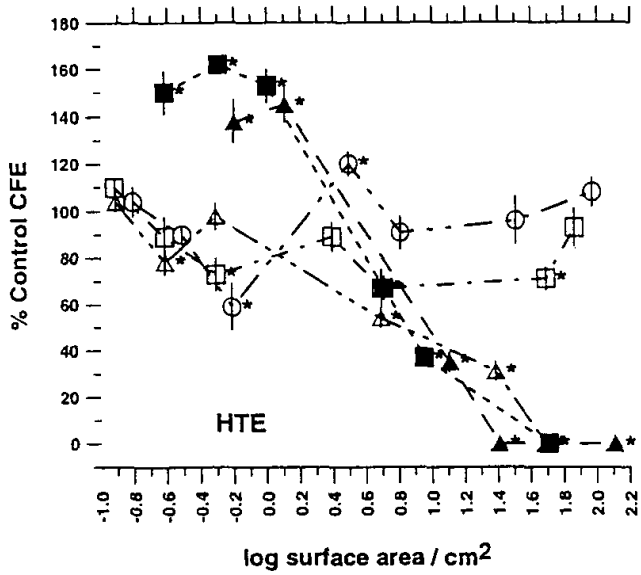

FIG. 6. Colony-forming efficiency (CFE) assays in HTE cells expressed as a function of surface areas of mineral samples (mm^2/cm^2). The symbol width is equal to or greater than one standard error. The standard error in CFE is indicated on the symbols. *$p < 0.05$ in comparison to untreated controls. (▲) Chrysotile; (■) crocidolite; (○) FD14; (□) S157; (△) CPS183.

concentration. The same concentrations of fibers greater than 5 μm of chrysotile and crocidolite that cause proliferation in HTE cells result in no effects when comparable concentrations of FD14 fibers are used, insignificant cytotoxicity with S157 fibers, and significant cytotoxicity with CPS183 fibers. It therefore seems likely that characteristics of the samples that are related to their mineralogy contribute to proliferation and/or cell growth inhibition.

As shown in Fig. 5, the response of RPM cells appears to be independent of the mineralogy of the samples. Neglecting the slight cytotoxic response of FD14 at low concentrations, the minimum concentrations of fibers per square centimeter necessary to cause significant decreases in CFE is between 10^3 and 10^4 fibers per square centimeter for all samples. In changing the size definition of a fiber (e.g., >8, ≤0.25 μm; >20 μm, all widths; all lengths, w < 0.28 μm), we found that the effective dose changed but the relationships among the samples did not (data not shown).

F6-F7

Figures 6 and 7 show CFE data in HTE and RPM cells, respectively, as a function of surface area. It is evident that surface area per se cannot explain cellular responses to minerals in HTE or RPM cells. Despite the fact that crocidolite and chrysotile have much larger surface areas per microgram, the range in the amount of sample administered resulted in similar doses between the asbestos and talc samples.

DISCUSSION

Asbestos is a term applied to a group of minerals that possess similar physical properties because of their habit of growth. However, different types of asbestos differ in their mineralogy and fiber size, which in turn may vary in preparations obtained from different geographic locations and sometimes even from the same locality (Guthrie and Mossman, 1993). The two most widely studied types of asbestos are the serpentine mineral chrysotile ($Mg_3Si_2O_5(OH)_4$), the most common type of asbestos in the Northern hemisphere and in commercial usage historically, and the asbestiform variety of the amphibole riebeckite, crocidolite ($Na_2Fe_3^{2+}Fe_2^{3+}Si_8O_{22}(OH)_2$), a high-iron-containing asbestos mined in parts of South Africa and Western Australia. Although crocidolite is implicated as more potent in the induction of mesothelioma, both chrysotile and crocidolite are linked occupationally to the development of lung cancer and asbestosis (Mossman and Gee, 1989; Mossman *et al.*, 1990, 1996; Guthrie and Mossman, 1993; Health Effects Institute, 1991).

How asbestos causes lung disease is uncertain, but acute toxicity, measured by a variety of techniques which have detected increases in membrane permeability, necrosis, release of oxygen-free radicals, exfoliation, and cell death (reviewed in Mossman and Begin, 1989) has been observed in a variety of cells exposed to high concentrations of fibers. At lower concentrations, both crocidolite and chrysotile asbestos cause cell proliferation in HTE cells and organ cultures, phenomena not observed with various synthetic fibers or nonfibrous analogs of asbestos (Marsh and Mossman, 1988; Woodworth *et al.*, 1983). These biological responses to asbestos may be important in the induction of neoplasms as cell injury may cause exfoliation and compensatory hyperplasia of surrounding cell types which are more sensitive to genetic damage. As suggested by Ames and Gold (1990), mitogenesis may facilitate mutagenesis and contribute to tumor development. In addition, cell proliferation is

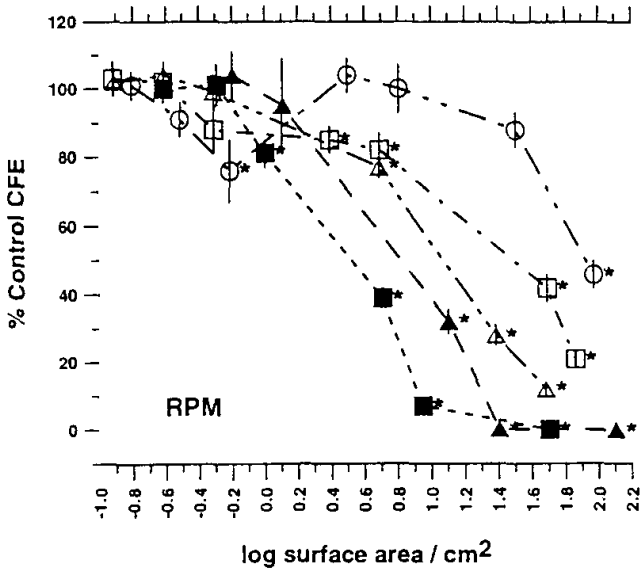

FIG. 7. Colony-forming efficiency (CFE) assays in RPM cells expressed as a function of surface areas of mineral samples (mm^2/cm^2). The symbol width is equal to or greater than one standard error. The standard error in CFE is indicated on the symbols. *$p < 0.05$ in comparison to untreated controls. (▲) Chrysotile; (■) crocidolite; (○) FD14; (□) S157; (△) CPS183.

an important component of tumor promotion and progression, and asbestos is a documented tumor promoter in epithelial cells of the respiratory tract (reviewed in Mossman *et al.*, 1990, 1996; Health Effects Institute, 1991).

Our results with asbestos samples are interesting in that HTE cells are unique in exhibiting increased CFE, in comparison to untreated and talc-exposed cells. Moreover, both cell types were more sensitive to the cytotoxic effects of equal weight dose amounts of asbestos in comparison to talc. The lack of response of RPM cells to the proliferative effects of asbestos may reflect the fact that single cells, as opposed to confluent monolayers (Marsh and Mossman, 1988; Woodworth *et al.*, 1983), were exposed to fibers here. For example, when added to confluent, growth-arrested RPM cells, crocidolite causes cell proliferation as measured by dual fluorescence techniques with an antibody to 5-bromodeoxyuridine (BrdU) and the DNA dye YOYO (Goldberg *et al.*, 1997). Moreover, increased numbers of both pleural mesothelial and bronchial epithelial cells incorporating BrdU are observed after inhalation of NIEHS crocidolite or chrysotile by rats (BeruBe *et al.*, 1996). As suggested by Gerwin *et al.* (1987), mesothelial cells may require growth factors, either produced endogenously or produced by other cell types, for proliferative responses to asbestos, and the small numbers of cells used in the CFE bioassay may not be sufficient for amounts of cytokines needed here.

Our experiments also show that fibrous talc does not cause proliferation of HTE cells or cytotoxicity equivalent to asbestos in either cell type despite the fact that talc samples contain durable mineral fibers with dimensions similar to asbestos. These results are consistent with the findings of Stanton *et al.* (1981) who found no significant increases in pleural sarcomas in rats after implantation of materials containing fibrous talc. Moreover, Smith and colleagues report no sarcomas in hamsters after implantation of FD14 (1979), and other rodent studies in which talcs of various types have been administered by inhalation of injection also have not shown an increased incidence of mesotheliomas or carcinomas (Stenback and Rowland, 1978; Wehner *et al.*, 1977). Epidemiological studies also indicate that talc in a number of occupational settings is less pathogenic than asbestos in the development of lung cancer, and the reports indicating excess lung cancer mortality may underestimate smoking habits, an important confounder, and exposure to commercial asbestos (reviewed in IARC, 1987a,b; Ross *et al.*, 1993). In essence, data have not proven that talc is a human carcinogen as small numbers of cohorts have been studied, smoking histories are poorly documented, and workers were often exposed to other dusts, including asbestos, that may cause lung disease.

Increases in cytotoxicity over time with CPS183, as opposed to the other talc samples, in both cell types also suggest the importance of mineralogic differences as the size distributions of CPS183 and S157 are similar. Since CPS183 fibers are mainly talc, while S157 contains more talc/amphibole and amphibole, mineralogical variability may affect the responses of cells to cytotoxic effects of talc. Nonfibrous particles such as quartz may also play a role in cytotoxicity of the talc samples since CPS183 higher number of quartz particles, a mineral known to be cytolytic (Mossman and Begin, 1989).

Data presented here lend increased uncertainty to the concept that long thin fibers [length >8 μm, width <0.25 μm, i.e., the Stanton hypothesis (Stanton *et al.*, 1981)] are the predominant factors predicting tumorigenicity and fibrogenicity (Mossman *et al.*, 1990; Health Effects Institute, 1991). In his elegant and comprehensive studies, Stanton and colleagues implanted two samples of fibrous talc (No. 6 and No. 7 samples) into rats. One of us (AW) examined talc No. 6 and found it to be similar in mineralogy, size distribution, and morphology to FD14, and little is known about No. 7 except that it was obtained from the Gouverneur District. Neither talc produced significant excesses in pleural sarcomas despite the fact that the dose of fibers >8 μm in length and <0.25 μm in width in sample No. 6 was large enough to predict a tumor probability of $>50\%$.

In summary, intrapleural injection studies in rats, epidemiologic investigations, and our *in vitro* work with fibrous talc here suggest caution in generalizing that durable fibers >5 μm or with aspect ratios approximating Stanton criteria are always more bioreactive and pathogenic. Our work is significant in that it supports reanalysis of the Stanton data by Wylie *et al.* (1987) and others (Oehlert, 1991; Nolan and Langer, 1993) and provides data implicating the importance of mineral type, rather than fiber length per se, in determining cellular outcomes associated with pathogenicity of mineral dusts.

ACKNOWLEDGMENTS

Work was supported in part by a grant from NIEHS (R01ES06499) to BTM and from R. T. Vanderbilt Company to AGW and CS. We thank Dr. Cynthia Timblin for her input into interpretation of CFE data.

REFERENCES

Ames, B. N., and Gold, L. S. (1990). Mitogenesis increases mutagenesis. *Science* **249,** 970–971.

BeruBe, K. A., Quinlan, T. R., Moulton, G., Hemenway, D., O'Shaughnessy, P., Vacek, P., and Mossman, B. T. (1996). Comparative proliferative and histopathologic changes in rat lungs after inhalation of chrysotile or crocidolite asbestos. *Toxicol. Appl. Pharmacol.* **137,** 67–74.

Campbell, W. J., Huggins, C. W., and Wylie, A. G. (1980). *Chemical and physical characterization of amosite, chrysotile, crocidolite, and nonfibrous tremolite for oral ingestion studies by the National Institute of Environmental Health Sciences, No. 8452 Bureau of Mines Report of Investigations.*

Davis, J., Addison, J., and Bolton, R. (1986). The pathogenicity of long versus short fiber samples of amosite asbestos administered to rats by inhalation and intraperitoneal injection. *Br. J. Exp. Pathol.* **67,** 415–430.

Engle, A. E. J. (1962). *The PreCambrian Geology and Talc Deposits of the Balmat-Edwards District, Northwest Adirondack Mountain, New York.* United States Geological Survey Open File Report.

Gerwin, B. I., Lechner, J. F., Reddel, R. R., Roberts, B. B., Robin, K. C., Gabrielson, E. W., and Harris, C. C. (1987). Comparison of production of transforming growth factor-B and platelet-derived growth factor by normal human mesothelial cells and mesothelioma cell lines. *Cancer Res.* **47,** 6180–6184.

Goldberg, J. L., Zanella, C. L., Janssen, Y. M. W., Timblin, C. R., Jimenez, L. A., Vacek, P., Taatjes, D. J., and Mossman, B. T. (1997). *Am. J. Respir. Cell Mol. Biol.*, in press.

Guthrie, G., Jr., and Mossman, B. (Eds.) (1993). *Health Effects of Mineral Dusts, Reviews in Mineralogy*, Vol. 28, pp. 1–584. Mineralogical Society of America, Washington, DC.

Health Effects Institute (1991). *Asbestos in Public and Commercial Buildings: A Literature Review and Synthesis of Current Knowledge*. Health Effects Institute-Asbestos Research, Cambridge, MA.

IARC (1987a). *IARC Monographs on the Evaluation of the Carcinogenic Risk of Chemicals to Humans: Silica and Some Silicates*, Vol. 42. World Health Organization, International Agency for Research on Cancer, Lyon.

IARC (1987b). *IARC Monographs on the Evaluation of the Carcinogenic Risk of Chemicals to Humans, Overall Evaluations of Carcinogenicity: An Updating of IARC Monographs 1 to 42*, Supplement 7. World Health Organization, International Agency for Research on Cancer, Lyon.

Janssen, Y., Heintz, N., Marsh, J., Borm, P., and Mossman, B. (1994). Induction of c-fos and c-jun protooncongenes in target cells of the lung and pleura by carcinogenic fibers. *Am. J. Respir. Cell Mol. Biol.* **11,** 522–530.

March, J. P., Mossman, B. T., Driscoll, K. E., Schins, R. F., and Borm, P. J. A. (1994). Effects of Aramid, a high strength synthetic fiber, on respiratory cells in vitro. *Drug Chem. Toxicol.* **17,** 75–92.

Marsh, J. P., and Mossman, B. T. (1988). Mechanisms of induction of ornithine decarboxylase activity in tracheal epithelial cells by asbestiform minerals. *Cancer Res.* **48,** 709–714.

Mossman, B. T., and Begin, R. (Eds.) (1989) *Effects of Mineral Dusts on Cells*. Springer-Verlag, Berlin.

Mossman, B. T., and Gee, J. B. L. (1989). Medical progress: Asbestos-related diseases. *N. Engl. J. Med.* **320,** 1721–1730.

Mossman, B. T., and Sesko, A. M. (1990). *In vitro* assays to predict the pathogenicity of mineral fibers. *Toxicology* **60,** 53–61.

Mossman, B. T., Bignon, J., Corn, M., Seaton, A., and Gee, J. B. L. (1990). Asbestos: Scientific developments and implications for public policy. *Science* **247,** 294–301.

Mossman, B. T., Ezerman, E. B., Adler, K. B., and Craighead, J. E. (1980). Isolation and spontaneous transformation of hamster tracheal epithelial cells. *Cancer Res.* **40,** 4403–4409.

Mossman, B. T., Kamp, D. W., and Weitzmon, S. A. (1996). Mechanisms of carcinogenesis and clinical features of asbestos-associated cancers. *Cancer Invest.* **14,** 466–480.

Nolan, R. P., and Langer, A. M. (1993). Limitations of the Stanton hypothesis. In *Health Effects of Mineral Dusts* (G. D. Guthrie and B. T. Mossman, Eds.), pp. 309–325. Mineralogical Society of America, Washington, DC.

Oehlert, G. W. (1991). A reanalysis of the Stanton *et al.* pleural sarcoma data. *Environ. Res.* **54,** 194–205.

Petruk, W., and Skinner, H. C. W. (1997). Characterizing particles in airborne dust by image analysis. *JOM* April, 58–61.

Ross, M., Nolan, R. P., Langer, A. M., and Cooper, W. C. (1993). Health effects of mineral dusts other than asbestos. In *Health Effects of Mineral Dust* (G. D. Guthrie and B. T. Mossman, Eds.), pp. 361–407. Mineralogical Society of America, Washington, DC.

Ross, M., Smith, W., and Ashton, W. H. (1968). Triclinic talc and associated amphiboles form Gouverneur Mining District, New York. *Am. Min.* **53,** 751–769.

Skinner, H. C. W., Ross, M., and Frondel, C. (1988). *Asbestos and Other Fibrous Materials*. Oxford Univ. Press, New York.

Smith, W. E., Hubert, D., Sobel, H., and Marquet, E. (1979). Biologic tests of tremolite in hamsters. *Dusts Dis.* 335–339.

Stanton, M. F., Layard, M., Tegeris, A., Miller, E., May, M., Morgan, E., and Smith, A. (1981). Relation of particle dimensions to carcinogenicity in amphibole asbestos and other fibrous minerals. *J. Natl. Cancer Inst.* **67,** 965–975.

Stemple, I. S., and Brindley, G. W. (1960). A structural study of talc and talc-tremolite relations. *J. Am. Ceram. Soc.* **43,** 34–42.

Stenback, F., and Rowland, J. (1978). Role of talc and benzo [*a*] pyrene in respiratory tumor formation: An experimental study. *Scand. J. Respir. Dis.* **59,** 130–140.

Timblin, C. R., Janssen, Y. M. W., and Mossman, B. T. (1995). Transcriptional activation of the proto-oncogene, c-jun, by asbestos and H_2O_2 is directly related to increased proliferation and transformation of tracheal epithelial cells. *Cancer Res.* **55,** 2723–2726.

Veblen, D. R., and Wylie, A. G. (1993). Mineralogy of amphiboles and 1:1 layer silicates. In *Health Effects of Mineral Dusts* (G. D. Guthrie and B. T. Mossman, Eds.), pp. 61–131. Mineralogical Society of America, Washington, DC.

Virta, R. L. (1985). *The Phase Relationship of Talc and Amphiboles in a Fibrous Talc Sample*, No. 8923 Bureau of Mines Report of Investigations.

Wehner, A. P., Zwicker, G. M., Cannon, W. C., Watson, C. R., and Carlton, W. W. (1977). Inhalation of talc baby powder by hamsters. *Food Cosmet. Toxicol.* **15,** 121–129.

Woodworth, C. D., Mossman, B. T., and Craighead, J. E. (1983). Induction of squamous metaplasia in organ cultures of hamster trachea by naturally occurring and synthetic fibers. *Cancer Res.* **43,** 4906–4913.

Wylie, A. G., Bailey, K. F., Kelse, J. W., and Lee, R. J. (1993). The importance of width in asbestos fiber carcinogenicity and its implications for public policy. *Am. Ind. Hyg. Assoc. J.* **54,** 239–252.

Wylie, A. G., Virta, R. L., and Segretti, J. M. (1987). Characterization of mineral population by index particle: Implications for the Stanton hypothesis. *Environ. res.* **43,** 427–439.

UNIVERSITY OF MARYLAND AT COLLEGE PARK

DEPARTMENT OF GEOLOGY

Prof. Fred Pooley
University of Wales, Cardiff
School of Engineering Division of Materials and Minerals
P.O. Box 925
Cardiff, CF2 1YF United Kingdom

November 3, 1994

Dear Fred;

Please accept my apologies for taking such a long time to respond. Unfortunately, I did not receive the photographs you sent until after I returned from my end of the summer vacation when I was quickly inundated with beginning of the year responsibilities. Furthermore, since I intended to disagree with your conclusion that the photographs were of amphibole, not amphibole intergrowths with other minerals, I wanted to discuss my conclusions with Tom Dagenhart, a mineralogist who has also studied fibrous talc. So now you know where I am going and I will proceed with the discussion.

While you provided me with the camera length, you did not give me the camera constant. Therefore, I was not able to make accurate measurements of d-spacings. The d-spacings I will discuss below are based on the assumption that the layer line spacing is approximately 5.3 A. Therefore, all d-spacings should be preceded with the word "approximately". Also, I will not discuss photographs 0532 (2) and 0583 (10). 0532 is not a zone axis picture, and 0583 appears to have at least two diffracting lattices that are not aligned. However, I did not see in these two photographs anything that would suggest conclusions different from those I draw from the other photographs.

Most of the photographs show a triplet pattern in the odd numbered layer lines. This pattern is very strongly developed in some (0537 (3) for example) and only slightly obvious in some. The only photograph that does not appear to display this pattern is 0560 (9). The triplet pattern can be caused from an epitaxial intergrowth between talc and anthophyllite with a-talc = c-anthophyllite, c-talc = a-anthophyllite and b-talc = b-anthophyllite. I am enclosing some computer generated diffraction patterns that show the origin of the triplet pattern. If you superimpose 100 anthophyllite and 001 talc, you will produce this pattern. The talc pattern forms the center of the triplets.

Between the triplets there should be an extinction. However,

DEPARTMENT OF GEOLOGY • UNIVERSITY OF MARYLAND AT COLLEGE PARK, MARYLAND 20742, USA
OFFICE: (301) 405-4365 • DIRECT LINE • FAX: (301) 314-9661

on most of the patterns on the odd numbered layer lines, in the position where there "should" be an extinction if 001 talc and 100 amphibole are responsible, there is a diffraction spot. In general, this spot is very weak in comparison to those in the triplet. This is illustrated in 0591 11)0531 (1), 0541 (4)0621 (13), 0544 (8) and 0543 (7). In most of the patterns there are also extra spots on the zero layer line. (As you know, Pnma symmetry does not allow reflections on from 010, 030, etc. (100 zone axis) or from 100, 300, etc. (010 zone axis). These "extra" spots cannot arise from anthophyllite unless they are due to double diffraction or they are actually in an adjacent plane in reciprocal space. If the latter were the case, the "extra" spots in the zero layer line would be either 110, 130, etc. or 110, 310, etc. All of these reflections are precluded by the Pnma symmetry and cannot be responsible. (Note: These "extra" spots are common in the diffraction patterns of the clinoamphiboles such as amosite. In monoclinic minerals, they could be the 110, 130, etc. since these are allowed reflections.) The even intensity and the ubiquitous nature of these "extra" spots suggest that they are not due to double diffraction. You should be able to test this by tilting a few degrees in the direction perpendicular to the fiber axis.

An alternate explanation for the "extra" spots is the presence of a quadruple chain. An orthorhombic quadruple chain would give (following the extinction pattern of anthophyllite) layer lines with 18 A spacing. Robert Felius produced a HRTEM image of a quadruple chain which gave rise to a diffraction pattern similar to the ones you have produced. The quadruple chain might explain the apparent 36A spacing observed on some of the first layer lines (See 0560 (9) for example.)

Another possibility that has been put forward by Dagenhart that explains the presence of the "extra" spots is the superposition of 101 anthophyllite and 101 talc. Their zone axes coincide so a pattern arising from the combination of the two is reasonable. If this orientation were responsible, there would be spacing of 18 A on the first and third layer line from the amphibole. However, every other (k even) spot is weaker in intensity. Every fourth amphibole spot (k even)coincides with a diffraction spot from talc. Therefore, if talc is present, this combination produces a three strong spot- one weak spot pattern along a row with an 18A spacing. This explanation does not, however, explain the "extra" spots in the zero layer line.

In the set of generated diffraction patterns, I am including those for an orthorhombic talc with the same lattice dimensions as those of the monoclinic talc. (Although talc is triclinic, its diffraction pattern is essentially identical to a monoclinic talc with twice the c-axis length. For reasons of limitations on computational time on the computer, monoclinic pattern rather than triclinic patterns were generated. The differences between the triclinic talc model and the monoclinic talc model is only 0.5 degrees in the angle the b-axis makes with the a-c plane.) While an orthorhombic talc has not been demonstrated to occur alone,

several researchers have suggested its existence based on the epitaxial growth of talc after anthophyllite. Talc may be orthorhombic when growth begins and revert to the more stable monoclinic form some distance away. The use of the orthorhombic model makes the "fit" between the talc and the amphibole just about perfect.

I am also including diffraction patterns generated for an Mg-cummingtonite with monoclinic C2/m symmetry. You will see that if you try to superimpose the monoclinic amphibole and talc, you will not generate a three spot pattern, despite what Stemple and Brindley published in 1960. Therefore, I do not believe that a monoclinic amphibole-talc intergrowth is indicated by these electron diffraction patterns.

In summary, I would conclude that the patterns that you sent do not represent amphibole alone because:

1) The intensity along the odd layer lines do not correspond to an amphibole pattern. By and large, the "triplet" is best explained by a talc-anthophyllite intergrowth, and

2) 18 A spots in the zero layer line and 36 A spacing of spots in the first layer line suggest the presence of a quadruple chain silicate (or some other pyrobole) also intergrown with talc and amphibole.

I believe these conclusions are supported by the photograph of the fiber which you included with the diffraction patterns. The striping on this particle is probably reflecting "layers" of different Mg silicate structures. I do not doubt that if one works hard enough, one could obtain the diffraction pattern of amphibole alone. However, my guess would be that somewhere else along that fiber, a mixed pattern would also be found. I think that the geologic conditions were such that pervasive alteration took place resulting in the "replacement" of amphibole by talc and other pyroboles. The composite nature of these fibers reflects alteration stopped in progress and a non-equilibrium assemblage resulted. The smearing of the spots in the b direction is ubiquitous in the diffraction patterns and could be interpreted as disorder in this direction. Rapid, non-equilibrium mineral growth would likely result in significant structural disorder. Support for the composite nature of fibrous talc also comes from its optical properties. The indices of refraction are variable, but most fall between pure Mg-talc and a pure Mg-amphibole, too high for talc, too low for amphibole.

I would be happy to discuss this further. I would also be most interested in your response.

Sincerely yours,

cc: J. Kelse
T. Dagenhart

Ann G. Wylie
Professor

Protocol for Sample analysis: Fiber number per microgram

OPTICAL MICROSCOPY (OM)

1. For those samples that are not ~~100%~~ UICC asbestos, the optical analysis can by facilitated by sieving to remove the smallest particles. Therefore, the samples should be dry sieved with a 325 sieve (44 micrometer) or other size appropriate for the sample. This process is not meant to divide the samples completely, and with fibers it cannot do so, but rather it is meant to separate the smallest particles and fibers to prevent interference. The majority of the particles in the smallest fraction will not be identifiable by OM so that TEM analysis will be necessary to characterize this fraction properly. The large size fraction, on the other hand, will contain particles that in general can be identified by OM and the role of TEM in the analysis of this size fraction will be lessened.

2. For those samples that contain a very high proportion of fiber, sieving may be of little benefit. This should probably be verified by attempting sieving.

3. For optical analysis, a high powered objective with a numerical aperture of at least 0.85 should be available. It is the objective of choice for samples that contain small particles. Objectives with this NA range in magnification from 45 to 64 X. Wide field eyepieces are easiest on the eyes. They should be 10 - 12.5 X. A micrometer ocular with the smallest divisions that calibrate to about 1 micrometer with a 50 X objective should be used.

4. For measurements to be made with the optical microscope, the following protocol is suggested:

a. Weigh a clean glass slide.

b. Place between 0.001 and 0.003 grams of material on the slide divided as equally as possible in two places. The amount of material within these limits is determined by sample characteristics, primarily particle size. Use less sample for populations of smaller particles and more for larger particles. The limits may be changed depending upon experience.

c. Weigh the slide plus material to determine the exact weight of the sample. After repeating this procedure a few times, you will be able to estimate 0.001 grams fairly precisely.

d. On each pile of material place two to three drops of oil and mix THOROUGHLY, taking care to liberate all particles that adhere to the slide so they become covered with oil. During the mixing, the oils and sample should be spread out to cover a square area 15 x 15mm. More oil is required for coarser samples. Enough oil should be mixed with sample so that when the mixture is covered with a 15 x 15 mm cover slip, it will fill the spaces

between cover slip and slide and there will not be excess around the edges. If the mixture fills greater than or equal to 90% of the space, the preparation is acceptable.

e. Place a 15 X 15 mm cover slip on the mixture. If less than 90% of the cover slip is filled, additional oil can be added by dropping oil at the edge of the cover slip and rocking the cover slip gently to disperse grains and oil evenly. This procedure generally leaves a drop of oil on the edge of the slip which should be removed with absorbing paper before optical examination in order to keep the objective clean.

f. Determine the area under the cover slip in terms of rows of fields of view. For example, you may have 53 rows for the 50 X objective.

g. Move the slide from one side of a single cover slip to the other and record the data for all particles that are visible within that row. Examine at lease 20 % of the slide (11 rows in my example above) and do so randomly but distributed over the breadth of the cover slip. Note magnification and number of rows examined.

h. Repeat the procedure for the other cover slip on the slide.

i. The number of preparations that must be counted in this way for each sample is largely governed by the precision desired and the abundance of the particles in each category. At a minimum, three preparations for each sample should be examined. Statistical analysis of these data will direct additional examination.

j. Record the length and width of each fiber meeting the specified dimensions in terms of divisions of the micrometer ocular. (You may wish to establish these categories in terms of micrometer ocular divisions that correspond to the desired micron divisions before you begin the measuring process. See amended data sheet.)

k. Calculate the number of fibers per microgram by determining the number of fibers counted/ weight of slide x proportion of slide examined.

Choice of immersion oils

The talc from Gouvernor contains very little iron. Therefore, the maximum magnitude of γ one would anticipate from this area is about 1.590-1.600. Certainly, if γ rises above 1.600, it is likely that some "amphibole" component or other structural abnormality is present and the material might be considered to be transitional or composite.

The amphibole from Gouvernor also contains no iron although

it may contain a small amount of Mn. The magnitude of α for tremolite from this locality has been measured at 1.598. Although there are no data on anthophyllite, it is likely by analogy with other studies of anthophyllite/tremolite co-occurrences that the magnitude of α for anthophyllite is also 1.598.

Given these relationships, mounting the samples that are likely to contain fibrous talc in 1.598 will enable the following distinctions to be made:

a. Fibers with α less than and γ less than or equal to 1.598. These are talc.

b. Fibers with α less than 1.598 and γ greater than 1.598. These fibers are "transitional" between talc and amphibole.

c. Fibers with α greater than or equal to and γ greater than 1.598. These fibers are most likely amphibole.

TRANSMISSION ELECTRON MICROSCOPY (TEM)

1. Weight a small amount of material (0.004 - 0.008 g) and disperse in distilled water with a small amount of surfactant.

2. Filter the mixture on to a 0.1 um Millipore filter and dry.

3. Measure area on filter that is covered with sample.

4. Prepare a TEM grid using direct transfer techniques. (Many references for this are available.)

5. Examine prepared carbon coated grid at 20,000 X magnification. Magnification can be changed for measurements but TEM must be calibrated at each magnification for accurate measurements.

6. Count and measure by length/width category all fibers in selected grid openings.

7. Record fiber measurements, number of grids examined, and calculate area of grid examined.

8. Fiber concentration = fibers counted / grid area examined x weight on filter/ filter area covered by sample.

9. Repeat as necessary.

American Mineralogist, Volume 65, pages 1075-1086, 1980

Anthophyllite asbestos: microstructures, intergrown sheet silicates, and mechanisms of fiber formation

DAVID R. VEBLEN

Department of Geology, Arizona State University
Tempe, Arizona 85281

Abstract

The complex microstructures of an anthophyllite asbestos specimen from Pelham, Massachusetts, have been elucidated by transmission electron microscopy and electron diffraction techniques. The specimen consists primarily of small amphibole crystallites that are greatly elongated in the *c* direction. Adjacent crystallites are crystallographically rotated with respect to each other, but are not related by a twinning operation. The anthophyllite possesses pervasive moderate chain-width disorder. Central screw dislocations are not present in the crystallites, indicating that they did not grow by a spiral growth mechanism around screw dislocations.

The grain-boundary structures between rotated crystallites have been characterized using high-resolution TEM methods. Low-angle grain boundaries may be largely structurally coherent, whereas high-angle grain boundaries are typically incoherent. Many of the grain boundaries are partially filled by talc, serpentine minerals, or chlorite. Unusual conformations of curved serpentine are present, and antigorite occurs in ordered 1- and 2-layer polytypes that are intimately intergrown with stacking-disordered antigorite. The curvature reversals in some areas of antigorite are non-periodic, with spacings much larger than those usually observed.

The microstructures strongly suggest that the primary mechanism of fiber formation in this asbestos is separation along the grain boundaries between individual crystallites. This process may be enhanced by the pervasive presence of sheet silicates along the grain boundaries. However, this is not the only mechanism of fiber formation that can occur in amphiboles, since in some other anthophyllite specimens crystals split preferentially along (100) stacking faults and (010) chain-width errors. Disaggregation along such planar defects may thus be an important secondary mechanism of fiber formation in commercial amphibole asbestos.

The correlation of chain-width errors with the asbestiform habit may result in part from the cellular structure of amphibole asbestos: hydrothermal fluids that produce these defects could diffuse much more rapidly along the incoherent grain boundaries than they could through the bulk structure of massive amphiboles. Rapid fluid conduction along these cellular grain boundaries can also account for the abundance of sheet silicates as grain-boundary fillings.

Introduction

Some of the most complex problems in mineralogy involve the relationships among physical properties, crystal structure, and defect structure. In many minerals, the ideal crystal structure clearly controls mechanical properties, such as cleavage, as well as other properties, such as color and electrical conductivity. In other cases, crystal defects exercise controlling influences on physical properties. For example, low concentrations of the defects referred to as color centers can severely alter light-absorption properties of alkali halides, and the mechanical deformation properties of most crystalline materials are dependent as much on the presence and motion of dislocations as they are on the ideal crystal structure.

One of the most important unanswered questions in rock-forming silicate crystallography involves the mechanical behavior of amphiboles. Most amphibole crystals ("massive or acicular amphiboles") are quite brittle and when broken exhibit excellent prismatic cleavage. On the other hand, some amphibole specimens ("amphibole asbestos") are not at all brittle

0003-004X/80/1112-1075$02.00

amphibole asbestos fibers can be attributed to spiral growth, at least in the present specimen.

Grain-boundary structures

Several different types of grain-boundary structures are observed between crystallites in the Pelham anthophyllite. The variations in structure are, in part, related to the orientation differences between adjoining grains. Where the orientation difference between two crystallites is very small, the interface is commonly a simple low-angle grain boundary that is mostly coherent, with partial dislocations absorbing the structural misfit (Fig. 5a; the relative rotation between the two crystals is about 0.5°). With larger differences in orientation between adjoining crystallites, structural coherency is lost, at least for most interface orientations (Fig. 5b; the relative rotation between the two crystals is about 9°).

Many grain boundaries between crystallites, however, are not simple amphibole-amphibole interfaces like those shown in Figures 5a,b. Instead, most of the high-angle grain boundaries, and also some of those with low angles, are at least partially filled with sheet silicates that include talc, serpentine minerals, and chlorite. An overview of the boundaries between three crystallites is shown in Figure 5c. At such boundaries containing sheet silicates, the interfaces between the sheet mineral and one of the crystallites usually exhibit strong structural control; these controlled interfaces are generally planar, while the interface of the sheet silicate with the other crystallite is irregular or ragged. The relationships between talc and anthophyllite at the controlled interfaces are typically the same as those commonly observed between talc and pyribole at Chester, Vermont (Veblen and Buseck, 1980): (1) $a_{tc} \parallel c_{an}$, $b_{tc} \parallel b_{an}$, and $c^*_{tc} \parallel a^*_{an}$; or (2) $(001)_{tc} \parallel (210)_{an}$. Boundaries having the first orientation relationship are typically parallel to (010), (210), or (100) of the anthophyllite. Where the sheet silicate occupying the boundary between anthophyllite crystallites is chlorite or serpentine, (001) of the sheet silicate is commonly parallel to (210) of the amphibole. This relationship is shown in Figure 5d, an interface between antigorite and anthophyllite; a large-scale undulation of the antigorite layers can also be seen in this figure.

Another grain-boundary relationship is shown in Figure 5e, where short talc layers are crystallographically related to one of the anthophyllite crystallites by relationship (1) above, but this controlled talc-amphibole interface is ragged rather than planar. In contrast, the boundary of the other anthophyllite crystallite is nearly planar and parallel to $(210)_{an}$. This situation is less common than those in which the crystallographically-controlled interface is planar. The fact that one of the anthophyllite boundaries is nearly always planar and has a rational crystallographic orientation of low index suggests that the interface energy is minimized by having one planar boundary and one ragged boundary, rather than two ragged boundaries with the sheet silicate. Another feature shown in Figure 5e is the local intercalation of 5Å layers in the talc; the structural configuration in such places is that of a chlorite mineral and has been observed in other occurrences where chain silicates have partially reacted to talc (Veblen and Buseck, 1980; in preparation).

Sheet silicates intergrown with Pelham anthophyllite

In addition to the features described in the last section on grain-boundary structure, there are many other fascinating microstructures in the sheet silicates in this asbestos specimen. In places, much of the anthophyllite has been replaced by talc and serpentine, so that there are sheet silicate grains in the tenth-micron size range, rather than simply as narrow grain-boundary fillings. Electron diffraction patterns indicate that this sheet silicate is oriented with its sheets more or less parallel to the pyribole silicate chains, as is typical in chain silicates that have partially reacted to sheet silicates. There is some variation in this orientation, however, just as there is variation in the orientations of the *c* axes of the anthophyllite, but the variations are not great enough to preclude simple interpretation of the HRTEM images.

The larger grains of talc are not very noteworthy. Like the talc that has been reported from intergrowths with pyroxenes, amphiboles, and wide-chain silicates from other localities, it exhibits stacking disorder in most areas, and the layers are commonly pulled apart locally (Veblen and Buseck, 1979b, 1980; in preparation).

The serpentine minerals, on the other hand, display remarkable diversity of structure. Like the fine-grained serpentine in certain uralites (Veblen and Buseck, 1979b), planar (lizardite) and curved (chrysotile) structures combine in some places to form complex patterns. More typical in this anthophyllite asbestos specimen, however, are curvature reversals in chrysotile, without the presence of lizardite structure. Figure 6 shows such microstructures in chrysotile that has grown, with talc, in two places along a low-angle (1.6°) grain boundary.

merous smaller fibers, as shown in Figure 9b, which also suggests that the resulting fibers are flexible. Such breakage along defects presumably occurs because the stacking faults and wide-chain slabs in the anthophyllite structure represent planes of high energy, even though the crystal structure is completely continuous across these planes.

Note that not all anthophyllite that contains chain-width errors is as fibrous as the material from Chester. An anthophyllite from the Cascades, Washington (Veblen and Buseck, 1979b) contains a moderate number of such errors (fewer than the Chester amphibole) but tends to form acicular amphibole particles when crushed. This difference in mechanical behavior suggests that the energies of the chain-width errors are different in the two cases, leading to easier fracture in the Chester case, that the density of chain-width errors is an important parameter in the degree of fibrousness, or that some other factor, such as deformation history or minor chemical differences, may play a role in the physical properties of these amphiboles.

Although breakage along chain-width errors and twin planes or stacking faults may not be the primary mechanism of fiber formation in most commercial-grade amphibole asbestos specimens, such breakage may still occur and contribute to the fiber properties, even when most of the fiber separation occurs along grain boundaries. For example, further splitting of fibrils that have separated along grain boundaries may occur along chain-width errors and stacking faults during milling. Such defects appear to be nearly universal in commercial-grade amphibole asbestos, having been reported in many different specimens by competent electron microscopists (Chisholm, 1973, 1975; Hutchison *et al.*, 1975; Alario Franco *et al.*, 1977); in addition, of several other amphibole asbestos specimens I examined, all contain at least

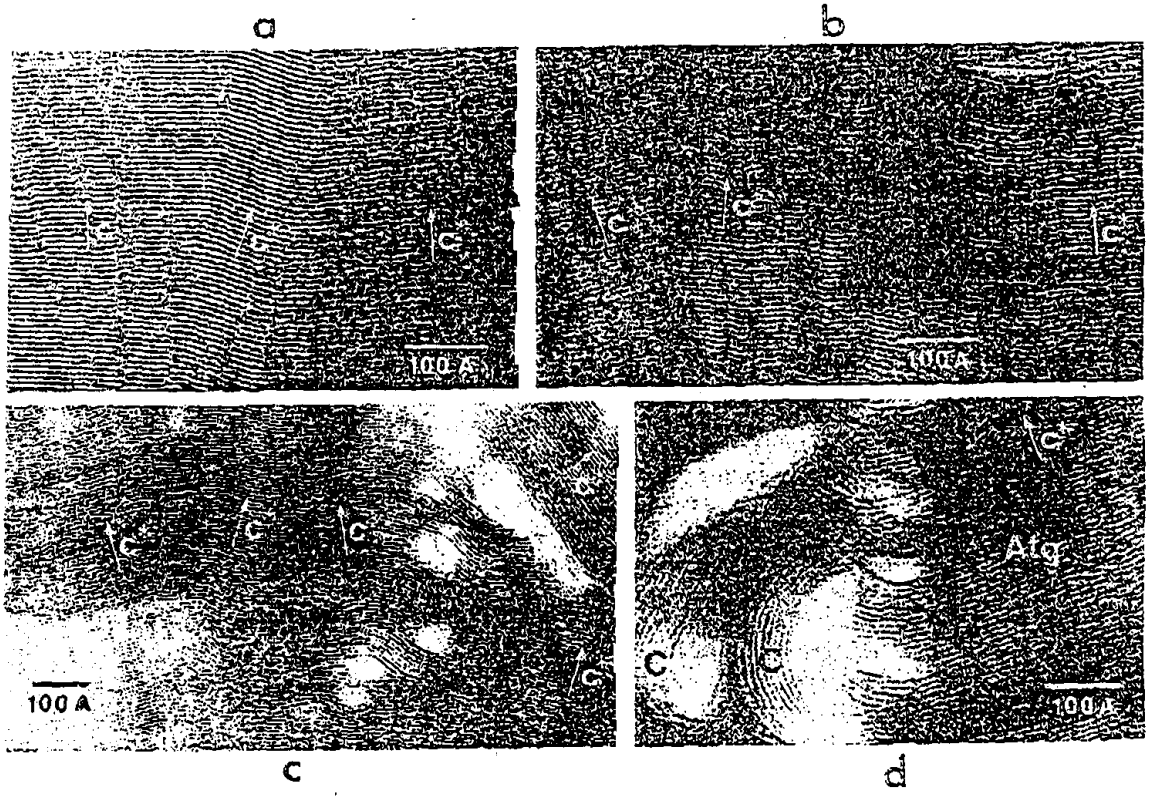

Fig. 8. Corrugation periodicity disorder and misorientation in antigorite. (a) A kink in the serpentine sheets. Local orientations of c^* are indicated. (b) Variation in layer curvature reversal can lead to orientation differences in different parts of an antigorite crystal. In the center and right portions of this figure the corrugation is nonperiodic, and the distance between curvature reversals is longer than that in typical antigorites. (c) Serpentine showing a highly sinuous arrangement of layers and resulting orientation differences. (d) Intergrowth of antigorite (Atg) and chrysotile (C) forms of serpentine.

RI 8923

Bureau of Mines Report of Investigations/1985

The Phase Relationship of Talc and Amphiboles in a Fibrous Talc Sample

By Robert L. Virta

UNITED STATES DEPARTMENT OF THE INTERIOR

Report of Investigations 8923

The Phase Relationship of Talc and Amphiboles in a Fibrous Talc Sample

By Robert L. Virta

UNITED STATES DEPARTMENT OF THE INTERIOR
William P. Clark, Secretary

BUREAU OF MINES
Robert C. Horton, Director

Library of Congress Cataloging in Publication Data:

Virta, Robert L

The phase relationship of talc and amphiboles in a fibrous talc sample.

(Report of investigations / United States Department of the Interior, Bureau of Mines ; 8923)

Bibliography: p. 9-11.

Supt. of Docs. no.: I 28.23: 8923.

1. Talc. 2. Amphiboles. 3. Phase rule and equilibrium. I. Title. II. Series: Report of investigations (United States. Bureau of Mines) ; 8923.

TN23.U43 [QE391.T2] 622s [549'.67] 84-600272

CONTENTS

ILLUSTRATIONS

TABLE

UNIT OF MEASURE ABBREVIATIONS USED IN THIS REPORT

Å	angstrom	μm	micrometer
ft	foot	wt %	weight percent
min	minute		

THE PHASE RELATIONSHIP OF TALC AND AMPHIBOLES IN A FIBROUS TALC SAMPLE

By Robert L. Virta[1]

ABSTRACT

The Bureau of Mines examined a fibrous talc sample from the Gouverneur talc district in New York by transmission electron microscopy (TEM) and polarized light microscopy to determine the mineralogical relationship of the fibrous talc to the amphiboles present in the sample. Two amphiboles, anthophyllite and tremolite, were present in the sample. Tremolite occurred as a separate mineral phase, which was blocky in habit. Only a few composite tremolite-talc grains were observed. Anthophyllite, however, was present only in the fibrous talc grains. Microdiffraction study of the fibrous talc grains containing anthophyllite showed that the anthophyllite was intermixed with the talc on a fine scale and that there was a crystallographic relationship between the talc and anthophyllite lattices in the fibrous talc grains. A mechanism similar to the process that forms biopyriboles could explain the structural defects, the fibrous habit of the talc, and the structural relationship between the talc and anthophyllite in the fibrous talc grains. Because of these characteristics, phase contrast microscopy and a provisional TEM technique for monitoring asbestos exposure would not distinguish between fibrous talc and fibrous amphiboles. TEM techniques employing electron diffraction and energy-dispersive X-ray analysis are recommended to positively identify the fibrous phases for regulatory purposes.

[1]Geologist, Avondale Research Center, Bureau of Mines, Avondale, MD.

INTRODUCTION

Health scientists are interested in occurrences of amphiboles in talc deposits because of the apparent association between cancer risk and the inhalation of pure amphibole asbestos (21).[2] Among the lesser studied occurrences are the fibrous amphiboles associated with the fibrous talc in the Gouverneur talc district, St. Lawrence County, NY.

Fibrous amphiboles are present in minor amounts throughout deposits in the Gouverneur district. In some localities, they have been altered through metamorphism (5, 8, 19). It is these amphiboles that are associated with fibrous talc (5, 8). Two fibrous talc samples from St. Lawrence County, were found to contain composite talc-amphibole fibers, rather than pure talc. In one case, tremolite occurred with talc; in the other, an unidentified Mg amphibole was present. In both cases, a crystallographic relationship between the talc and amphibole lattices was observed (1, 22). Studies of a partially altered fibrous anthophyllite from Vermont have also shown that chain width disorder and intergrown sheet structures are sometimes found in the amphibole structure (23, 25). Missing structural units were explained as providing sites for ion migration and structural reordering to form the sheet silicate structures from the amphibole double-chain structure (24).

Asbestiform amphiboles, whether occurring with fibrous talc or not, are monitored because of the health risk they pose (4, 9, 14-15). Monitoring is performed using phase contrast microscopy; particles that are equal to or longer than 5 μm and that have a length-to-width ratio greater than 3 to 1 are classified as asbestos (18). When fibrous amphiboles occur with platy talcs, this monitoring process is relatively definitive for asbestos because of the morphological differences. It is when fibrous amphiboles occur with fibrous talc that morphology alone is inadequate to distinguish between phases (16). For this reason, TEM has been recommended for regulatory use. Particle morphology, electron diffraction (ED) and energy dispersive X-ray analysis (EDX) are used to positively identify the particles (6). To provide a relatively rapid analysis for regulatory use, a provisional Environmental Protection Agency (EPA) technique that relies on particle morphology, EDX, and qualitative ED for particle identification was developed (20). In this technique, a 5.3-Å repeat spacing parallel to the long axis of the fiber and an Mg and Si spectrum are used to classify a particle as the amphibole anthophyllite. These characteristics, however, are similar to those of fibrous talc and could result in the misidentification of talc as anthophyllite.

The purpose of this Bureau of Mines study is to determine the phase relationships between the talc and amphiboles present in the sample and examine possible problems that could be encountered in monitoring for asbestos because of the presence of fibrous talc.

ACKNOWLEDGMENTS

The assistance of Dr. A. G. Wylie, crystallography and mineralogy, and C. W. Huggins, X-ray diffraction, both of the Bureau of Mines Avondale Research Center is gratefully acknowledged.

EXPERIMENTAL WORK

SAMPLE AND SAMPLING REGION

The sample selected for this study is a coarsely ground fibrous talc sample from Talcville, St. Lawrence County, NY. The talc deposits in this area consist of lenses of talc interbedded with metasedimentary and metasomatic rocks of the

[2]Underlined numbers in parentheses refer to items in the list of references at the end of this report.

Precambrian Grenville series. Talc, tremolite, anthophyllite, serpentine, chlorite, mica, quartz, and diopside are present in deposits along the talc belt (2-3 5, 8, 13, 19). Most of the talc and the amphiboles formed through the prograde metamorphism of quartzite and dolomite. Anthophyllite and talc have also been reported to have formed through the retrograde alteration of tremolite (19). Engel (8) reported the occurrence of fibrous talc and serpentine which are pseudomorphous after tremolite as a late-stage reaction product of the dynamothermal metamorphism of the region. Stemple (22) examined one sample of talc from St Lawrence County by electron microscopy and reported the occurrence of fibrous talc-tremolite particles. They observed a crystallographic relationship between the fibrous talc and tremolite. Barr (1) reported the presence of amphibole-talc particles in a talc sample from St. Lawrence County. The amphibole was identified only as a Mg-rich monoclinic amphibole.

The sample used in this study was randomly selected. Consequently, it may not be representative of the morphology or the morphological characteristics of particles in the entire deposit.

SAMPLE PREPARATION

Samples were prepared for X-ray diffraction analysis (XRD) by freezer milling to minus 325 mesh and briquetting in a pellet press. Quartz present in the sample was used as an internal calibration standard.

Samples for infrared spectrophotometric analysis (IR) were prepared by freezer milling to minus 325 mesh and mixing 2 mg of sample in 200 mg of KBr powder in a mixer mill. Pellets were made in a vacuum press under 9 tons of pressure for 2 min.

Samples for TEM analysis were ground and suspended in water with sonification. A drop of the suspension was placed on a collodian-coated TEM grid, dried on a hotplate, and carbon-coated in a vacuum evaporator.

ANALYSIS AND RESULTS

Talc, quartz, tremolite, phlogopite, and carbonate were identified by polarized light microscopy (PLM). Talc is the major phase with 1 to 3 wt % quartz and 1 to 3 wt % tremolite present. Phologite and carbonate were trace constituents. Talc particles had lengths ranging from 5 to several hundred micrometers. The particle morphology of the talc ranged from platelets to individual fibers to fiber bundles with splayed ends (fig. 1). The

FIGURE 1. - *A*, Variation of particle sizes and shapes in the talc sample, including platelets and fiber bundles of talc; *B*, talc fiber bundles splaying into thin talc fibrils.

quartz and tremolite had particle sizes of 10 to 150 μm. Quartz grains were generally anhedral and often contained inclusions of fibers. The tremolite was present in a blocky habit with a few prismatic grains. Several tremolite particles had partially altered to talc, forming composite talc-tremolite grains similar to those described by Wright (27). No gradations in the refractive indices between minerals were observed in these composite grains or in the fibrous talc particles. Gradations in the refractive indices have been reported in particles where amphibole are altering to talc (1).

Talc, quartz, tremolite, anthophyllite, and phlogopite were identified using XRD (table 1). Slightly less than 5 wt % anthophyllite was estimated to be present using mixed standards. Tremolite, whose major peak intensities were less than those of anthophyllite, was present in lesser concentration than anthophyllite. The maximum concentration of 5 wt % for anthophyllite was verified using mixed standards for IR analyses.

TABLE 1. - Powder X-ray diffraction data, briquetted fibrous talc

hkl	2θ[1]	d_{obs}	d_{111}[2]	I	Other minerals
	8.83	10.014		45	Phlogopite.
002	9.44	9.368	9.34	>100	Talc.
	10.53	8.400		20	Tremolite.
	10.70	8.267		8	Anthophyllite.
	17.66	5.021		6	Phlogopite.
004	18.96	4.680	4.66	85	Talc.
020	19.40	4.575	4.55	20	Talc.
	20.85	4.260		25	Quartz.
	21.11	4.208		5	Tremolite.
	26.66	3.344		>100	Quartz.
	27.23	3.274		6	Tremolite
	27.65	3.226		12	Anthophyllite.
006	28.60	3.121	3.116	>>100	Talc.
	29.33	3.044		64	Anthophyllite.
	31.92	2.803		8	Tremolite.
	32.64	2.743		7	Anthophyllite?
	35.30	2.542		3	Anthophyllite.
	35.76	2.510		4	Phlogopite.
132	36.18	2.482	2.476	3	Talc.
	36.55	2.458		20	Quartz.
008	38.46	2.340	2.335	11	Talc.
	38.83	2.319		3	Tremolite or anthophyllite.
	39.48	2.282		8	Quartz.
	40.31	2.237		6	Quartz.
	42.47	2.128		8	Quartz.
	45.14	2.008		14	Phlogopite.
	45.81	1.980		7	Quartz.
	48.13	1.890		18	Tremolite.
0·0·10	48.61	1.872	1.870	35	Talc.
	49.38	1.845		6	Anthophyllite?
	50.20	1.817		20	Quartz.
	54.91	1.672		11	Quartz.
313	58.20	1.585		22	Talc?

See footnotes at end of table.

TABLE 1. - Powder X-ray diffraction data, briquetted fibrous talc--Continued

hkl	2θ[1]	d_{obs}	d_{lit}[2]	I	Other minerals
0·0·12	59.20	1.560	1.557	16	Talc.
	60.03	1.541		24	Quartz.
060, $33\bar{2}$	60.68	1.526	1.527	17	Talc.
062, 330	61.68	1.503	1.509	6	Talc.
	64.88	1.437		2	Tremolite.
	67.80	1.382		15	Quartz.
	68.20	1.375		25	Quartz.
	68.36	1.372		19	Quartz.
	68.50	1.369		4	Unidentified.
	69.38	1.354		11	Talc?
0·0·14	70.33	1.338	1.336	14	Talc.
260	71.43	1.320	1.317	4	Talc.
	73.53	1.288		4	Quartz.
	75.73	1.256		7	Quartz.
	77.73	1.228		4	Quartz.
	79.96	1.199		5	Quartz.
	80.75	1.190		4	Unidentified.
	81.13	1.183		5	Quartz.
	81.53	1.180		8	Quartz.
	83.88	1.153		3	Quartz.

[1]Naturally occurring quartz found in talc fibers used as internal standard for minor 2-theta corrections.

[2]Values from JCPDS card 13-558.

Based on the results of the PLM, XRD, and IR analyses, the sample is estimated to be composed of greater than 90 wt % talc, 3 to 5 wt % anthophyllite, 1 to 3 wt % tremolite, 1 to 3 wt % quartz, and trace amount of phlogopite and a carbonate.

Although tremolite and anthophyllite were detected by XRD, only tremolite was observed by PLM. This suggests that anthophyllite is closely associated with the talc on a submicroscopic scale. Electron microscopy (EM) further confirmed this relationship of the anthophyllite to the talc. The morphological characteristics observed by PLM were observed by TEM on particles whose size was below the resolution limit of PLM (fig. 2). Both platy and fibrous particles were observed. Several fiber bundles composed of fine fibrils were also present. The individual fibrils are approximately 1,000 Å wide.

Identification of the individual fibers was performed using selected area electron diffraction (SAED) and EDX. The SAED spot patterns for various particle orientations of talc, tremolite, and anthophyllite were plotted using the reflection conditions specified in the

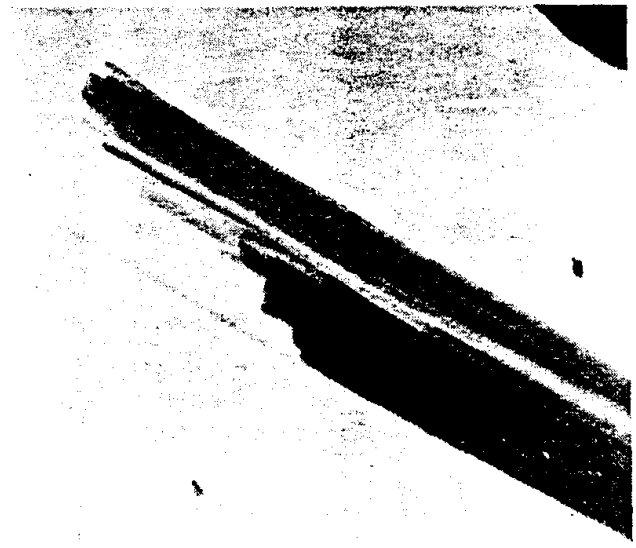

FIGURE 2. - Fibrous talc particle pseudomorphic after anthophyllite. Note the narrow fibrils of talc separating from the particle.

International Tables for X-ray Crystallography (10). These predicted SAED patterns and calculated d spacings were then used to identify the mineral phases. For tremolite, the body-centered cell described by Warren (26) was used to determine reflection conditions.

All fibrous particles were identified as either talc or talc-amphibole particle using SAED and EDX. Figures 3 and 4 show an elongated talc particle and a fibrous talc-amphibole particle respectively. The talc is oriented with its b*

FIGURE 3. - *A*, Fibrous talc particle; *B*, corresponding SAED pattern with a* oriented parallel to the particle length and b* oriented perpendicular to the particle length (TEM photomicrographic).

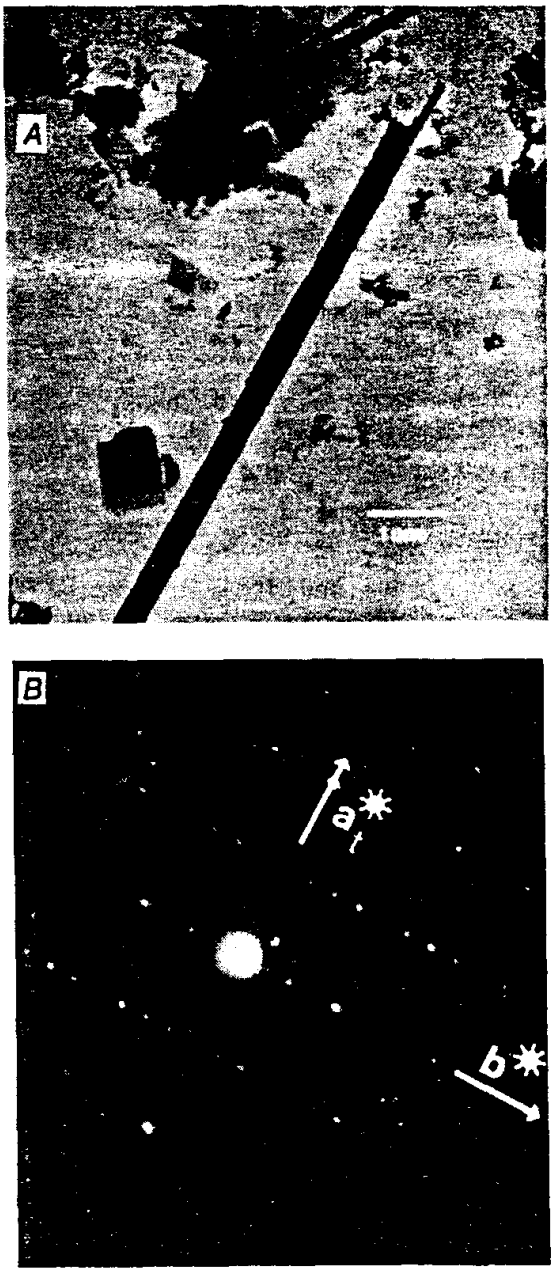

FIGURE 4. - *A*, Fibrous talc-amphibole particle; *B*, corresponding SAED pattern with a* (talc) and c* (amphibole) parallel to the particle length and b* (talc) and b* (amphibole) perpendicular to the particle length (TEM photomicrographic).

direction perpendicular to the length of the fiber and its a* direction parallel to the fiber length (fig. 3*B*). For talc-amphibole particles, the amphibole ED pattern is superimposed on the talc pattern (fig. 4*B*). The amphibole is oriented with the c* direction parallel to the fiber length and b* perpendicular to the fiber length. This ED pattern is shown schematically in figure 5, where the b* talc axis is parallel to the b* amphibole axis and the a* talc axis is parallel to the c* amphibole axis. The a* amphibole axis and c* talc axis were parallel to the electron beam. Dominant orientation of the (100) amphibole face perpendicular to the electron beam has been reported in the literature for amphibole asbestos (17). The maximum crystal growth of the fibrous talc is along the a axis with limited growth along the b axis and c axis. In platy talcs, the a and b lattice directions usually have equivalent crystal growth (7).

Many of the fibrous talc-amphibole particles exhibit a streaking of the ED pattern in the b* (amphibole) direction, suggesting possible defect structures in the b* lattice direction (fig. 4*B*). Other fibrous particles displayed distinct ED spot patterns, indicating that structural defects were minimal. These generally exhibited only a talc ED pattern.

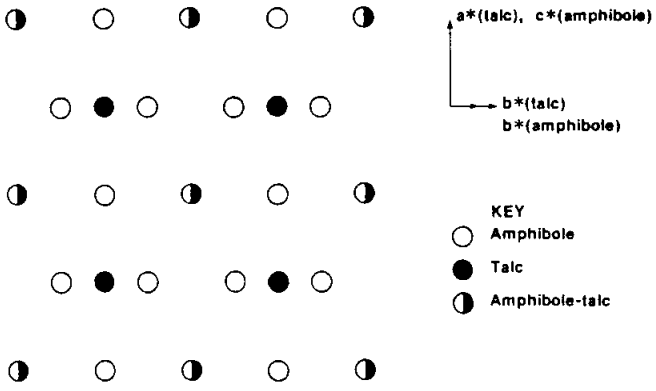

FIGURE 5. - Representation of superimposed talc-amphibole reciprocal lattices show in figure 4*B*. a* (talc) is parallel to c* (amphibole), and b* (talc) is parallel to b* (amphibole). b* (talc) ≈1/2 b* (amphibole).

Microdiffraction (μD) was used to determine if the mixed talc-amphibole ED pattern observed using conventional SAED could be attributed to alteration on a submicroscopic scale or partial alteration of an entire portion of the individual fibrous grains. Microdiffraction images were observed using a nominally rated 200-Å-diameter electron beam in the scanning transmission electron microscope mode along both the length and the width of the particles. Most of the fibrous particles exhibited either a talc μD pattern or a mixed talc-amphibole μD pattern. Only a few fibrous particles exhibited a mixed talc-amphibole μD pattern in one portion of a grain and a talc μD pattern in another portion of the same grain. No fibrous particles exhibited only an amphibole μD pattern.

Approximately 50 fibrous particles were examined qualitatively using EDX and found to be composed primarily of Mg and Si. Less than 2% of the particles contained any Ca or Fe, suggesting that tremolite is a minor to trace phase and that anthophyllite is the predominant amphibole. Semiquantitative EDX analyses were performed on particles with thicknesses less than approximately 1 μm using the Cliff-Lorimer technique (11). A pure Italian talc sample was used as the EDX standard. The Italian talc was composed of 19.8 wt % Mg and 29.0 wt % Si as determined using wet chemical techniques. Accuracy of the Cliff-Lorimer technique was approximately ±5 wt % relative under the operating conditions used in this study. A 4.5 wt % water content of the talc was assumed.

The fibrous particles ranged from 18.2 to 21.2 wt % Mg with an average value of 20.4±0.6 wt %. Silicon ranged from 27.9 to 30.6 wt % with an average value of 28.9±0.6 wt %. No Fe was detected. Several blocky particles exhibited EDX spectra similar to that of tremolite.

The percentage of amphibole in each fibrous particle could not be determined accurately using EDX because of the similarity of the Mg and Si content of the

talc and amphiboles. The particles would have to contain approximately 40 wt % anthophyllite before any significant shift in talc composition would be observed using semiquantitative techniques. The presence of more than 5 wt % tremolite would be detected because of the presence of Ca in the EDX spectrum. No significant variations in elemental concentrations (less than 2 wt %) were detected in different portions of most analyzed grains.

DISCUSSION

The intergrowth of talc with amphiboles, serpentine, chlorite, mica, and pyroxenes has been reported in several papers (1, 22-23, 25). The crystallographic relationship between the amphibole and fibrous talc in the sample examined is similar to that observed by Stemple (22), except that anthophyllite and possibly tremolite is intergrown with talc rather than only tremolite. Since both tremolite and anthophyllite are found in talc deposits and retrograde alteration of amphiboles has been reported in geological studies of the sampling area, the alteration of either mineral to fibrous talc could be expected.

Within the fibrous portion of the sample, the EDX and ED data indicate that no amphiboles occur as a free phase and that amphiboles occur only as composite talc-amphibole grains. The amphibole structures were determined to be interspersed on an extremely fine scale (several hundred angstroms in width) using μD and EDX. In all cases, either talc or superimposed talc and amphibole diffraction patterns were observed. No diffraction patterns and EDX spectra corresponding to a pure amphibole phase were observed. Had the composite particles been composed of coarse lamallae of talc and amphibole or had partial alteration of an entire portion of a grain occurred, only ED patterns and EDX spectra typical of an amphibole would have been observed.

Veblen (25) describes structural defects in pyroxenes and amphiboles which are believed to contribute to the alteration of their chain structures. The missing structural units were explained as providing sites for ion migration and structural reordering in the amphibole to form the sheet structure (24). Similar structural changes are likely to have been involved in the alteration of the amphibole to fibrous talc. The crystallographic relationship between the fibrous talc and amphibole and the fine intermixing of the two minerals are consistent with such an alteration mechanism. Defect structures in the lattice structure parallel to the b* direction of amphibole suggested by the streaking observed in the ED patterns are also consistent with the chain width disorder of chain silicate alteration described by Veblen (25).

A positive identification of the amphibole within the talc fibers could not be made by EM because all fibers had their a axis of amphibole parallel to the electron beam and the a* spacing was not determined. Tilting of the sample through angles of ±25° had almost no effect on the ED pattern. This phenomenon is explained as a result of the ED formation process related to the particle thickness (12). However, the data indicate that anthophyllite, rather than tremolite, is the major amphibole occurring in the fibrous talc grains. The 1 to 3 wt % nonfibrous tremolite observed as a free amphibole phase by PLM represents the bulk of the tremolite in the sample. Intermixing of the anthophyllite with talc fibers could account for its not being observed as a free amphibole phase by PLM despite its presence in the sample in greater quantities than tremolite. This also suggests that the fibrous talc and fibrous talc-anthophyllite particles formed from anthophyllite. Further, the fibril dimensions and dominant (100) orientation of the amphibole lattice, similar to what would be observed with asbestos, suggest that the fibrous morphology is due to the alteration of fibrous, if not asbestiform, anthophyllite. The dominant (001) crystal face of the talc would be developed in the alteration products due to the nature of the alteration process.

Based upon the results of this study and of studies on fibrous talc from other regions of the Gouverneur talc district, fibers of talc or talc-amphibole composites could be expected as a result of the alteration of fibrous amphiboles. This is one area of consideration when regulating for asbestos in talcs. The current phase contrast technique for asbestos monitoring uses the criteria of length equal to or greater than 5 μm, aspect ratio equal to or greater than 3 to 1, and parallel sides for classifying particles as asbestos. Many of the fibrous talc particles observed would meet these criteria, so other means of evaluating air monitoring filters would be required in these cases. Individual fibers could be positively identified with TEM using particle morphology, ED, and EDX. The use of ED, however, requires photographing and indexing each ED pattern. For regulatory purposes, a more rapid TEM technique would be required to permit analysis of large numbers of samples. A proposed technique using ED and the 5.3-Å repeat spacing would be appropriate if fibrous talc was not present. The 5.3-Å c spacing is very similar to the 5.28-Å a spacing observed on the fibrous talc grains, and both are oriented parallel to the fiber length. The 5.28-Å spacing would be indistinguishable from the 5.3-Å spacing for amphiboles using qualitative techniques. The particle morphology and the Mg and Si composition are similar to those of fibrous anthophyllite. To increase the accuracy of this technique, the spacings perpendicular to the 5.3-Å spacing should be determined. Assuming that most fibrous talc grains would lie on the 00ℓ face as they were in this study, the 18-Å b spacing of amphiboles would be distinguishable from the 9-Å b spacing in talc. On grains without this orientation, the more thorough quantitative ED technique would be required. An accurate assessment of whether fibrous talc should be suspected to be present in the sample prior to TEM analysis could be accomplished by determining the mineralogy through PLM and XRD.

CONCLUSIONS

The fibrous talc sample contained talc, anthophyllite, tremolite, quartz, and carbonate. Anthophyllite is present only within the fibrous talc grains. The intermixing of the talc and anthophyllite on a submicroscopic scale and the crystallographic relationship between the talc and anthophyllite crystal lattices suggest an alteration mechanism similar to that observed in the formation of some biopyriboles. Tremolite, however, was observed as a physically distinct nonfibrous amphibole phase, and little, if any, was present within the fibrous talc grains. The fibrous morphology, the lattice relationships in the talc-anthophyllite intergrowths, and the dominant (100) orientation of the amphibole lattice are suggested to result from alteration of fibrous or asbestiform anthophyllite. The possible presence of fibrous talc in samples containing fibrous amphiboles suggests that phase contrast microscopy and qualitative TEM techniques alone may be inappropriate for the regulation of amphibole asbestos in talcs. These techniques would not positively distinguish between amphiboles and fibrous talc because of the characteristics of the fibrous talc resulting from the alteration of fibrous amphiboles.

REFERENCES

1. Barr, T. A Structural Study of Talc From Governeur, New York, Univ. MD Senior Geology Thesis, May 1, 1978, 20 pp.

2. Bateman, A. M. Economic Mineral Deposits. Wiley, 2d ed., 1965, 916 pp.

3. Bates, R. L. Geology of the Industrial Rocks and Minerals. Dover, 1969, 459 pp.

4 Brown, D. P., J. M. Dement, and J. K. Wagoner. Mortality Patterns Among Miners and Millers Occupationally

Exposed to Asbestiform Talc. Paper in Dusts and Disease (Proc. Conf. on Occupational Exposure to Fibrous and Particulate Dusts and Their Extension Into the Environment, Washington, DC, Dec. 4-7, 1977), ed. by R. Lemen and J. M. Dement. Pathotox Pub., Inc. Park Forest South, IL, 1979, pp. 317-324.

5. Brown, J. S., and A. E. J. Engel. Revision of Grenville Stratigraphy and Structure in the Balmat-Edwards District, N. W. Adirondacks, NY. Bull. Geol. Soc. America, v. 67, 1956, pp. 1599-1622.

6. Chatfield, E. J. Measurement of Asbestos Fibre Concentrations in Ambient Atmospheres. Ontario Research Foundation, Ontario, Canada, May 1983, 115 pp.

7. Deer, W. A., R. A. Howie, and J. Zussman. Rock Forming Minerals. Wiley, v. 2, 1963, 379 pp.

8. Engel, A. E. The Talc Deposits of the Gouverneur District, New York. Econ. Geol., v. 42, 1947, p. 419.

9. Gamble, J., W. Feliner, and M. J. DiMeno. Respiratory Morbidity Among Miners and Millers of Asbestiform Talc. Paper in Dusts and Disease (Proc. Conf. on Occupational Exposure to Fibrous and Particulate Dusts and Their Extention Into the Environment, Washington, DC, Dec. 4-7, 1977), ed. by R. Lemen and J. M. Dement. Pathotox Pub., Inc., Park Forest South, IL, 1979, pp. 307-316.

10. Henry, N. F. M., and K. Linsdale (eds.). International Tables for X-ray Crystallography, v. I. International Union of Crystallography, Kynoch Press, Birmingham, England, 1952, 558 pp.

11. Hren, J. J., J. I. Goldstein, and D. C. Joy. Introduction to Analytical Electron Microscopy. Plenum, 1979, 601 pp.

12. Hutchison, J., and E. J. W. Whittaker. The Nature of Electron Diffraction Patterns of Amphibole Asbestos and Their Use in Identification, Environ. Res., v. 20, 1979, pp. 445-449.

13. Jansen, M. L., and A. M. Bateman. Economic Mineral Deposits. Wiley, 3d ed., 1979, 593 pp.

14. Kleinfeld, M., J. Messite, O. Kooyman, and M. H. Zaki. Mortality Among Talc Miners and Millers in New York State. Arch. Environ. Health, v. 14, 1967, p. 663.

15. Kleinfeld, M., J. Messite, and M. H. Zaki. Mortality Experiences Among Talc Workers! A Follow-up Study. J. Occup. Med., v. 16, 1974, p. 16.

16. Krause, J. B., and W. H. Aston. Misidentification of Asbestos in Talc. Paper in Proceedings, Workshop on Asbestos: Definitions and Measurement Methods, NBS, Gaithersburg, MD, July 18-20, 1977, ed. by C. C. Gravatt, P. D. LaFleur, and K. F. J. Heinrich. NBS Spec. Pub. 506, 1978, pp. 339-354.

17. Lee, R. J., J. S. Lally, and R. M. Fisher. Identification and Counting of Mineral Fragments. Paper in Proceedings, Workshop on Asbestos: Definitions and Measurement Methods, NBS, Gaithersburg, MD, July 18-20, 1977, ed. by C. C. Gravatt, P. D. LaFleur, and K. F. J. Heinrich. NBS Spec. Pub. 506, 1978, pp. 387-402.

18. Leidel, N. A., S. G. Bayer, R. D. Zumwalde, and K. A. Busch. USPHS/NIOSH Membrane Filter Method For Evaluating Airborne Asbestos Fibers. NIOSH Tech. Rept. 79-127, 1979, 89 pp.

19. Ross, M., W. Smith, and W. Ashton. Triclinic Talc and Associated Amphiboles From Gouverneur Mining District, N.Y. Am. Mineral., v. 53, 1968, pp. 751-769.

20. Samudra, A. V., C. F. Harwood, and J. D. Stockham. Electron Microscope Measurement of Airborne Asbestos Concentrations. U.S. EPA, EPA-600/2-77-178, 1978, 47 pp.

21. Selikoff, L. J., and E. C. Hammon (eds.). Health Hazards of Asbestos Exposure, Ann. NY Acad. Sci., v. 330, 1979, 814 pp.

22. Stemple, I. S., and G. W. Brindley. A Structural Study of Talc and Talc Tremolite Relations. J. Am. Ceramic Soc., v. 43, No. 1, Jan. 1960, pp. 35-42.

23. Veblen, D. R. Anthophyllite Asbestos: Microstructures, Intergrown Sheet Silicates, and Mechanisms of Fiber Formation. Am. Mineral., v. 65, 1980, pp. 1075-1086.

24. Veblen, D. R., and P. B. Buseck. Microstructures and Reaction Mechanisms in Biopyriboles. Am. Mineral., v. 65, 1980, pp. 599-623.

25. _____. Hydrous Pyriboles and Sheet Silicates in Pyroxenes and Uralites: Intergrowth Microstructures and Reaction Mechanisms. Am. Mineral., v. 66, 1981, pp. 1107-1134.

26. Warren, B. E. Structure of Tremolite. Z. Krist., v. 72, 1927, pp. 42-57.

27. Wright, H. D. An Optical Study of Talc-Tremolite Relations. J. Am. Ceram. Soc., v. 43, No. 1, Jan. 1960, pp. 42-43.

☆U.S. GPO: 1985-505-019/5090

INT.-BU.OF MINES,PGH.,PA 27858

Two Submissions to the National Toxicology Program on the

Mineralogy and Experimental Animal Studies of Tremolitic Talc

GL Nord PhD, CW Axten PhD CIH, RP Nolan PhD

An Evaluation of the Epidemiological Evidence Concerning "Talc" and Respiratory Cancer In Humans with Specific Attention to "Talc" as Produced by the Gouverneur Talc Company at its Mines in New York State and Factors to Consider in Evaluating Causation

GW Gibbs, MScPhD, LRSc, PhD

December 1, 2000

Environmental Sciences Laboratory
Brooklyn College, The City University of New York
2900 Bedford Avenue
Brooklyn, NY 11210-2889

Executive Summary

The nomenclature of asbestiform talc is not specific enough to define a class of carcinogens. The proper nomenclature should be fibrous talc and transitionals. Microscopic analyses indicate the fibrous particulates in talc are not surrogates for asbestos. This fact is further substantiated by the results of several animal studies which indicate significant differences in that fibrous talc and transitionals lack the carcinogenic potency of asbestos fibers. As such, fibrous talc and transitionals do not meet the criteria for inclusion in the NTP Report on Carcinogens and should be removed from further consideration.

Introduction

The nomenclature of asbestiform talc is not specific enough to define a class of carcinogens. An understanding of the mineralogy of tremolitic talc is required to evaluate whether this assemblage of minerals can cause cancer in humans or experimental animals. This is particularly important if you wish to justify the assumption that talc is a surrogate for asbestos as was done in the Report on Carcinogens (ROC Report) Background Document for Talc Asbestiform and Non-Asbestiform. The ROC document reviews the medical and scientific literature and offers a premise for concluding that "talc asbestiform" materials are either "known to be a human carcinogen" or "reasonably anticipated to be a human carcinogen". (Summary of Review Group 1 & 2, ROC, 2000). The two review groups are of differing opinion concerning the evaluation of the information within the background report. Although the summaries are remarkably similar, no explanation for the difference in evaluation is offered, we are of the opinion that neither review group's claim is justified on the basis of the available information for tremolitic talc. Furthermore, the assumption that asbestiform talc is a surrogate for asbestos has not been justified in the ROC document and we will show that such an assumption is not scientifically justifiable.

The medical and scientific literature that the ROC used to describe "talc asbestiform" largely refers to tremolitic talc. This complex assemblage of minerals contains three phases (three different minerals), which can occur as asbestos minerals and two additional minerals that can occur in fibrous form. The ROC relies on relating these

phases to the carcinogenic risks associated with the commercial asbestos minerals to strengthen their case that asbestiform talc is a human and animal carcinogen. We will describe the tremolitic talc mineral assemblage and show that this extrapolation to asbestos is not justified. Examples from experimental animal studies will be used to emphasize the relevance of the mineralogy to carcinogenic risk.

Mineralogy of Tremolitic Talc

New York State tremolitic talc is an assemblage of five principal minerals, which can vary in abundance and particle size to form the various commercial grades (Table 1). Specific grades have properties useful in the fabrication of various products including ceramics and paints. Each grade contains three phases - anthophyllite, tremolite and serpentine – which can exist as asbestos or non-asbestos minerals but asbestos is not typically found in talc (Table 2). The two-amphibole minerals occur more commonly in nature in a nonasbestos habit, although each can occur as asbestos. Commercial deposits of these asbestos minerals have been rare and small and together they represent the least important of the commercial asbestos minerals (Ross, in press). The serpentine asbestos mineral is chrysotile – another serpentine mineral is antigorite, a platy particle. In addition, tremolitic talc can contain two fibrous particulates – fibrous talc sometimes referred to as agalite and an intergrowth of talc and anthophyllite referred to as an intermediate or transitional.

Each of the phases that can occur either as asbestos mineral or as a fibrous particulate was examined and characterized using polarized light microscopy, continuous scan x-ray diffraction and analytical transmission electron microscopy. A variety of tremolitic talc samples and reference standards were used for comparison. NYTAL400, a fine particle size grade of tremolitic talc, which is rich in fibrous particulates, was selected for analysis. Reference standards of the following minerals were selected for comparison:

- NYTAL 400 obtained from Gouverneur Talc Company, Inc., 1837 State Highway 812, Gouverneur, NY 13642.
- Tremolite Asbestos, Korea obtained from John Addison, Cottingham, Hull, United Kingdom.
- Tremolite Nonasbestos Respirable (NTP Animal) obtained from RT Vanderbilt, Inc., 30 Winfield Street, P.O. Box 5150, Norwalk, Ct 06856-5150.
- High Fiber Concentrate obtained from RT Vanderbilt, Inc., 30 Winfield Street, P.O. Box 5150, Norwalk, Ct 06856-5150.
- Anthophyllite Asbestos, UICC, Paakkila, Finland.
- Anthophyllite Asbestos, Anglo Dutch, Republic of South Africa, obtained from Prof DR Bowes.
- Anthophyllite Asbestos, Svedlovsk Region, Russian Federation.

Tremolite

Examination by TEM shows that tremolite particles in the NYTAL 400 tremolitic talc sample range from 20 micrometers to 5 micrometers in length and 1 to 4 micrometers in width with aspect ratios of 6 to 4. The sides of the particles are generally rough and not parallel with irregular to squared off terminations. The width is similar to the thickness indicating the particles are prismatic in shape. The particles are usually too thick to be electron transparent even at 200 keV accelerating voltages. Bright-field images (Figure 1) show the particles to be featureless in areas that were electron transparent.

Selected area electron diffraction patterns of tremolite particles (Figure 2) showed no evidence of disorder or the presence of additional phases or alteration. By tilting on the c-axis open planar fractures can be seen parallel to the c-axis (Figure 3). Selected area electron patterns indicate the open fractures are the {110} cleavage planes.

Fibrous Talc and Transitionals

Examination by TEM shows that fibrous talc particles in the NYTAL 400 tremolitic talc. Fibrous talc is identified in the image by its curved edges, bent and twisted shapes and frayed ends as in flax. It ranges from very thin ribbons with high aspect ratios (Figure 4) to equidimensional mats (Figure 5). Fibrous talc intergrown with anthophyllite appears as relatively straight lath-shaped particulates – commonly with small curved portions of talc-rich material separating from the larger particle at the

sides and ends. In bright-field images long linear features run along the length of the particles (Figure 6). These features are due to diffraction contrast from a talc and anthophyllite intergrowth, these fibrous particulates are the transitional.

Transitionals arise from the alteration of anthophyllite to talc; they are part anthophyllite and part talc intimately intergrown. The compositions of both phases are almost identical so that only an excess of OH^- is needed for the alteration, which easily migrates through the structure. The crystal structures of both phases also are similar so that there is an orientation relationship maintained between anthophyllite and talc. This relationship can be seen in [100] electron diffraction patterns of the transitionals where diffraction from both phases is present (Figure 7). The [100] zone shows layer lines with $l = 3n$ that are intense relative to those with $l \neq 3n$. The addition of the second phase, talc, with its characteristic psuedohexagonal [001] zone axis pattern results in diffraction spot triplets in the $l = 3n$ layer lines. These triplets are characteristic of anthophyllite and talc intergrowths, transitionals, with an interface parallel to (010).

Platy Talc

Talc is a sheet silicate and when growing freely naturally grows fastest parallel to the plane of the sheet as platelets. Sliding between the sheets gives talc its characteristic low hardness and lubricating properties. In the NYTAL 400 talc also occurs as platelets, generally less than 5 micrometers in diameter (Figure 8). A hexagonal arrangement of spots is characteristic of the diffraction pattern (Figure 9).

Serpentine

Serpentine occurs as a platy mineral identified mainly by the high Mg/Si ratio in energy dispersive spectroscopy (EDS) patterns (theoretically 1.5). The serpentine phase is antigorite or lizardite, most likely antigorite, both have a platy habit. No rolled tubes indicative of the chrysotile serpentine mineral (the asbestos variety) were observed.

Anthophyllite

Anthophyllite in the NYTAL 400 sample occurs as tabular crystals similar to popsicle sticks with the large flat face indexed as (100) (Figure 10). The length of the particle is parallel to the c-axis, the width is parallel to the b-axis and the thickness is parallel to the a-axis. This are the same common crystal faces expected in hand-specimen sized anthophyllite crystals. The particles are invariably thin and in most cases electron transparent from one side to the other. Electron diffraction patterns contain no extra spots due to talc alteration (Figure 11 – compare with Figure 7).

The longest particle measured on the sample grid had a length of 200 micrometers and a width of 3 micrometers for an aspect ratio of 67. Aspect ratios of other anthophyllite particles were smaller, ranging down to 2. The width of the smaller particles appeared to be constant at about 2 to 3 micrometers indicating the smaller aspect ratio particles were fragments of larger ones.

The terminations of the anthophyllite particles are generally right angles. Small amounts of alteration material adhering to the terminations indicate the particles break along planes of alteration parallel to (001). Long particles also split along (010) again along bands of alteration. These are seen in images as bands of material that have different diffraction contrast conditions than the adjacent anthophyllite.

Quartz

Quartz in the NYTAL 400 sample occurs as rare irregular shaped featureless particles generally several micrometers in diameter. These were identified by EDS spectra with only Si and O present.

Tremolitic Talc and Experimental Animal Studies

The tremolite present in tremolitic talc are cleavage fragments and should not be referred to as asbestos or asbestiform (Langer et al 1991). Smith et al 1979 evaluated the carcinogenic activity of tremolitic talc, tremolite non-asbestos and tremolite asbestos by intrapleural injections in hamsters. Only tremolite asbestos produced tumors (Table 3, Figure 12) and this is not present in tremolitic talc. The phases present in the tremolitic talc used by Smith et al 1979 were similar to Table 1 in this report with tremolite non-asbestos, talc fibers, talc plates and transitionals (Smith, 1974).

More recently, Davis et al 1991 evaluated six tremolite samples in rats by intraperitoneal injection (see Nolan et al 1991 for a review). Each tremolite sample was prepared as a respirable size range sample. The three-asbestos/asbestiform tremolites produced mesotheliomas in almost all animals. Davis et al 1991 goes on to conclude:

> Two samples of non-fibrous tremolite produced respirable dust samples containing numerous elongated fragments with aspect ratios greater than 3:1, which therefore fitted the definition of respirable fibers. Both these samples produced relatively few tumors, although one had more long "fibers" than did the brittle tremolite that produced 70% tumors. This study has therefore demonstrated that different morphologic forms of tremolite produce dusts with very different carcinogenic potential (p. 489).

Therefore, fibrous morphology alone does not define whether a mineral is carcinogenic or not (Nolan et al, 1991). Stanton et al 1981 reported on 72 experiments relating an index of fiber morphology to carcinogencity. Although the fiber morphology produced some correlation with carcinogenicity it was not without exceptions. For example, two tremolite asbestos samples containing fewer long thin fibers than a fibrous talc sample produced tumor probability of 100% while the fibrous talc produced no tumors (Table 4) (Nolan and Langer, 1993 for a review). Two other platy talc samples tested by Stanton et al 1981 also did not produce

tumors while four other platy talcs produced 1 tumor each corresponding to a tumor probability of 7% or less. The two tremolite asbestos samples which caused tumors are not found in tremolitic talc while fibrous talc which did not produce tumors would be found in tremolitic talc.

Again, there was no increase in the number of tumors in this location, although this procedure appears to have a similar sensitivity as the intraperitoneal injection technique.

The primary animal data set used to classify non-asbestiform talc as an animal carcinogen is the inhalation study conducted by the NTP (NTP 1993). This appears to be a well-conducted and reported study of non-asbestiform talc in rats and mice. The exposure levels (6 and 18 mg/m3) correlate well with the lung burdens in rats although the data for mice are not shown. The concentration of talc in the lungs of the rats increases linearly with dose and time, until 18 months. The evidence for carcinogenic activity is confined to the rat, e.g. the mouse studies were negative. In the rat a significant increase in lung tumors was observed in females, but not males, at 18mg/m3 but not at 6 mg/m3.

However, pheochromocytomas (tumors comprised of chromaffin cells of the adrenal medulla) were increased in both males and females at both exposures. This type of tumor in rats has little relevance to humans because it is related to an epigenetic mechanism as a result of chronic stress related to pulmonary pathology (Tishler et

al., 1988, 1994, 1996, 1999). Chromaffin cell proliferation appears to be under the control of neural signals, which explains tumor formation with the anti-hypertensive drug reserpine (Sietzen et al., 1987). Proof of this mode of action has been offered by Tishler et al. (1994), who showed that chromaffin cell proliferation induced by reserpine could be abolished by adrenal denervation. Pheochromocytomas in rats have also been induced in rats by common food components, e.g. vitamin D, lactose (milk sugar) and xylitol probably as a result of altered calcium homeostasis (Tishler et al., 1999).

Because this type of tumor is such a nonspecific effect and not related to non-asbestiform talc *per se*, it would be interesting to determine how the animal exposures (8 and 16 mg/m3) compare with those encountered by humans. Such information could then be used for margin of exposure analyses, especially since talc is not genotoxic (see below).

Hamsters have also been exposed by inhalation to nonasbestiform talc (talc baby powder) (Wehner et al., 1979). Again, no treatment related tumors were observed, but the study was of too short a duration to make a definitive statement about carcinogenicity.

There was one subcutaneous injection study of talc in mice. No tumors were observed. This is an important study because many solid materials, both fibrous

and nonfibrous particulates cause tumors using this technique and not finding any neoplasms is biologically significant.

The NTP report mentions two intraperitoneal injection studies of non-asbestiform talc in rats, both of which were negative for tumor induction. These are in addition to the negative studies reported earlier for tremolitic talc and some of the various mineral phases of tremolitic talc in rats and hamsters. These are particularly significant result because this technique (route of exposure) is highly sensitive to the induction of tumors (typically mesotheliomas), particularly with fibrous particulates, both naturally occurring and synthetic. In fact, many researchers feel that this technique is overly sensitive and that positive results may not indicate that the mineral phase has a carcinogenic potential for humans. On the other hand, a negative result should be viewed as meaning that it has minimal or no carcinogenic potential. In addition, it needs to be remembered that this technique results in a large and direct exposure to the ovary and surrounding tissues. If talc can cause tumors in this organ, it seems reasonable to expect that tumors would have been found in this exaggerated exposure condition. The negative results of these studies are buttressed by a study in rats where non-asbestiform talc was injected directly into the ovary with no tumor formation (Hamilton et al., 1984).

There was one intrathoracic injection study in mice, which showed a non-significant increase in lymphoid tumors (3/47), and adenocarcinomas (2/47) compared to 0/48 in the concurrent controls. The lymphoid tumors are not biologically significant

because they are not found with other types of fibrous and nonfibrous particulates, including asbestos. The adenocarcinomas are also an unusual response; the typical response is induction of mesotheliomas, none of which were observed.

While the ROC background document attempts to provide a definitive argument for classifying talc as carcinogenic in humans, the summary is not complete in its survey of the medical and scientific literature. For example, the most recent reference in Table 4-6 is 1977. There have been several informative and relevant inhalation studies of fibrous particulates including asbestos in the last 23 years that are not included. The studies undertaken and reported since 1977 represent the state-of-the-art for the inhalation studies of synthetic vitreous fibers in rats and hamsters where different types of asbestos were used as a positive control. If these well-known studies are missing, has other data also been omitted? Furthermore the NTP did not even mention its' own ingestion studies in rats and hamsters of several types of asbestos and non-asbestos tremolite. Finally, why are the talc studies conducted by Stanton using intrapleural instillation and those of Pott using intraperitoneal injection, both of which were negative for tumors, not included in the Table? The review of the medical and scientific literature needs to be re-reviewed and brought up-to-date.

Probably the least justifiable assumption in the ROC background report is the claim that asbestos is a "surrogate for talc". No mineralogical or biological basis has been offered for this assumption. Our review of the medical and scientific literature

indicates the tremolitic talc contains a class of minerals, which are sufficiently different to be considered as a separate and distinct class of minerals from asbestos (see above). It appears that the NTP relies on asbestos-related experimental animal studies to support its claim that talc is carcinogenic in animals because the data specific to asbestiform and non-asbestiform itself is so weak. The weakness of the data may simply reflect that lack of carcinogenic potential in the talc (asbestiform and non-asbestiform) which the ROC report is recommending as either known or probably a human carcinogen.

Genotoxicity

Determining the genotoxicity for particulates and fibers is always problematic because most fibers are relatively insoluble and therefore do not have the same potential to interact with DNA as chemicals. However, it is clear from the data that asbestiform and non-asbestiform talc has not been shown to be genotoxic or clastogenic either *in vitro* or *in vivo*. In contrast, asbestos has been shown to be clastogenic in several types of *in vitro* systems and some *in vivo* ones. The problem is that while the ROC background report states that talc, with or without asbestiform fibers, is not genotoxic, asbestos is and by inference, talc should also be considered positive, in spite of the evidence to the contrary. This is another weakness in the talc as a surrogate for asbestos argument.

Other Relevant Data

The discussion, in this particularly important part of the document, on deposition, clearance and retention is less than thorough. For example, there is no mention of the possibility of dissolution within the body, aspects of surface chemistry or the biological differences between asbestiform and non-asbestiform talc. The report seems to make the argument that because talc particles are found in the lungs and lavage samples from individuals many years after exposure, this means that a potential carcinogenic response is possible. This is a particularly weak argument. For example, using this argument, a coal-miner would be expected to show cancer because coal particles are found in his/her lung or sputum. Well-conducted studies of miners have shown no evidence of coal-related lung cancer, even in the presence of severe pneumoconiosis and high lung burdens. The ROC background report lacks a scientific balance and a modern approach.

Similarly, the document seems to suggest that because talc particulates have been found in ovarian tissues, in both cancerous and normal ovaries, that this indicates cause/effect. At best this is an observation and only of limited value in establishing etiology. One would have to examine ovarian tissue from a large number of individuals, exposed and non-exposed, to make this claim for an etiological role for talc in ovarian cancer. In fact, such a study has been done, and there was no correlation (Heller et al., 1996a, b see ROC Report for reference).

As another example, it is commonly known that asbestos bodies can be found in the lung and lymph nodes of most individuals living in urban environments, there is no evidence to show that such individuals are at an increased risk for asbestos-related cancer, nor do many researches believe these are meaningful risk factors. The most persuasive evidence that talc is not a significant hazard to the ovary is the intraperitoneal injection and intra-ovarian injection studies of huge amounts of talc in rodents. If talc were carcinogenic in this tissue, surely one or more of these studies would have shown a positive result. The ROC background report should be revised to reflect the importance of these animal studies and improve the scientific balance of the report.

Very importantly, in discussing the possible mechanisms of talc toxicity (6.2.2), there are a number of significant reports in medical and scientific literature showing inflammation and resulting production of cytokines and growth factors are important in the mechanism of particulate induced cancer. However, the preeminent investigators in this field, e.g. Driscoll, Kane, Oberdorster, Mossman, etc. are not referenced or their work considered in the document. The ROC report is weak on a state-of-the-art review of mechanisms of fibrous and non-fibrous particulate induced cancer.

Summary

In summary, the document fails to make a case that talc, either asbestiform or non-asbestiform, meets the criteria for inclusion in the NTP Report on Carcinogens. The standard for inclusion of a material into the NTP Report on Carcinogens should be a clearly supported by sound science and judgment establishing the material as a carcinogen. To "list" talc on the basis that asbestos is a "surrogate for talc" is without mineralogical or biological merit and should be rejected.

To the extent that the ROC document relies on asbestos to justify the claim that tremolitic talc is carcinogenic the NTP needs to reconsider their approach. The logic, used within the ROC document, contains conflicts in that the six commercial asbestos minerals are well defined and regulated by OSHA and other regulatory agencies. Such minerals are not exempt from the standard because they occur in association with talc, anymore than they would be exempt because they are used to fabricate a building material. To the extent that commercial asbestos minerals occur in association with talc, exposure would carry the same cancer risk. If the ROC wishes to go beyond simply classifying asbestos as a carcinogen and define other mineral phases present in tremolitic talc as carcinogens they should define the phases that they claiming are carcinogenic – not rely on claims of similarity to asbestos – and produce convincing evidence of carcinogenic effects in human and experimental animals.

References

Davis JMG, Addison J, McIntosh C, Miller BG & Niven K (1991) Variations in the carcinogenicity of tremolite dust samples of differing morphology. ANYAS 643: 473-490.

Hamilton TC, Fox H, Buckley CH, Henderson WJ & Griffiths K (1984) Effect of talc on the rat ovary. Br J Exp Path **65:** 101-106.

IARC (1987) Talc In: Silica and some silicates (42), IARC Monograph on the Evaluation of Carcinogenic Risk to Humans, International Agency for Research on Cancer, Lyon, France, pp. 185-224.

Langer AM, Nolan RP & Addison J (1991) Distinguishing between amphibole asbestos fibers and elongate cleavage fragments of their non-asbestos analogues. In: NATO Advanced Research Workshop on Mechanisms in Fibre Carcinogenesis. R.C. Brown, J. Hoskins, N. Johnson, (eds), Albuquerque, New Mexico, October 22-25, 1990. pp. 253-267.

Nolan RP, Langer AM, Oechsle GW, Addison J & Colflesh DE (1991) Association of tremolite habit with biological potential. In: NATO Advanced Research Workshop on Mechanisms in Fibre Carcinogenesis. RC. Brown, J. Hoskins, N. Johnson, (eds), Albuquerque, New Mexico, October 22-25, 1990. pp. 231-251.

Nolan RP & Langer AM (1993) Limitations of the Stanton Hypothesis. In: Health Effects of Mineral Dusts. (Eds) Guthrie GD, Mossman BT. Reviews in Mineralogy **28:** 310-328.

NTP, 1993. Toxicology and Carcinogenesis Studies of Talc (CAS N° 14807-96-6)(Non-Asbestiform) in F344/N Rats and B6C3F1 Mice (Inhalation Studies). TR-421, National Toxicology Program, Research Triangle Park, NC.

Ross M, Virta RL (2000) Occurrence, Production and Uses of Asbestos In: The Health Effects of Chrysotile Asbestos: Contribution of Science to Risk Management Decisions (RP Nolan, AM Langer, M Ross, F Wick, RF Martin, eds) Canadian Mineralogist Special Publication.

Sietzen M, Schober M, Fischer-Colbrie R, Scherman D, Sperk G & Winkler H (1987) Rat adrenal medulla: levels of chromogranins, enkephalins, dopamine beta-hydroxylase and of the amine transporter are changed by nervous activity and hypophysectomy. Neuroscience **22:** 131-139.

Smith WE (1974) Experimental studies on biological effects of tremolite talc on hamsters In: Proceedings of the Symposium on Talc. Washington, DC, Information Circular 8639. US Bureau of Mines, pp. 43-44.

Smith WE, Hubert DD, Sobel HJ & Marquet E (1979) Biological tests of tremolite in hamsters In: Dust and Disease. (Eds.) Lemen RA, Dement J, Pathotox Publishers, Illinois, pp. 335-339.

Stanton MF, Layard M, Tegeris A, Miller E, May M, Morgan E & Smith A (1981) Relationship of particle dimensions to carcinogencity of amphibole asbestoses and other fibrous minerals. J Nat'l Cancer Inst **67:** 965-975.

Tishler AS and DeLellis RA (1988) The rat adrenal medulla. II. Proliferative lesions. J. Amer. Coll. Toxicol., 7:23-44.

Tishler AS and Coupland RE (1994) Changes in structure and function of the adrenal medulla. In, Pathobiology of the Aging Rat, Vol 2. eds. Mohr, U., Dungworth, D.L., Capen, C.C., ILSI Press, Washington, DC, pp245-268.

Tishler AS (1996) Cell proliferation in the adult adrenal medulla: In, Endocrine System, 2nd Edition, ILSI Monographs on the Pathology of Laboratory Animals, eds., Jones, T.C., Capen, C.C. Mohr, U., Springer-Verlag, Berlin, Heidelberg, NY, pp. 405-411.

Tishler AS (1999) The effect of therapeutic drugs and other pharmacological agents on activity of porphobilinogen deaminase, the enzyme that is deficient intermittent acute porphyria. Life Sci **65:** 207-214.

Tishler AS, Powers JF, Pignatello M, Tsokas P, Downing JC and McClain (1999) Vitamin D3-induced proliferative lesions in the rat adrenal medulla. Toxicol. Sci. 51:9-18.

Wehner AP, Stuart BO & Sanders CL (1979) Inhalation of talc baby powder by hamsters. Food Cosmet Toxicol **15:** 121-129.

Figure 1: Tremolite particle, 6 μm by 1 μm. (Plate 727)

Figure 2: [100] Zone Axis, Selected Area Electron Diffraction Pattern (Plate 724)

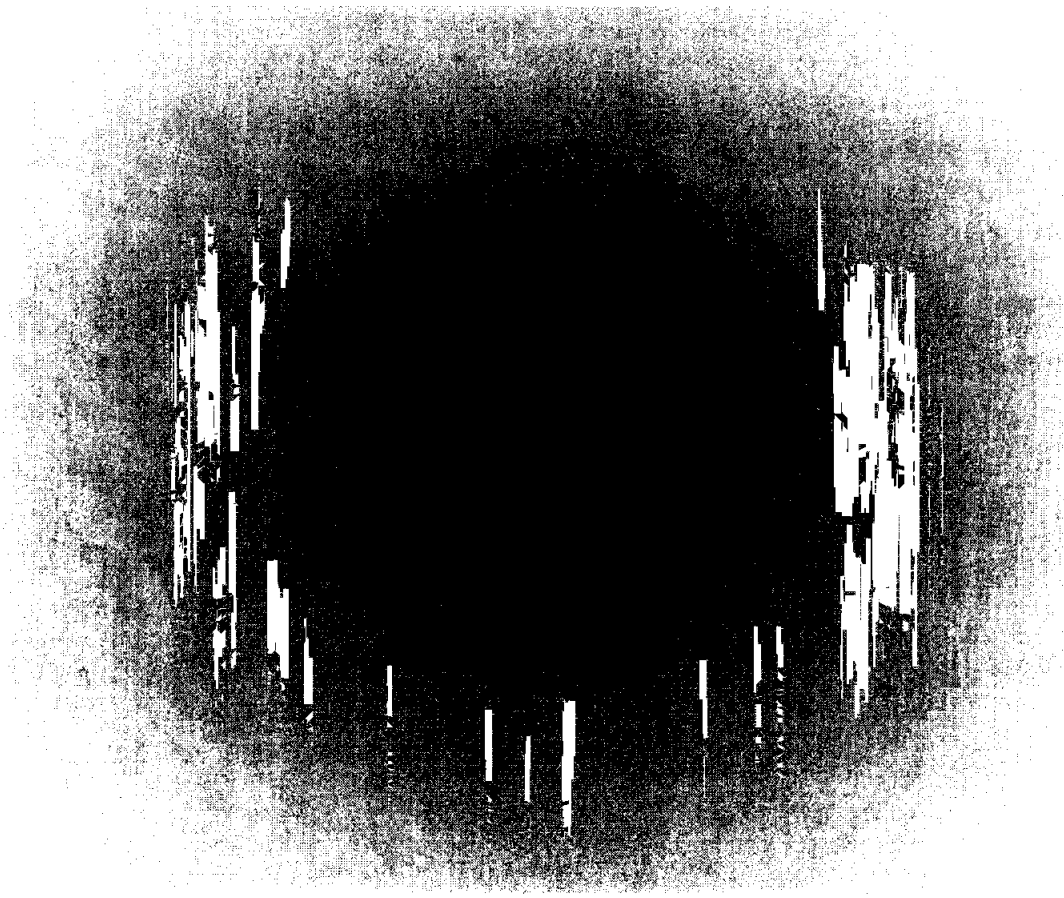

Figure 3: Open Fractures parallel to the c-axis are {110} cleavage planes (Plate 729)

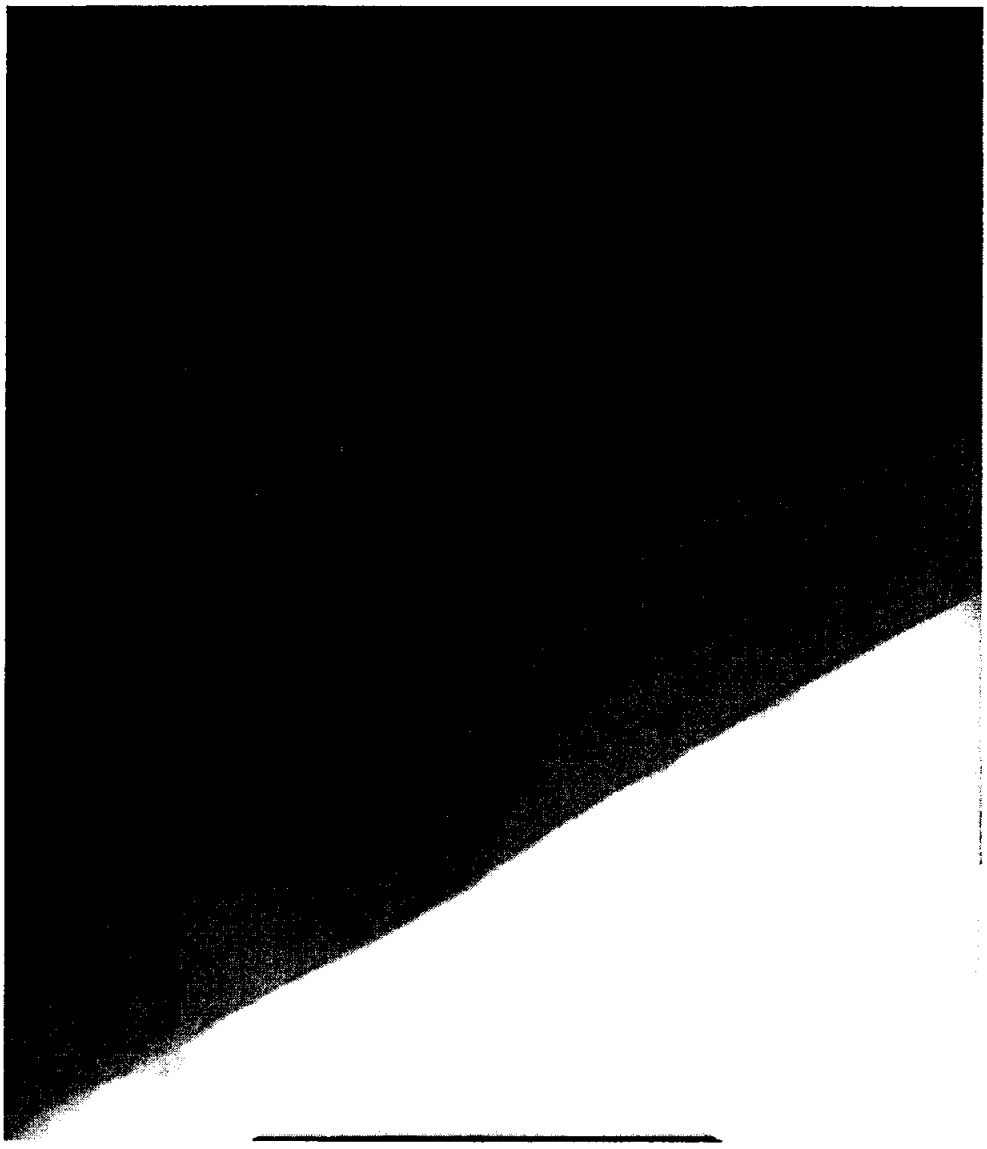

Figure 4: Curved fibrous talc particle with high aspect ratio. (Plate 730)

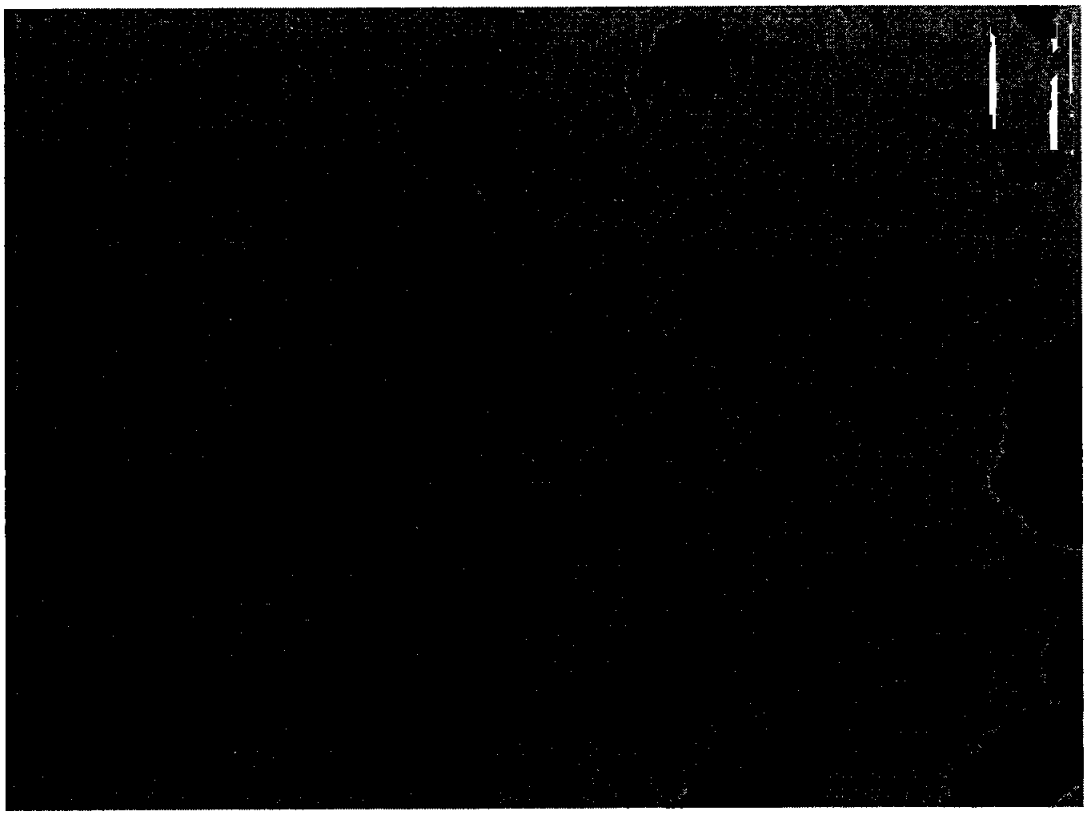

Figure 5: Fibrous talc particle (Plate 531)

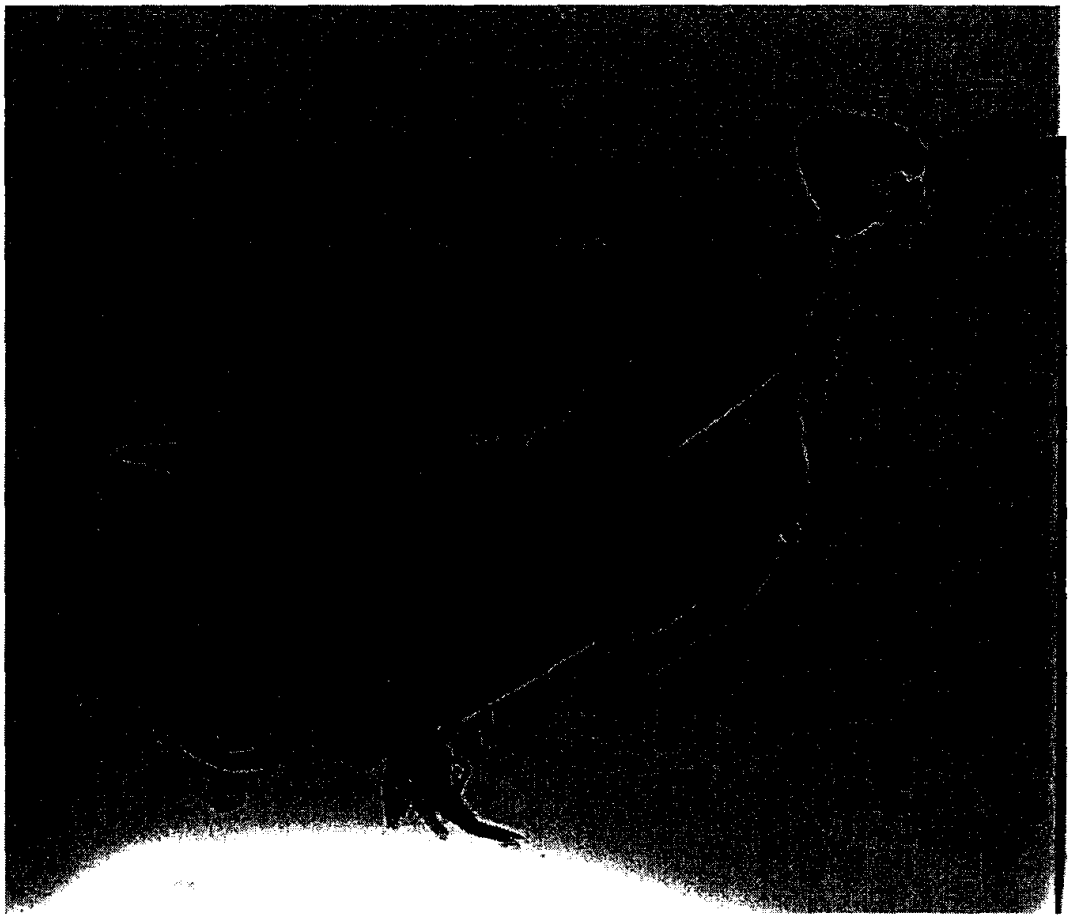

Figure 6: "Transitional" showing linear features from the intergrowth. (Plate 686)

Figure 7: [001] Zone Axis showing both anthophyllite and talc spots in "Transitional" particle. (Plate 562)

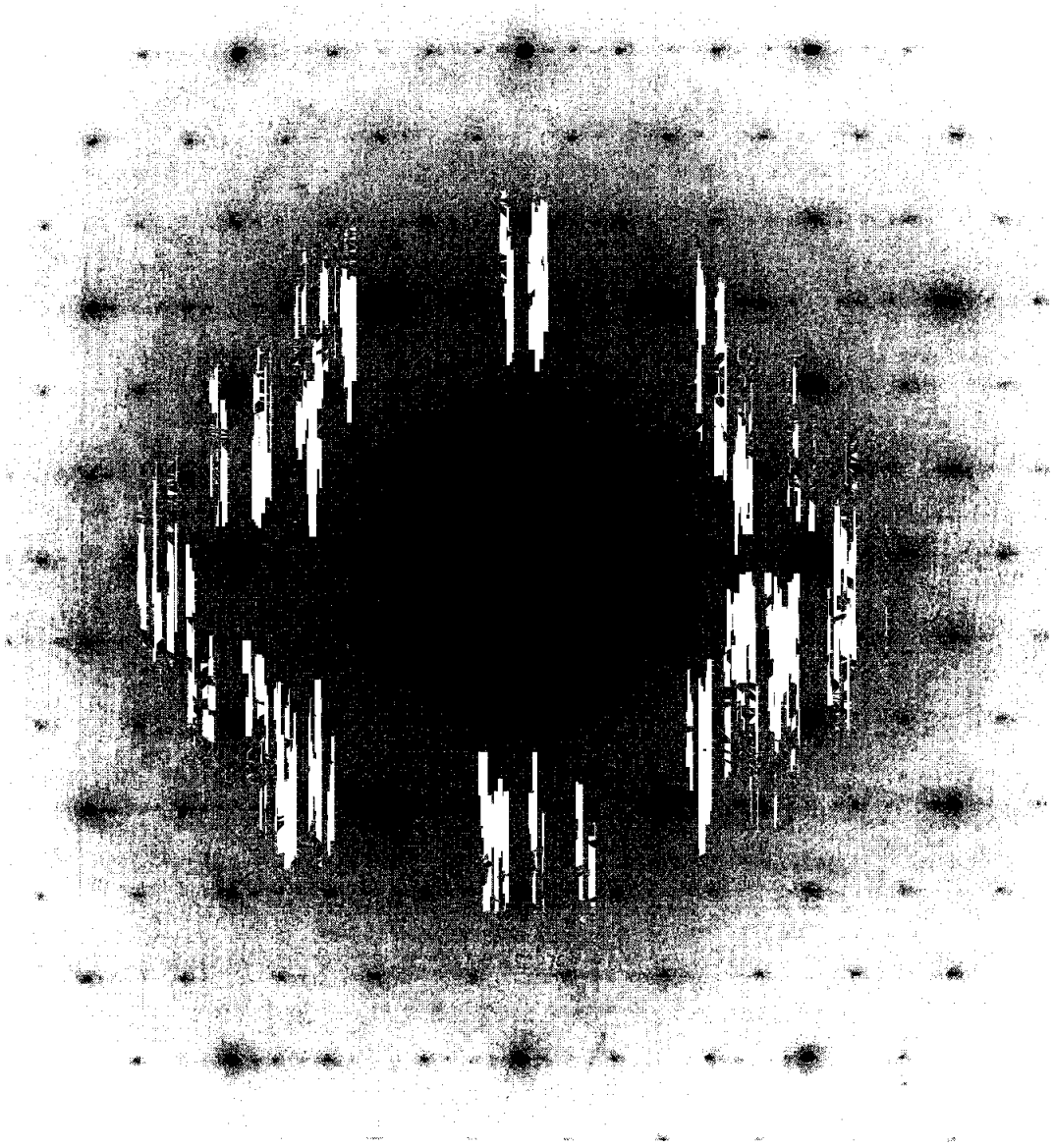

Figure 8: Talc Plate (Plate 706)

Figure 9: [001] Zone Axis from Talc Plate (Plate 707)

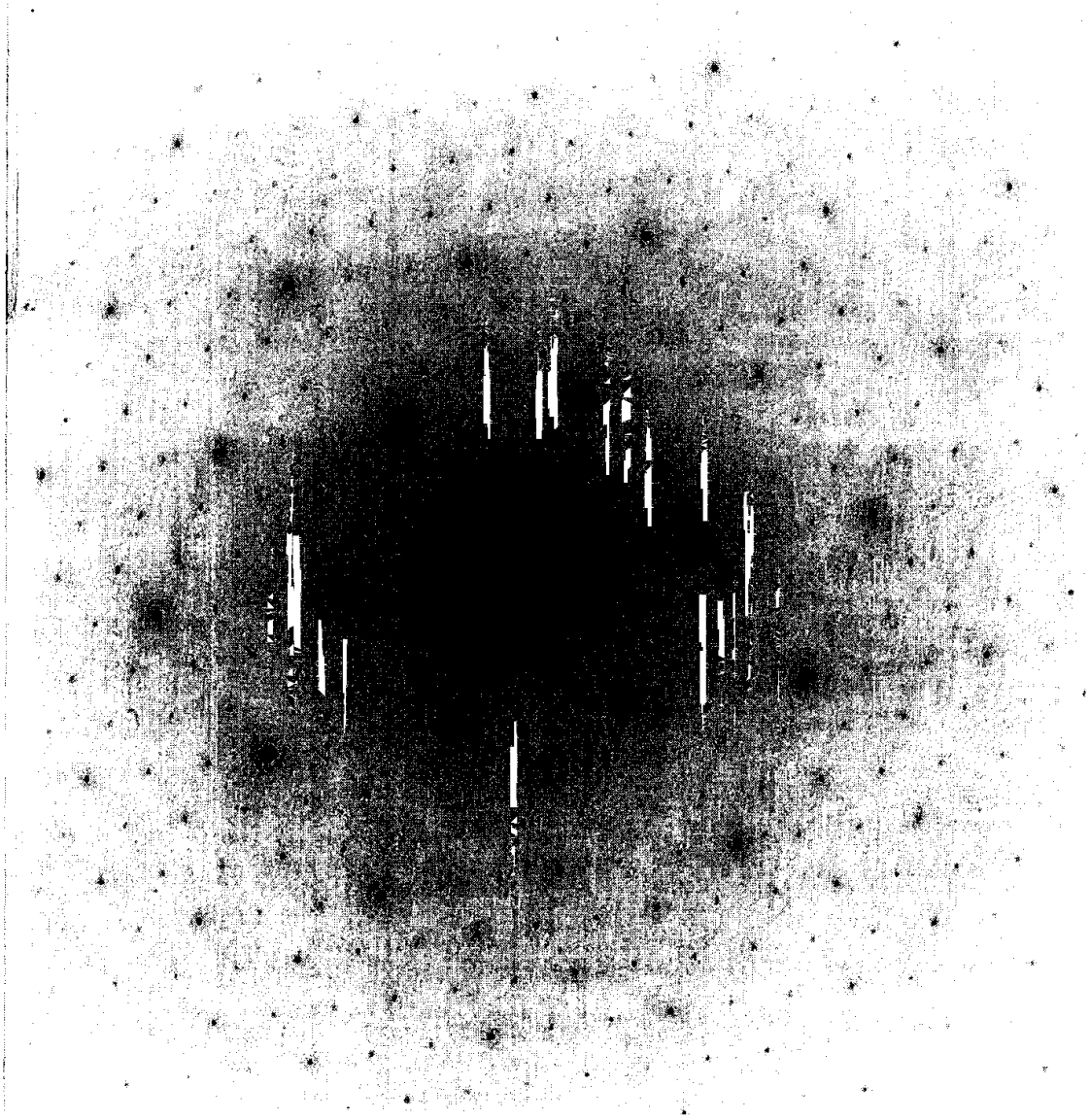

Figure 10: Bright Field electron micrograph of an anthophyllite particle. The width is 0.5 micrometers and the length is 6 micrometers with an aspect of 12. (Plate 709)

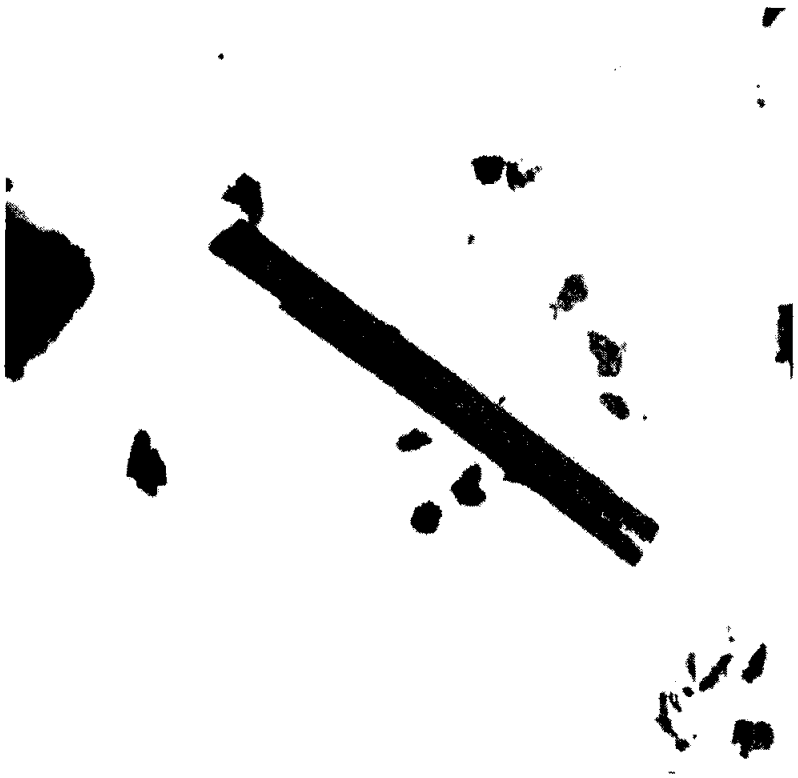

Figure 11: Selected area electron diffraction pattern of the [100] zone axis. Very weak spots from intergrown talc are also present. (Plate 711)

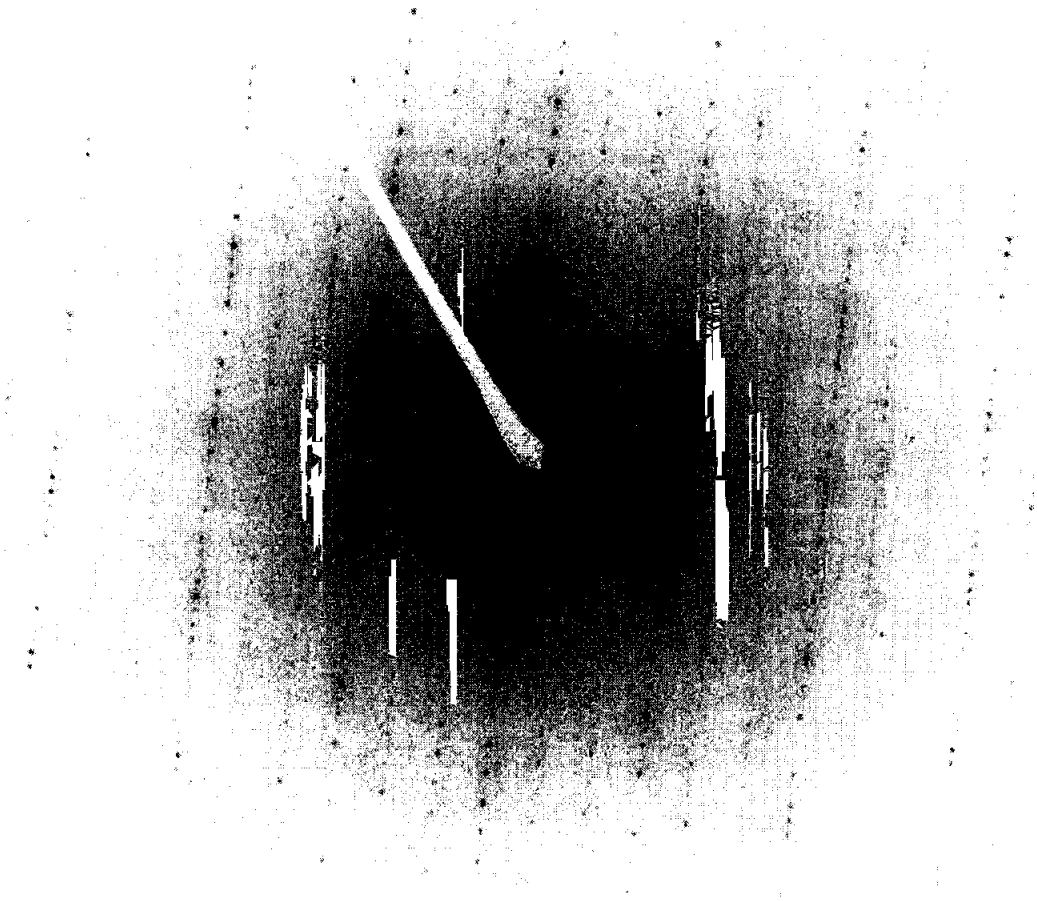

MAGNESIUM SILICATE FIBERS

FOUND IN [redacted] PAINT

Prepared for
R.T. Vanderbilt Co., Inc.

by

RJ Lee Group, Inc.
350 Hochberg Road
Monroeville, PA 15146

Project # ATH208337

April 2, 1993

Introduction

A sample of [redacted] Paint, RJ Lee Group sample number 43694HTP4, was examined for magnesium silicate fibers because this paint was reported to contain anthophyllite asbestos instead of fibrous talc, one of the intended components. The inorganic paint components were isolated and the fibrous particles were analyzed by transmission electron microscopy (TEM) and polarized light microscopy (PLM). The results of these analyses conflict with the assertion that this paint contains anthophyllite asbestos.

Two types of talc fibers are present in these samples, ordinary talc and transitional talc. Ordinary talc fibers exhibit a ribbon-like morphology and typical TEM and PLM properties for talc. Transitional talc fibers exhibit somewhat higher refractive indices and complex selected area electron diffraction (SAED) patterns. Transitional talc fibers are more equidimensional in cross section than ribbon talc, i.e., more rod like than ribbon-like. Because the transitional talc fibers are the fibers readily confused with simple anthophyllite asbestos, this report focuses almost exclusively on transitional talc.

TEM Analyses - Sample Preparation and Equipment

The sample was prepared for TEM analysis using standard procedures commonly applied to asbestos bulk samples. An aqueous suspension of the inorganic paint components was deposited on a mixed cellulose ester filter. The filter was collapsed with acetone vapor, coated with evaporated carbon, transferred to TEM grids, and dissolved with acetone. This process yields an electron-transparent carbon replica of the filter surface which supports the paint particles on a copper TEM grid.

The particles were studied using a JEOL 2000 FX TEM operated at an accelerating potential of 200 kv and magnifications of 1,000X to 100,000X. The TEM grids were also studied using a Philips CM 12 TEM operated at an accelerating potential of 100 kv and magnifications of 1,000X to 100,000X. Numerous fibers were examined by TEM in order to determine their typical composition, crystal structure and morphology.

TEM Chemical Analyses

Qualitative fiber composition was measured using energy dispersive X-ray spectroscopy (EDXS) with a Tracor Northern 5500 system on the JEOL TEM and an EDAX 9800+ system on the Philips TEM. Qualitative EDXS of numerous fibers indicates that these fibers are silicates of magnesium with only minor amounts of other elements (see figures 1 and 2 for typical EDXS spectra).

Quantitative EDXS of several representative fibers was performed using the EDAX 9800+ system and several natural minerals as standards. The quantitative EDXS data demonstrate that these fibers have an atomic ratio of magnesium to silicon (Mg:Si) between 6:8 and 7:8 (see tables 1A and 1B). The minor amounts of aluminum present are added to the silicon to calculate these ratios since much (if not all) aluminum occurs in tetrahedral structural sites substituting for silicon. Similarly, the minor amounts of other elements present (e.g., iron) are added to the magnesium to calculate these ratios since such elements occur in the octahedral (and other larger structural sites) substituting for magnesium. These Mg:Si ratios, approximately 6.5:8, correspond to the ratios expected from a talc and magnesio-anthophyllite intergrowth. Ideal talc has a 6:8 (3:4) ratio and ideal magnesio-anthophyllite has a 7:8 ratio (see Figure 7).

One fiber analyzed by EDXS yielded chemical data typical of pure talc (see table 1C). The analysis was performed on the tip of the fiber where only talc was present by SAED. This fiber tip has a Mg:Si ratio of 5.94:8 which is very close to the ideal ratio for talc, of 6:8.

Conventional TEM/EDXS analysis does not yield information on hydrogen and oxygen content. These components are computed from stoichiometric requirements of the particular mineral species. The oxygen calculation is simple and uses the assumption that the minor iron present is in the ferrous state. The hydrogen calculation is more complex because it is present as hydroxyl (OH) and talc and magnesio-anthophyllite contain different amounts of hydroxyl. Talc has four hydroxyls for every 8 silicons and magnesio-anthophyllite has 2 hydroxyls for every 8 silicons. Hydroxyl is calculated to fulfill the structural requirements of a compound fiber containing talc and magnesio-anthophyllite in the proportions indicted by the Mg:Si ratio.

The elemental ratios produced by EDXS analysis are converted into weight percentages of component oxides by standard mineralogical calculations. The weight percentages are normalized to total 100 percent in this process; so the 100 percent sum should not be taken as a

representation that these analyses are perfect. Coefficients of variance are approximately 0.05 for the major elements, magnesium and silicon, and 0.20 for the minor elements.

For convenience in evaluating these fibers as hypothetical simple amphiboles, the site occupancies for an amphibole have been calculated from the EDXS analytical data for each fiber (see tables 1A and 1B). These fibers clearly have a deficiency in cations compared to a normal amphibole. However, this compositional deficiency is expected due to the intergrown talc. The magnesium-to-ferrous-iron ratio indicates that these fibers are so magnesium rich that any amphibole present must be magnesio-anthophyllite and not ordinary anthophyllite.

TEM Structural Analyses

Crystal structural information was determined in the TEM by SAED analysis of the fibers. The SAED patterns generated by these fibers include numerous diffraction maxima, some of which are produced by a talc-like structure and some by a magnesio-anthophyllite structure (see table 2 and figures 3.1 to 3.3). These SAED patterns are distinguished by the consistent presence of both talc-like and magnesio-anthophyllite maxima in the same pattern. The term talc-like is used because, as will be discussed below, the talc-like phase appears to be orthrhombic talc (ortho-talc).

The patterns indicate not only that ortho-talc and magnesio-anthophyllite structures are present in the same fiber, but also that both structures share common crystallographic axes. The following crystallographic relations were noted (see Figure 8):

a-axis (ortho-talc) = c-axis (magnesio-anthophyllite)
b-axis (ortho-talc) = 0.5 X b-axis (magnesio-anthophyllite)
c-axis (ortho-talc) = a-axis (magnesio-anthophyllite)

This rigorous alignment of crystal structures indicates that the two structures are intimately intergrown and thus inseparable. Similar talc/anthophyllite oriented intergrowths have been noted by Veblen (1980) and Virta (1987).

Calculated SAED patterns for talc and magnesio-anthophyllite were prepared to check the validity of the proposed intergrowth. Superimposing analogous patterns of the two minerals should yield a compound pattern which matches the experimentally observed patterns. An excellent match was achieved for the [100] pattern of magnesio- anthophyllite plus the [001] pattern of talc. However, the other compound calculated patterns indicated a minor

dimensional incompatibility between the two structures (compare figures 4.1 - 4.3 and 5.1 - 5.3 to figures 3.1 - 3.3).

The incompatibility was resolved by assuming an orthorhombic cell for talc (see figures 6.1 - 6.3). In nature, talc generally has a monoclinic or triclinic (pseudo-monoclinic) unit cell, but calculated patterns with these symmetries do not align properly with the calculated magnesio-anthophyllite patterns. Calculated orthorhombic talc (ortho-talc) patterns combined with calculated magnesio-anthophyllite patterns match the observed SAED patterns well in most orientations. Because the calculated compound patterns explain the observed compound patterns, the presence of ortho-talc is considered to be proven. An ortho-talc has also been noted by Veblen (1980), but no details of its identification are provided. Our discovery of ortho-talc proceeded independently.

The unit cell parameters chosen to calculate the SAED patterns were taken from the literature and may not perfectly match the actual phases under consideration. Therefore, small mismatches are found in some of the patterns. In a few patterns, the SAED data match regular monoclinic talc as well as ortho-talc.

The ortho-talc patterns were calculated using unit cell parameters like regular monoclinic talc with two exceptions. First, the beta angle must be 90 degrees in order for the structure to be orthorhombic. Second, the c-axis was shortened by multiplying times the sine of beta for monoclinic talc. These manipulations of the monoclinic talc cell to produce a hypothetical orthorhombic talc cell are analogous to the transformations required to relate the monoclinic cell of magnesio-cummingtonite to magnesio-anthophyllite and to relate the monoclinic cell of clino-enstatite to enstatite (see table 4). In these two examples, the a-axis is shortened by sine beta multiplication, not the c-axis. However, the a-axes of these minerals are the axes which are structurally related to the c-axis of talc. This type of relationship between polymorphs is referred to as unit-cell twinning.

The space group of the ortho-talc is unresolved. $Ccm2_1$, Pnmn, Ccmm, C2cm, Cc2m, and $C222_1$ have been found or predicted as space groups for other orthorhombic sheet silicates and may be applicable to ortho-talc. More detailed study of systematic SAED extinctions is required to narrow the choice of space groups. From the data we do have, it appears that the space group may be C-centered. To calculate hypothetical SAED patterns, the maximum symmetry C-centered space group, Cmmm, was assumed.

The ortho-talc may be only pseudo-orthorhombic (e.g., staurolite). Therefore, the space group may not be one of those suggested above. Even if the ortho-talc is pseudo-orthorhombic, the conclusions reached above are valid because the unit cell parameters are essentially correct.

In most of the SAED patterns, the talc maxima exhibited streaking in the direction of the b-axis. This streaking is attributed to chain-width disorder from intergrown biopyriboles or strain in the talc structure. The strain would be caused by the small misfit between the talc and anthophyllite b dimensions, 9.171 and 9.007 Angstroms respectively (9.007 is actually half the anthophyllite b dimension, but is the structurally relevant dimension of the anthoplyllite sub-cell which would match up with the talc cell). The strain should be greatest if the intergrowth is along a composition plane parallel to [010], e.g. (001). Other streaking along the same layer line direction may be due to disorder in either the talc or the anthophyllite structures.

A few obvious cleavage fragments of anthophyllite were detected and yielded an SAED pattern characteristic of anthophyllite alone. The vast majority of fibers were not like this cleavage fragment.

TEM Morphological Analyses

TEM morphological analysis of the fibers indicates that most fibers have dimensions in the following ranges:

diameter	0.15 to 0.80 micrometers
length	2.3 to >7.3 micrometers
aspect ratio	3.0 to >49

If regulation of fibers was based on morphology alone, many of these fibers would clearly be regulated. However, the regulated status of a given fiber depends on morphology and mineral species and will be discussed below.

Other Particles Detected by TEM

In addition to the ortho-talc / magnesio-anthophyllite fibers (transitional talc) which were the target of this study, particles of ordinary fibrous talc, non-fibrous talc and tremolite cleavage fragments were noted in the sample. The normal talcs and tremolite are very low in iron like the transitional talc. Both minerals also have chemistries close to their ideal end-member composition.

PLM Analyses

The fibers were examined using Nikon Labophot PLM's at magnifications ranging from 40X to 400X. The fibers were mounted on glass slides in various refractive index oils to determine the optical properties of the fibers.

The highest refractive index (gamma) was consistently between 1.600 to 1.590 and was parallel to the fiber length for transitional talc fibers. The other fibers of ordinary ribbon talc which were present exhibit more normal refractive indices (approximately 1.584) parallel to the fibers. The highest birefringence exhibited by the transitional fibers was below that of talc and above that of magnesio-anthophyllite. The fibers consistently reached extinction parallel to the ocular cross hairs. These optical properties are all consistent with properties which we have calculated for theoretical intimate ortho-talc / magnesio-anthophyllite intergrowths (see table 3). Gamma refractive indices in this range indicate a composition of 50 - 80% ortho-talc and 20 - 50% magnesio-anthophyllite.

Tremolite cleavage fragments and non-fibrous talc were also detected in the sample by PLM.

Evaluation of Available XRD Data

RJ Lee Group was provided with powder X-ray diffraction (XRD) data collected by McCrone Environmental Services, Inc. from three transitional "talc" fibers. The data were collected with a Debye-Scherrer camera and include d-values for both magnesio-anthophyllite and talc. The only unambiguous talc values are (001) reflections. Since these reflections are identical for talc and ortho-talc, this data neither supports nor refutes the ortho-talc described above. The XRD data do support the general findings above, i. e., the "talc" fibers consist of an intimate intergrowth of magnesio-anthophyllite and talc.

Discussion

The congruency between the TEM and PLM data indicate the sample contains fibers which are an intimate intergrowth of ortho-talc and magnesio-anthophyllite structural units. In addition, the data also prove that these fibers are not the material regulated as anthophyllite asbestos for the following reasons:

1. These paint fibers have such a disordered structure that they do not fit the definition of a mineral. "A mineral is a naturally occurring **homogeneous** solid with a definite (but generally not fixed) chemical composition and an **ordered** atomic arrangement" (Hurlbut and Klein, 1977). Two parts of this definition (highlighted in bold) are violated by the paint fibers. The fibers are not homogeneous and the crystal structure is somewhat disordered. The inhomogeneity is structural and due to the intimate intergrowth of talc and magnesio-anthophyllite structural units. A substance such as this is best described by the term mineraloid and should not be assigned a conclusive mineral name.

2. PLM is generally recognized as the benchmark analytical technique for identifying regulated asbestos in bulk materials. Since the PLM data indicate these paint fibers exhibit optical properties outside the range recognized for anthophyllite, these fibers must not be the material regulated as anthophyllite asbestos.

3. The composition of the magnesio-anthophyllite / ortho-talc intergrowths is so iron poor that the anthophyllite structural units must have a chemistry which falls into the compositional range for magnesio-anthophyllite, which is a different mineral species than anthophyllite. Magnesio-anthophyllite is clearly not federally regulated under OSHA (29 CFR 1910.1001 and 1926.58), AHERA (40 CFR 763 subpart F), MSHA (30 CFR 56 subpart D), or NESHAP (40 CFR 61). The definition of magnesio-anthophyllite clearly predates these federal regulations (Leake, 1978). Therefore, magnesio-anthophyllite cannot be considered a regulated mineral.

This regulatory interpretation makes sense because most commercial "anthophyllite" asbestos has a chemistry which falls within the anthophyllite compositional range, not within the magnesio-anthophyllite range (Dagenhart, 1989). The "anthophyllite" asbestos with a composition within the magnesio-anthophyllite range contains so much iron that its composition lies near the boundary between anthophyllite and magnesio-anthophyllite. These paint fibers have essentially no iron and are clearly compositionally distinct from commercial anthophyllite asbestos. These paint fibers exhibit a chemistry at the opposite end of the magnesio-anthophyllite compositional range from commercial "anthophyllite" asbestos.

Summary

The fibers in the [redacted] paint sample are composed of a magnesium silicate mineraloid which contains intimately intergrown regions of talc-like and magnesio-anthophyllite-like structure.

No one mineral predominates within these fibers and therefore a mineral name cannot be assigned to them. Even though these fibers may be commercially described as "fibrous talc", they are mineralogically best described as talc-like mineraloids. On the basis of these findings, we conclude that the reported identification of anthophyllite asbestos in paint samples containing Vanderbilt talc was incorrect.

References

Dagenhart, T.V. (1989) *A Review of Asbestos Mineralogy Contrasting Regulatory Definitions and Mineralogical Definitions.* Paper presented to National Asbestos Council, Sixth Annual Asbestos Abatement Conference and Exposition, Anaheim, CA.

Hey, M. H. (1956) *On the Correlation of Physical Properties With Chemical Composition in Multivariate Systems.* Mineralogical Magazine 31:69.

Hurlbut, C.S. and C. Klein (1977) *Manual of Mineralogy.* 19th Edition. John Wiley and Sons, New York.

Leake, B. E (1978) *Nomenclature of the Amphiboles.* American Mineralogist 63:1023-1052.

Ross, M., W. L. Smith, and W.H. Ashton (1968) *Triclinic Talc and Associated Amphiboles from Government Mining District.* New York. American Mineralogist 53: 751-769.

Veblen, D. (1980) *Microstructures and Reaction Mechanisms in Biopyriboles.* American Mineralogist 65:599-623.

Virta, R. L. (1985) *The Phase Relationship of Talc and Amphiboles in a Fibrous Talc Sample.* U.S. Bureau of Mines. Report of Investigations 8923.

List of Tables

Table 1A

MINERAL CHEMICAL ANALYSIS BY TRANSMISSION ELECTRON MICROSCOPY AND ENERGY DISPERSIVE X-RAY SPECTROSCOPY

Date: February, 1993
Analyst: TVD
TEM: Philips CM 12
EDX Unit: EDAX 9800+
K-Ratios: February 1993, 100kv

Specimen: "Talc" Fiber A
Gildden Paint, 43694HTP4

Location:

Correct Species Name: Talc / Magnesio-Anthophyllite Intergrowth ~50.0% amphibole ~50.0% talc

Chemical Composition:

Element	Peak Area (cps)	Peak Area Ratio (X/Si)	K-Ratio Used	Atoms per Formula	Oxide	Wt. % Oxide
Na			6.000		Na2O	
Mg	51.016	0.364	2.161	6.188	MgO	32.11
Al	1.727	0.012	1.300	0.126	Al2O3	0.83
Si	140.277	1.000	1.000	7.874	SiO2	60.91
K			0.745		K2O	
Ca	2.639	0.019	0.713	0.106	CaO	0.76
Ti			0.675		TiO2	
V			0.658		V2O3	
Cr			0.650		Cr2O3	
Mn	2.306	0.016	0.646	0.084	MnO	0.76
Fe	1.957	0.014	0.642	0.071	FeO	0.65
					Fe2O3*	
Co			0.639		CoO	
Ni	1.457	0.010	0.636	0.052	NiO	0.50
Cu			0.634		CuO	
Zn			0.633		ZnO	
H (as OH)*	N/A	N/A	N/A	3.000	H2O*	3.48
			TOTAL	14.500	TOTAL*	100.00

Calculated site occupancies (cations nominally assigned to amphibole structural sites):

Tetrahedral Site	Si	7.874	M4 Site	Mg	1.188
	Al	0.126		Ni	0.052
	Cr			FeII	0.071
	FeIII			Mn	0.084
	Ti			Ca	0.106
				Na	
	Sum T	8.000			
				Sum M4	1.500
M1,2,3 Sites	Al	0.000			
	Cr		A Site	Na	
	FeIII			K	
	Ti				
	Mg	5.000		Sum A	
	Ni				
	FeII				
	Mn			Mg / (Mg + FeII)	0.989
	Sum M1.2.3	5.000		Total Oxygens:	22.44

Assumptions:

*Normalized to 8 Si and Al cations in the tetrahedral site.

All iron assumed to be present as ferrous iron. Number of hydroxyls computed to fulfill stoichiometric requirements of the computed talc-amphibole proportions. Total weight percent normalized to 100 percent. Weight percent values less than 2 percent are imprecise.

Table 1B

MINERAL CHEMICAL ANALYSIS BY TRANSMISSION ELECTRON MICROSCOPY AND ENERGY DISPERSIVE X-RAY SPECTROSCOPY

Date: February, 1993
Analyst: TVD
TEM: Philips CM 12
EDX Unit: EDAX 9800+
K-Ratios: February 1993, 100kv

Specimen: "Talc" Fiber B
Glidden Paint, 43694HTP4

Location:

Correct Species Name: Talc / Magnesio-Anthophyllite intergrowth ~51.6% amphibole ~48.4% talc

Chemical Composition:

Element	Peak Area (cps)	Peak Area Ratio (X/Si)	K-Ratio Used	Atoms per Formula	Oxide	Wt. % Oxide
Na			6.000		Na2O	
Mg	64.041	0.369	2.161	6.256	MgO	32.53
Al	2.503	0.014	1.300	0.147	Al2O3	0.97
Si	173.722	1.000	1.000	7.853	SiO2	60.87
K			0.745		K2O	
Ca	3.501	0.020	0.713	0.113	CaO	0.82
Ti			0.675		TiO2	
V			0.658		V2O3	
Cr			0.650		Cr2O3	
Mn	2.453	0.014	0.646	0.072	MnO	0.66
Fe	1.314	0.008	0.642	0.038	FeO Fe2O3*	0.35
Co			0.639		CoO	
Ni	1.306	0.008	0.636	0.038	NiO	0.36
Cu			0.634		CuO	
Zn			0.633		ZnO	
H (as OH)*	N/A	N/A	N/A	2.968	H2O*	3.45
			TOTAL	14.516	TOTAL*	100.00

Calculated site occupancies (cations nominally assigned to amphibole structural sites):

Tetrahedral Site	Si	7.853	M4 Site	Mg	1.256
	Al	0.147		Ni	0.038
	Cr			Fe II	0.038
	Fe III			Mn	0.072
	Ti			Ca	0.113
				Na	
	Sum T	8.000		Sum M4	1.516
M1,2,3 Sites	Al	0.000			
	Cr		A Site	Na	
	Fe III			K	
	Ti				
	Mg	5.000		Sum A	
	Ni				
	Fe II			Mg / (Mg + Fe II)	0.994
	Mn				
	Sum M1,2,3	5.000		Total Oxygens:	22.44

Assumptions:

*Normalized to 8 Si and Al cations in the tetrahedral site.

All iron assumed to be present as ferrous iron. Number of hydroxyls computed to fulfil stoichiometric requirements of the computed talc-amphibole proportions. Total weight percent normalized to 100 percent. Weight percent values less than 2 percent are imprecise.

Table 1C

MINERAL CHEMICAL ANALYSIS BY TRANSMISSION ELECTRON MICROSCOPY AND ENERGY DISPERSIVE X-RAY SPECTROSCOPY

Date: February, 1993
Analyst: TVD
TEM: Philips CM 12
EDX Unit: EDAX 9800+
K-Ratios: February 1993, 100kv

Specimen: "Talc" Fiber C
Gildden Paint, 43694HTP4

Location:

Correct Species Name: Talc / Magnesio-Anthophyllite intergrowth ~0% amphibole ~100% talc

Chemical Composition:

Element	Peak Area (cps)	Peak Area Ratio (X/Si)	K-Ratio Used	Atoms per Formula	Oxide	Wt. % Oxide
Na			6.000		Na2O	
Mg	56.901	0.337	2.161	5.695	MgO	30.16
Al	2.804	0.017	1.300	0.169	Al2O3	1.13
Si	169.074	1.000	1.000	7.831	SiO2	61.83
K			0.745		K2O	
Ca	2.518	0.015	0.713	0.083	CaO	0.61
Ti			0.675		TiO2	
V			0.658		V2O3	
Cr			0.650		Cr2O3	
Mn	1.832	0.011	0.646	0.055	MnO	0.51
Fe	1.605	0.009	0.642	0.048	FeO	0.45
					Fe2O3*	
Co			0.639		CoO	
Ni	1.985	0.012	0.636	0.058	NiO	0.57
Cu			0.634		CuO	
Zn			0.633		ZnO	
H (as OH)*	N/A	N/A	N/A	4.000	H2O*	4.73
			TOTAL	13.939	TOTAL*	100.00

Calculated site occupancies (cations nominally assigned to amphibole structural sites):

Tetrahedral Site	Si	7.831	M4 Site	Mg	0.695
	Al	0.169		Ni	0.058
	Cr			Fe II	0.048
	Fe III			Mn	0.055
	Ti			Ca	0.083
				Na	
	Sum T	8.000		Sum M4	0.939
M1,2,3 Sites	Al		A Site	Na	
	Cr			K	
	Fe III				
	Ti				
	Mg	5.000		Sum A	
	Ni				
	Fe II				
	Mn			Mg / (Mg + Fe II)	0.992
	Sum M1,2,3	5.000		Total Oxygens:	21.85

Assumptions:
*Normalized to 8 Si and Al cations in the tetrahedral site.
All iron assumed to be present as ferrous iron. Number of hydroxyls computed to fulfil stoichiometric requirements of the computed talc-amphibole proportions. Total weight percent normalized to 100 percent. Weight percent values less than 2 percent are imprecise.

Table 2. SAED Evaluation of Magnesium Silicate Fibers in Glidden Paint

Negative Number	Particle Dimensions: Length (um)	Width (um)	Aspect Ratio	Talc/Ortho–Talc SAED Interpretation: d1/hkl (Angstrome) observed	expected	obs./exp.	d2/hkl (Angstrome) observed	expected	obs./exp.	angle/zone axis observed	expected	obs.–exp.	[uvw] ^ [0 0 1]	Magnesio–anthophyllite SAED Interpretation: d1/hkl (Angstrome) observed	expected	obs./exp.	d2/hkl (Angstrome) observed	expected	obs./exp.	angle/zone axis observed	expected	obs.–exp.	[uvw] ^ [1 0 0]
18262	5.3	0.30	17.7	4.537 (0 2 0) Talc	4.586	0.989	4.436 (1 1 1)	4.265	1.041	61.95 [1 0 –1]	62.29	–0.34	14.72	9.073 (0 2 0)	9.007	1.007	4.879 (1 1 1)	4.888	0.998	74.97 [1 0 1]	74.26	0.71	15.69
				* 4.537 (0 2 0) Ortho–talc	4.586	0.989	4.436 (1 1 1)	4.449	0.998	61.95 [1 0 1]	60.98	0.97	15.79										
18267	>6.6	0.50	> 13.0	4.421 (0 2 0) Talc	4.586	0.964	4.349 (1 1 1)	4.265	1.020	61.60 [1 0 –1]	62.29	–0.69	16.06	8.842 (0 2 0)	9.007	0.982	4.782 (1 1 1)	4.888	0.978	74.47 [1 0 1]	74.26	0.21	15.69
				* 4.421 (0 2 0) Ortho–talc	4.586	0.964	4.349 (1 1 1)	4.449	0.978	61.60 [1 0 1]	60.98	0.62	15.79										
18269	2.3	0.33	7.0	No Talc Pattern, Cleavage Fragment										3.696 (4 3 0)	3.671	1.007	3.020 (4 3 1)	3.014	1.002	35.26 [3 4 0]	34.81	0.47	52.31
18276	>4.7	0.80	> 5.9	4.549 (0 2 0) Talc	4.586	0.992	4.496 (1 1 0)	4.532	0.992	60.24 [0 0 1]	60.39	–0.15	0	9.096 (0 2 0)	9.007	1.010	4.976 (0 1 1)	5.067	0.982	72.90 [1 0 0]	73.66	–0.76	0
				* 4.549 (0 2 0) Ortho–Talc	4.586	0.992	4.496 (1 1 0)	4.500	0.982	60.24 [0 0 1]	60.04	0.20	0										
18278 (same fiber as 18276)	>2.4	0.80	> 3.0	4.513 (0 2 0) Talc	4.586	0.984	4.413 (1 1 –1)	4.558	0.968	61.47 [1 0 1]	60.20	1.27	16.06	9.026 (0 2 0)	9.007	1.002	4.833 (1 1 1)	4.888	0.989	74.32 [1 0 1]	74.26	0.06	15.69
				* 4.513 (0 2 0) Ortho–talc	4.586	0.984	4.413 (1 1 1)	4.449	0.992	61.47 [1 0 1]	60.98	0.49	15.79										
18284	>6.6	0.15	> 45.3	* 4.068 (0 2 2) Talc	4.117	0.988	4.319 (1 1 1)	4.265	1.013	54.60 [0 1 1]	54.68	–0.08	25.81	8.135 (2 1 0)	8.248	0.986	4.884 (1 1 1)	4.888	0.999	68.40 [1 2 1]	69.00	–0.60	63.00
				4.068 (0 2 2) Ortho–Talc	4.117	0.988	4.319 (1 1 2)	4.113	1.050	54.60 [1 1 1]	53.39	1.21	29.52										
18287 (same fiber as 18284)	>7.3	0.15	> 48.7	4.542 (0 2 0) Talc	4.586	0.990	4.456 (1 1 –1)	4.558	0.978	59.87 [1 0 1]	60.20	–0.33	16.06	9.083 (0 2 0)	9.007	1.008	4.917 (1 1 1)	4.888	1.006	73.59 [1 0 1]	74.26	–0.67	15.69
				4.542 (0 2 0) Ortho–Talc	4.586	0.990	4.456 (1 1 1)	4.449	1.002	59.87 [1 0 1]	60.98	–1.11	15.79										
18289	3.96	0.35	11.3	4.072 * (0 2 2) Talc	4.117	0.989	4.255 (1 1 1)	4.265	0.998	54.87 [0 1 1]	54.68	0.19	25.81	8.144 (2 1 0)	8.248	0.987	4.931 (1 1 1)	4.888	1.009	69.85 [1 2 1]	69.00	0.85	63.00
				4.072 (0 2 2) Ortho–Talc	4.117	0.989	4.255 (1 1 2)	4.113	1.035	54.87 [1 1 1]	53.39	1.48	29.52										
18291 (same fiber as 18289)	3.96	0.35	11.3	4.595 * (0 2 0) Talc	4.586	1.002	4.493 (1 1 0)	4.532	0.991	60.22 [0 0 1]	60.39	–0.17	0	8.985 (0 2 0)	9.007	0.998	5.049 (0 1 1)	5.067	0.996	73.73 [1 0 0]	73.66	0.07	0
				4.595 (0 2 0) Ortho–Talc	4.586	1.002	4.493 (1 1 0)	4.500	0.981	60.22 [0 0 1]	60.04	0.18	0										
18299	6.5	0.65	10.0	4.473 (0 2 0) Talc	4.586	0.975	4.539 (1 1 0)	4.532	1.002	59.82 [0 0 1]	60.39	–0.57	0	8.945 (0 2 0)	9.007	0.993	5.020 (0 1 1)	5.067	0.991	72.83 [1 0 0]	73.66	–0.83	0
				* 4.473 (0 2 0) Ortho–Talc	4.586	0.975	4.539 (1 1 0)	4.58	0.991	59.82 [0 0 1]	60.04	–0.22	0										
				Averages:		0.966			1.001							0.998			0.995				

For both talc and anthophyllite, the first d–values were measured along the obvious layer lines in each SAED pattern.
The (020) and (021) d–values of talc are biased low due to overlap of talc diffraction maxima with magnesio–anthophyllite maxima.

RJ Lee Group Sample Number 43694-TP4

Table 3. Calculated Optical Properties for Talc / Magnesio–Anthophyllite Oriented Intergrowths

Input Data and Assumptions:

Mg–rich Talc Refractive Indices (Ross, et al., 1968)

alpha =	1.545	(parallel to c*–axis of talc)	birefringence = 0.039
beta =	1.584	(parallel to a–axis of talc)	
gamma =	1.584	(parallel to b–axis of talc)	

Magnesio–Anthophyllite Refractive Indices (from regression equations of Hey, 1956)

alpha =	1.602	(parallel to a–axis of anthophyllite)	birefringence = 0.019
beta =	1.614	(parallel to b–axis of anthophyllite)	
gamma =	1.621	(parallel to c–axis of anthophyllite)	

Refractive indices are calculated for talc / magnesio–anthophyllite intergrowths which exhibit the following relative orientations as shown by TEM–SAED:
a (talc) = c (Mg–anthophyllite) b (talc) = b (Mg–anthophyllite) c* (talc) = a (Mg–anthophyllite)

The talc and Mg–anthophyllite are assumed to be intergrown in a mosaic so fine that individual phases cannot be resolved by light microscopy. The calculated optical properties are valid only for talc / Mg–anthophyllite intergrowths near end member compositions. Optical properties are assumed to vary linearly with relative proportions of the two minerals.

Calculated Optical Properties for Varying Proportions of Talc and Mg–Anthophyllite:

Talc Fraction	Mg–Anthophyllite Fraction	Refractive Indices alpha	beta	gamma	average	birefringence
100%	0%	1.545	1.584	1.584	1.571	0.039
90%	10%	1.551	1.587	1.588	1.575	0.037
80%	20%	1.556	1.590	1.591	1.579	0.035
70%	30%	1.562	1.593	1.595	1.583	0.033
60%	40%	1.568	1.596	1.599	1.588	0.031
50%	50%	1.573	1.599	1.603	1.592	0.029
40%	60%	1.579	1.602	1.606	1.596	0.027
30%	70%	1.585	1.605	1.610	1.600	0.025
20%	80%	1.591	1.608	1.614	1.604	0.023
10%	90%	1.596	1.611	1.617	1.608	0.021
0%	100%	1.602	1.614	1.621	1.612	0.019

Talc Fraction	Mg–Anthophyllite Fraction	Maximum Retardation for Particles of Given Thickness (micrometers) 0.10	0.30	1.00	3.00	10.00	30.00
100%	0%	3.9	11.7	39.0	117.0	390.0	1170.0
90%	10%	3.7	11.1	37.0	111.0	370.0	1110.0
80%	20%	3.5	10.5	35.0	105.0	350.0	1050.0
70%	30%	3.3	9.9	33.0	99.0	330.0	990.0
60%	40%	3.1	9.3	31.0	93.0	310.0	930.0
50%	50%	2.9	8.7	29.0	87.0	290.0	870.0
40%	60%	2.7	8.1	27.0	81.0	270.0	810.0
30%	70%	2.5	7.5	25.0	75.0	250.0	750.0
20%	80%	2.3	6.9	23.0	69.0	230.0	690.0
10%	90%	2.1	6.3	21.0	63.0	210.0	630.0
0%	100%	1.9	5.7	19.0	57.0	190.0	570.0

Table 4. Comparison of Unit Cell Dimensions for Monoclinic and Orthorhombic Polymorphs of Magnesium Silicates

Mineral Group	Monoclinic Minerals	Orthorhombic Minerals
Pyroxene Group	Clino–Enstatite	Enstatite
	a = 9.620	a = 18.276
	b = 8.825	b = 8.850
	c = 5.188	c = 5.184
	beta = 108.33	beta = 90.00
	a(mono) X 2 X sine (beta) = 18.264 = predicted a–value for orthorhombic polymorph	
Amphibole Group	Magnesio–Cummingtonite	Anthophyllite
	a = 9.49	a = 18.555
	b = 18.00	b = 18.014
	c = 5.30	c = 5.2803
	beta = 102.00	beta = 90.00
	a(mono) X 2 X sine (beta) = 18.565 = predicted a–value for orthorhombic polymorph	
Talc Group	Talc	"Ortho–Talc"
	a = 5.287	a = 5.287
	b = 9.171	b = 9.171
	c = 18.964	c = 18.698
	beta = 99.61	beta = 90.00
	c(mono) X sine (beta) = 18.698 = predicted c–value for orthorhombic polymorph	

Notes: Unit cell dimensions reported in Angstroms and angles reported in degrees. Unit cell parameters culled from various references for all minerals except ortho–talc. Ortho–talc parameters predicted as part of this study.

The "a" dimensions of both pyroxenes and amphiboles describe the thickness of their chain silicate structures in a direction at (or nearly at) right angles to the plane formed by the basal oxygens of the chain. In talcs, the "c" dimension describes the thickness of the sheet silicate structure at (or nearly at) right angles to the plane formed by the basal oxygens of the sheet. Thus the talc "c" is analogous to the "a" of pyroxenes and amphiboles. Since silicate sheets are essentially infinitely wide silicate chains, they have the same thickness as chains. Talc contains two sheets in its basic structure; hence the talc "c" is actually twice the "a" of chain silicates.

The monoclinic chain silicates are related to the orthorhombic chain silicates by a concept described as unit cell twinning. Orthorhombic "a" dimensions are almost doubled compared to monoclinic "a" dimensions. This is due to twinning of the monoclinic unit cell on the (100) plane. The other cell parameters remain unchanged (except for beta which becomes 90 degrees). The doubled orthorhombic "a" value must be reduced by multiplying by the sine of the monoclinic beta angle to maintain the proper geometric relationships.

Orhto–talc may be derived from monoclinic talc in a similar way except the "c" axis is involved. For ortho–talc, the relationship may be better described as intra–unit–cell twinning since the talc unit cell is already two layers thick. Each layer may be considered a subcell which is related across an (001) twin plane to the the other layer. Thus, to derive ortho–talc, the "c" axis need not be doubled, only multiplied by sine beta of monoclinic talc. This may not be twinning in the most rigorous sense because the two subcells may not be related by a simple mirror plane due to minor structural variations within the each layer.

List of Figures

Figure 1

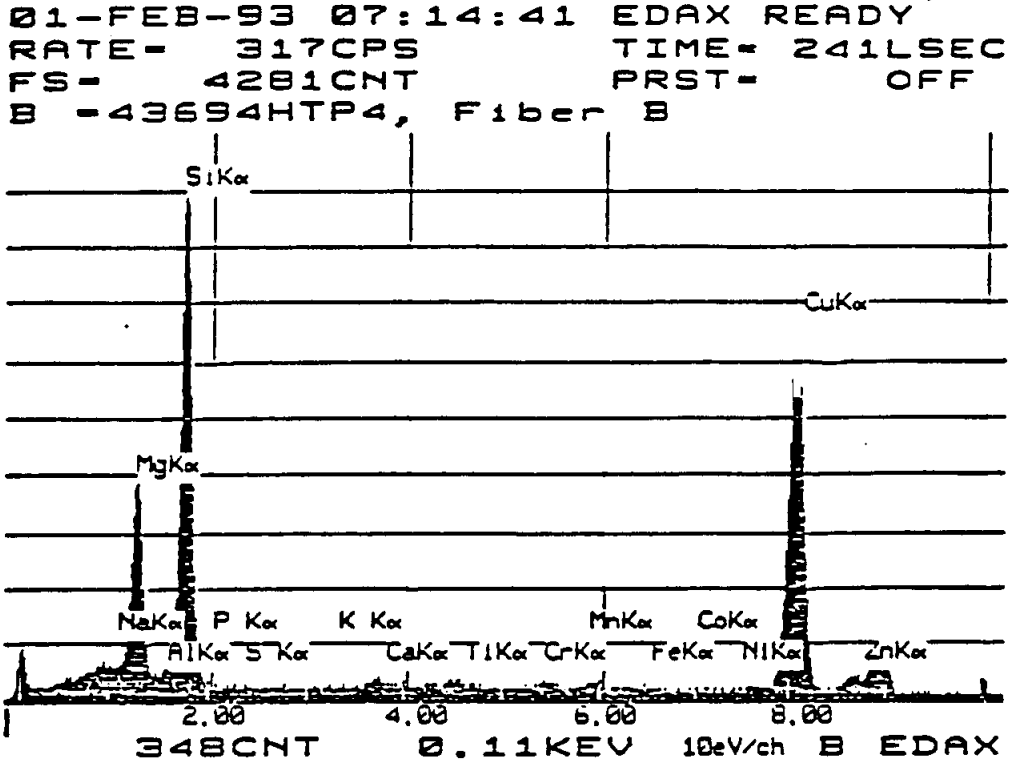

Figure 2

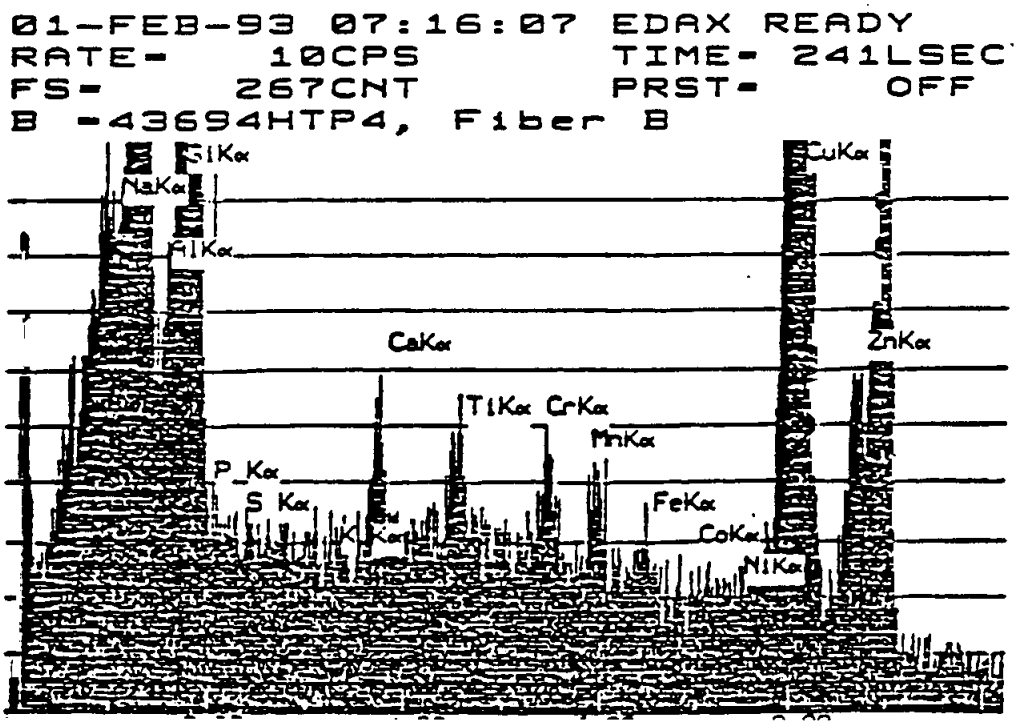

Figure 3.1

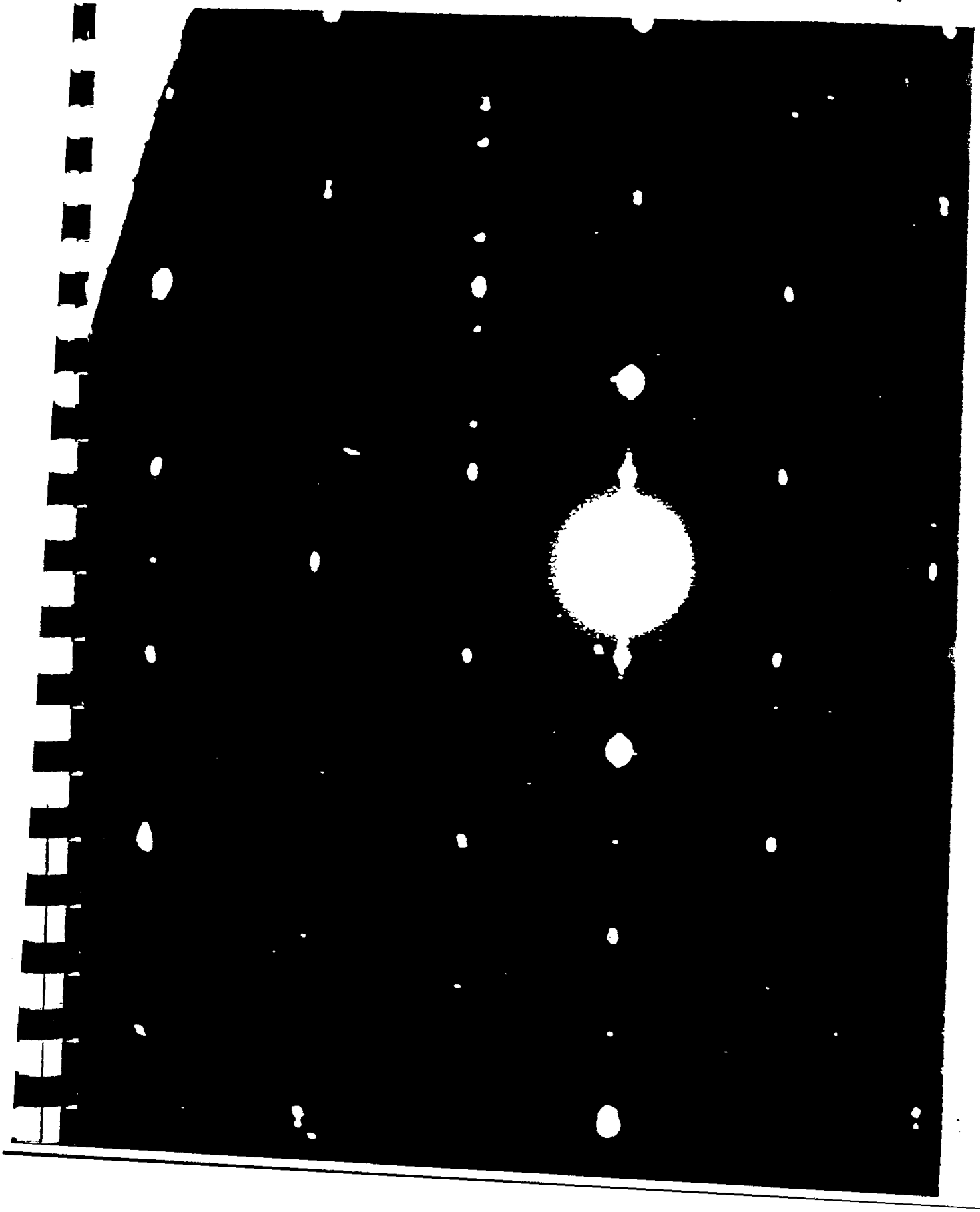

Figure 3.2

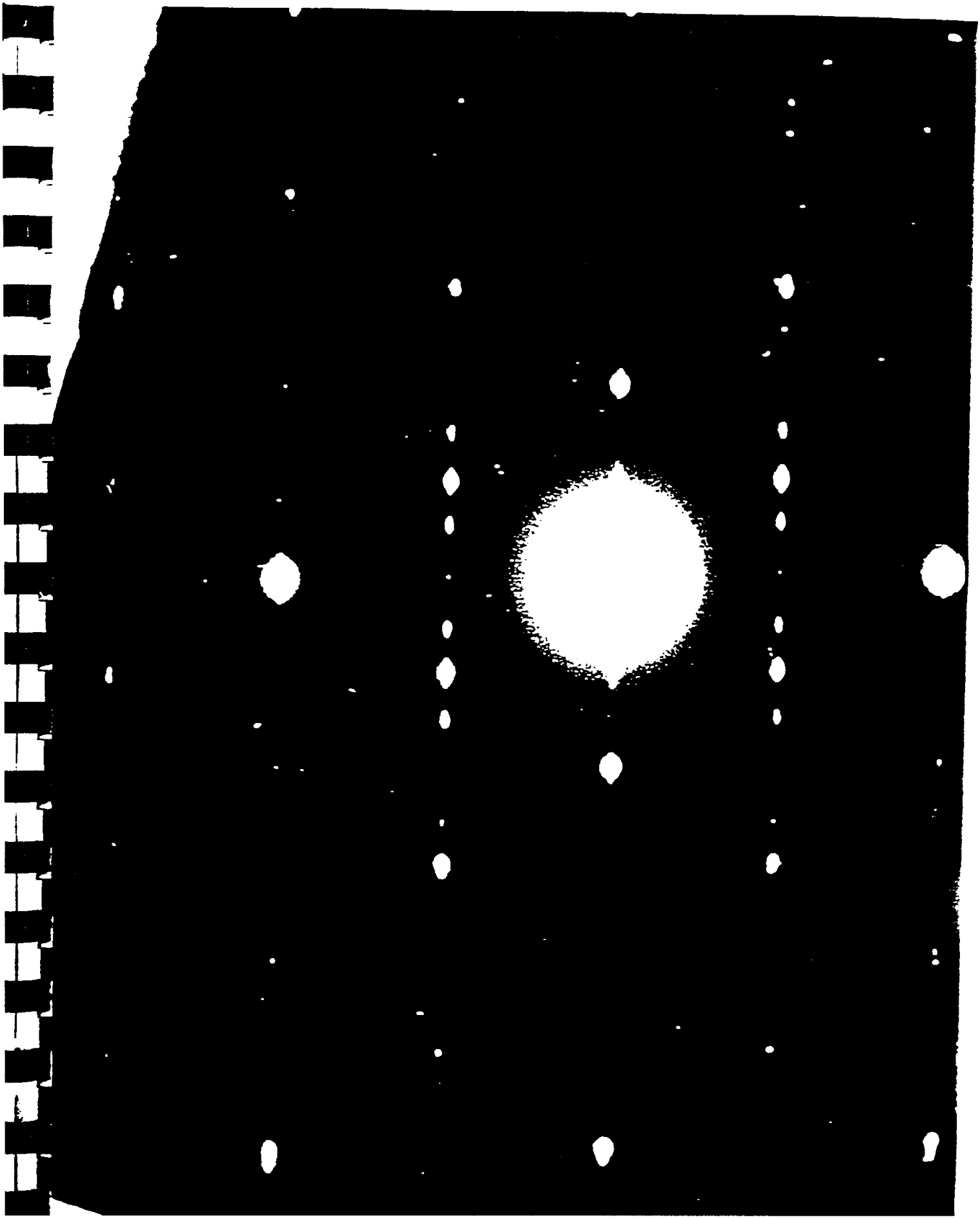

Figure 3.3

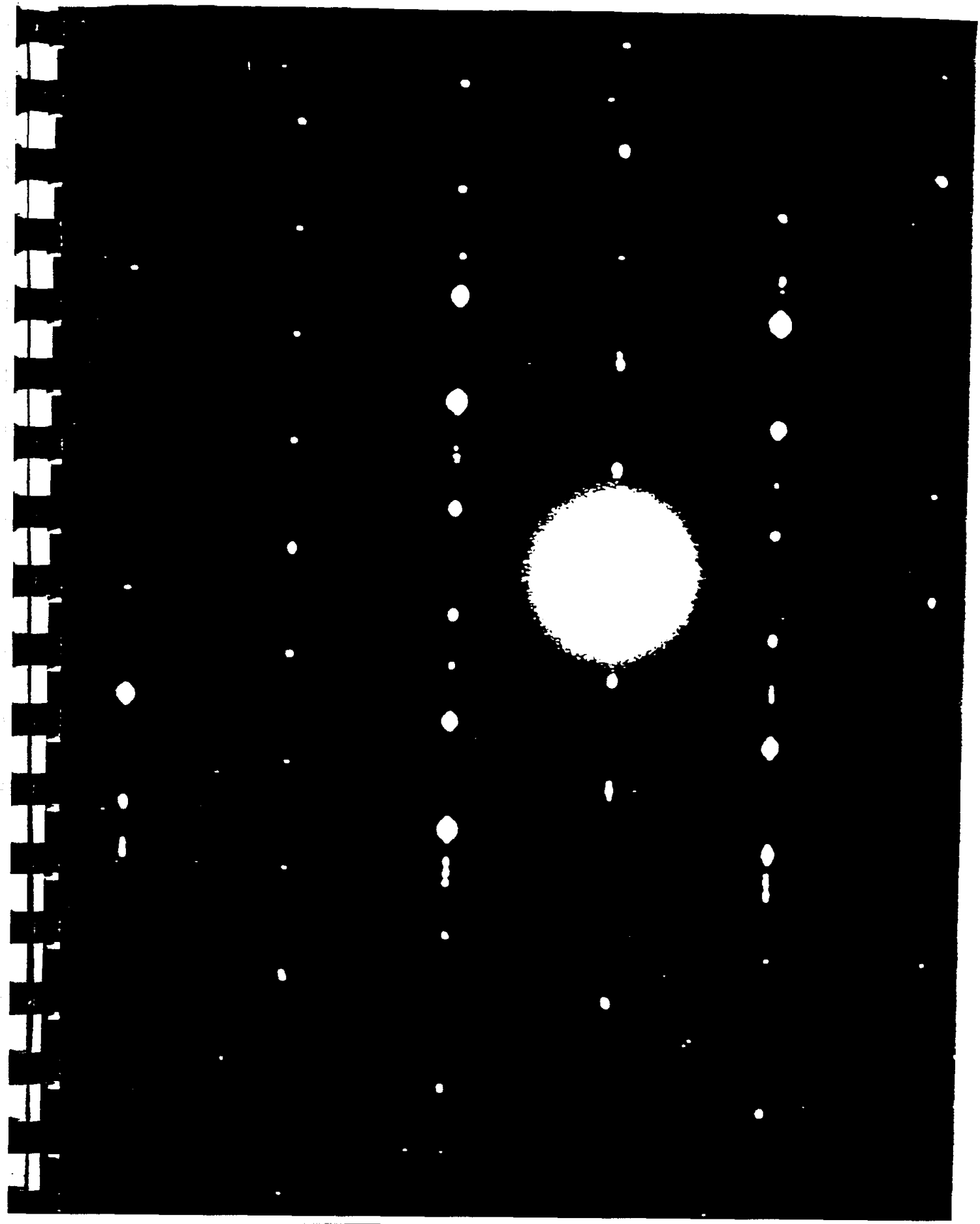

Anthophyllite 1 0 0 ZONE AXIS

a = 18.555 Å b = 18.014 Å c = 5.280 Å ß = 90.00° Space Group = P nma

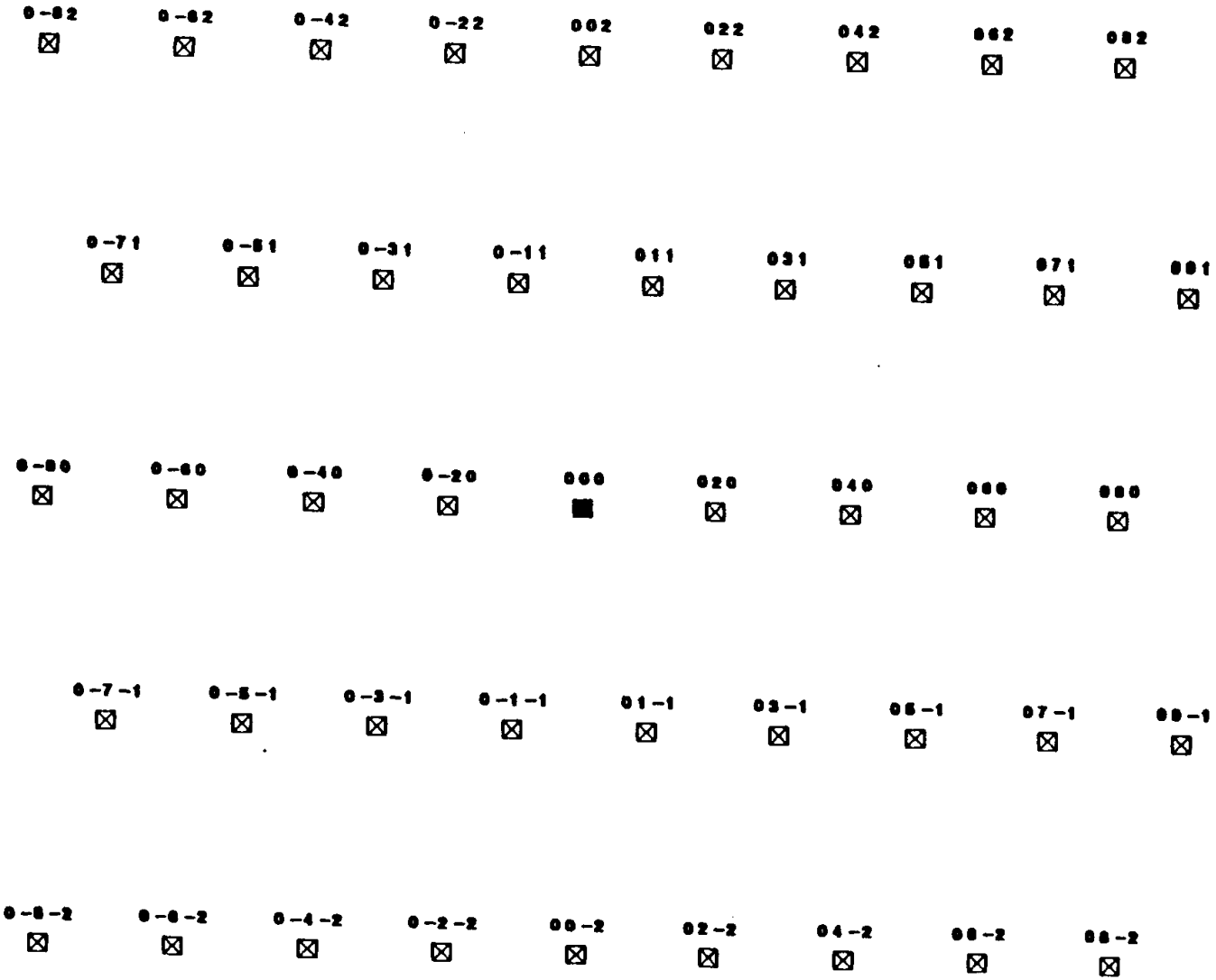

Squares are non-extinct Diamonds are extinct Camera Constant = 120.0 mm Å

Figure 4.1

Anthophyllite 1 0 1 ZONE AXIS

a = 18.555 Å b = 18.014 Å c = 5.280 Å ß = 90.00° Space Group = P nma

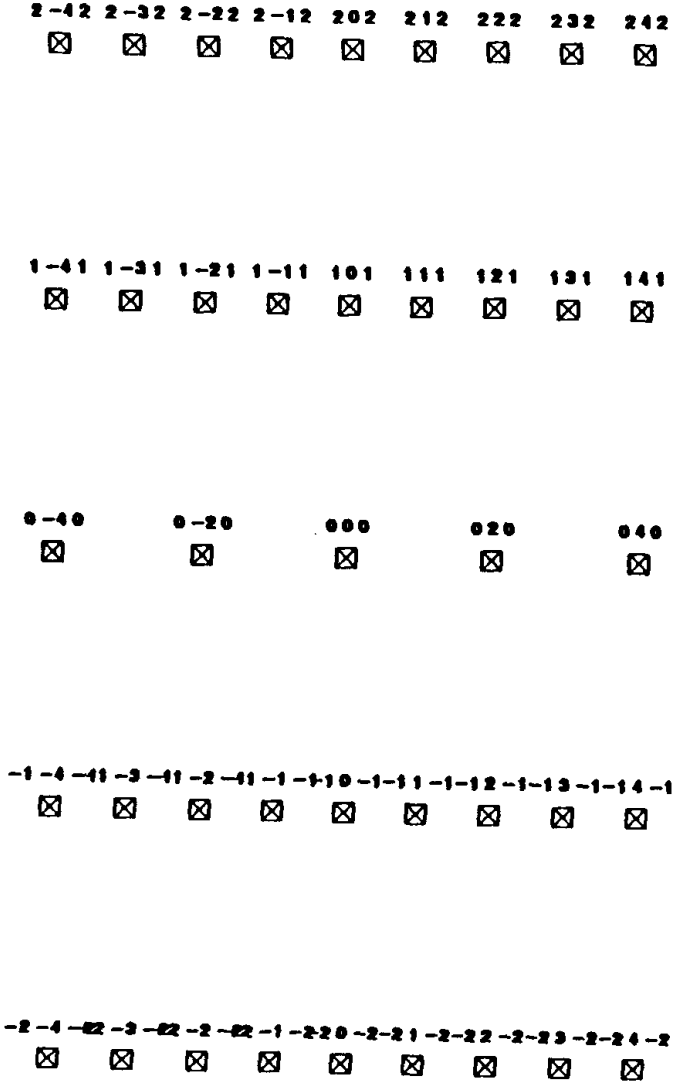

Squares are non-extinct. Diamonds are extinct. Camera Constant = 180.0 mm-Å

Figure 4.2

Anthophyllite 1 2 1 ZONE AXIS

a = 18.555 Å b = 18.014 Å c = 5.280 Å ß = 90.00° Space Group = P nma

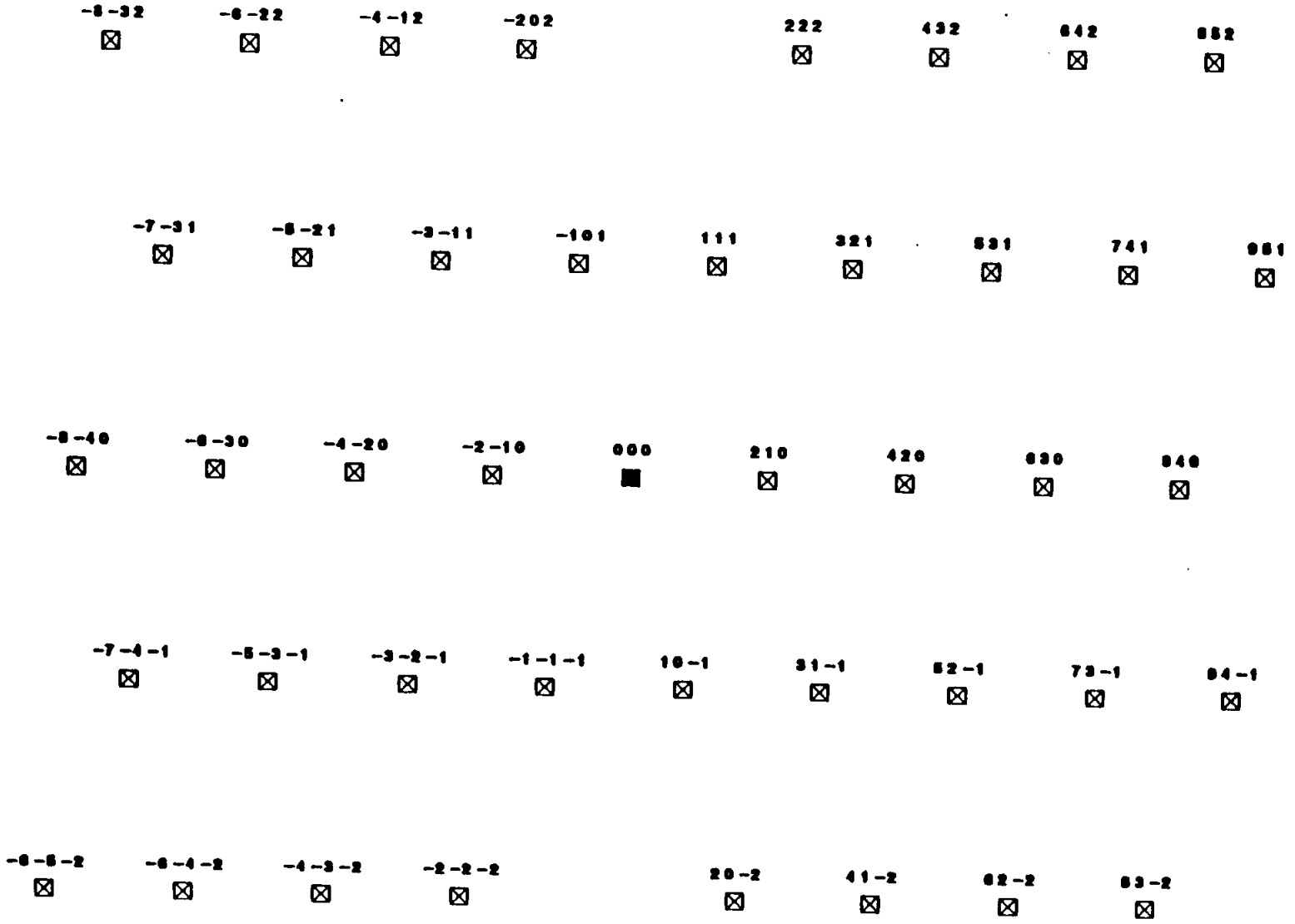

Squares are non−extinct. Diamonds are extinct. Camera Constant = 180.0 mm−Å

Figure 4.3

TALC 0 0 1 ZONE AXIS

a = 5.287 Å b = 9.171 Å c = 18.964 Å ß = 99.61° Space Group = C 2/c

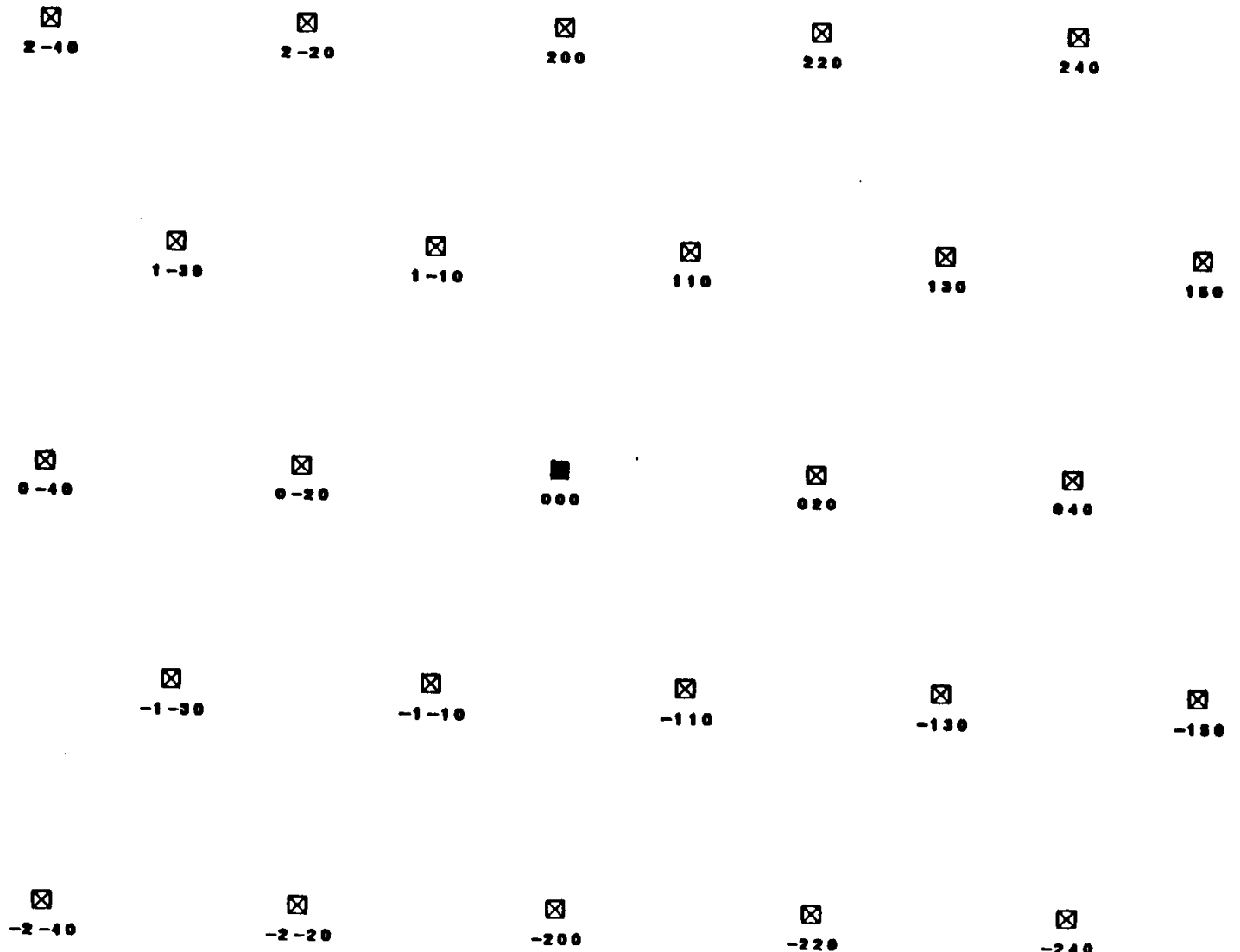

Squares are non−extinct. Diamonds are extinct. Camera Constant = 180.0 mm−Å

Figure 5.1

TALC 1 0 1 ZONE AXIS

a = 5.287 Å b = 9.171 Å c = 18.964 Å ß = 99.61° Space Group = C 2/c

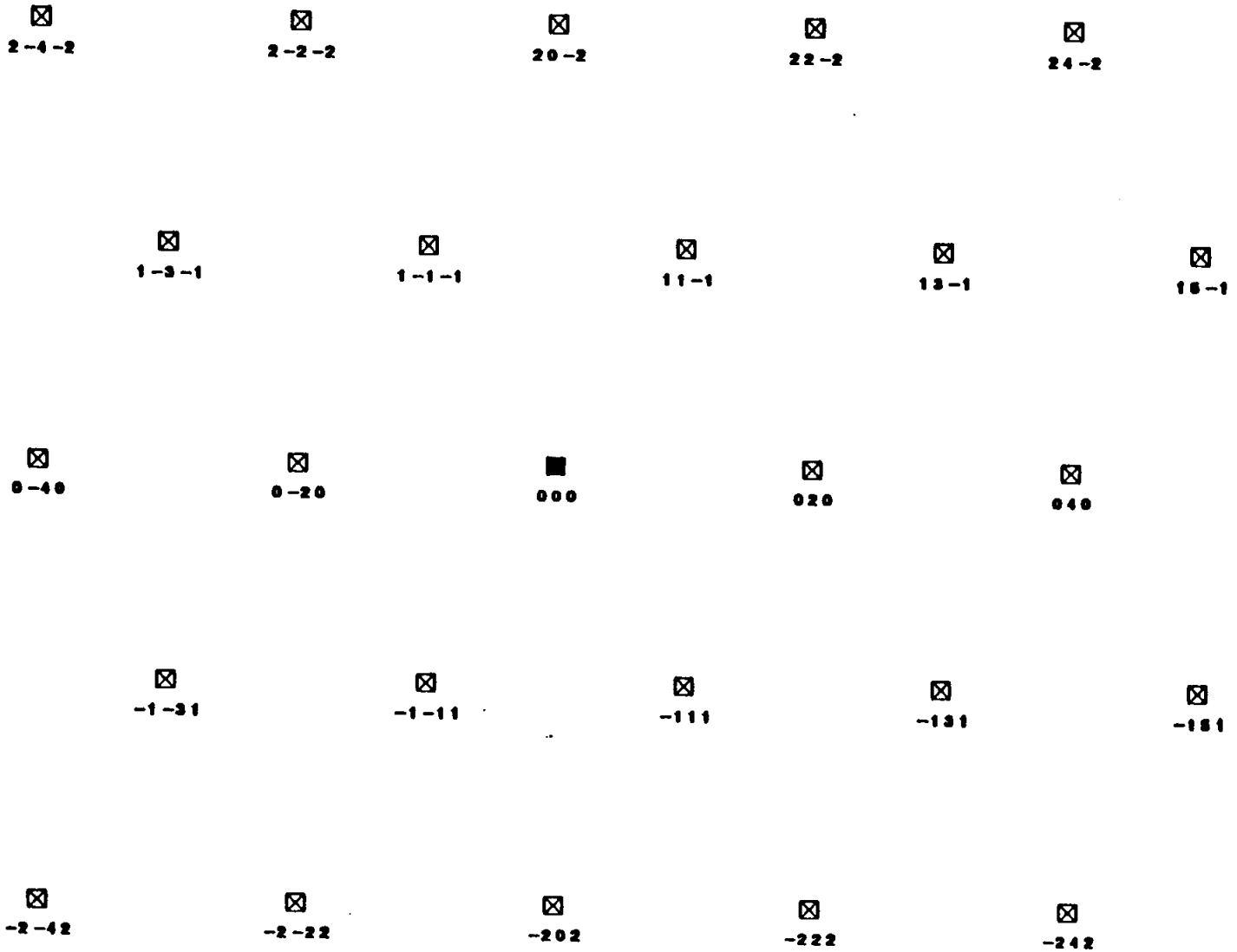

Squares are non−extinct. Diamonds are extinct. Camera Constant = 180.0 mm−Å

Figure 5.2

TALC 1 1 1 ZONE AXIS

a = 5.287 Å b = 9.171 Å c = 18.964 Å ß = 99.61° Space Group = C 2/c

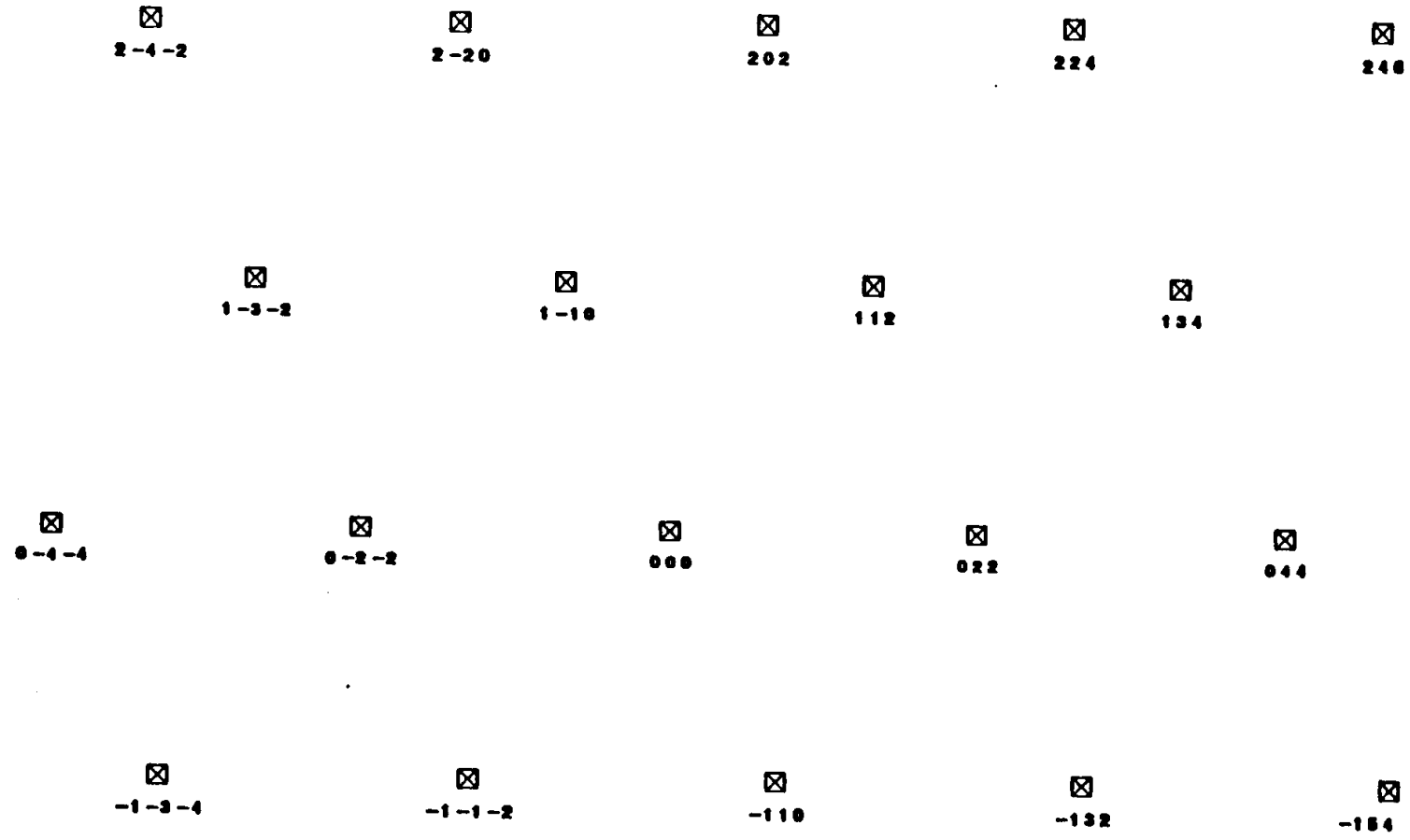

Squares are non−extinct. Diamonds are extinct. Camera Constant = 180.0 mm−Å

Figure 5.3

"Ortho–Talc" 0 0 1 ZONE AXIS

a = 5.287 Å b = 9.171 Å c = 18.698 Å ß = 90.00° Space Group = C mmm

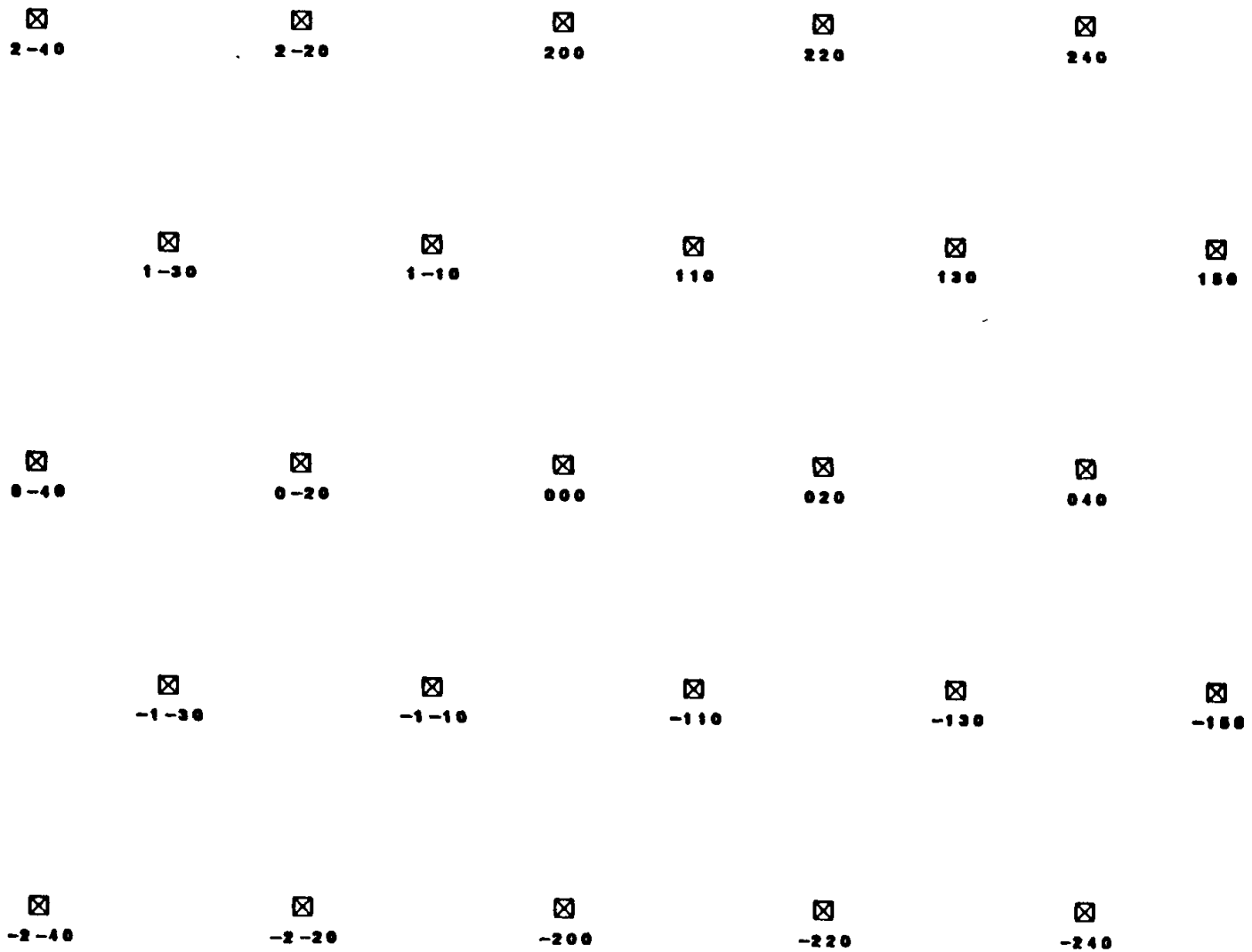

Squares are non–extinct. Diamonds are extinct. Camera Constant = 180.0 mm–Å

Figure 6.1

"Ortho–Talc" 1 0 1 ZONE AXIS

a = 5.287 Å b = 9.171 Å c = 18.698 Å ß = 90.00° Space Group = C mmm

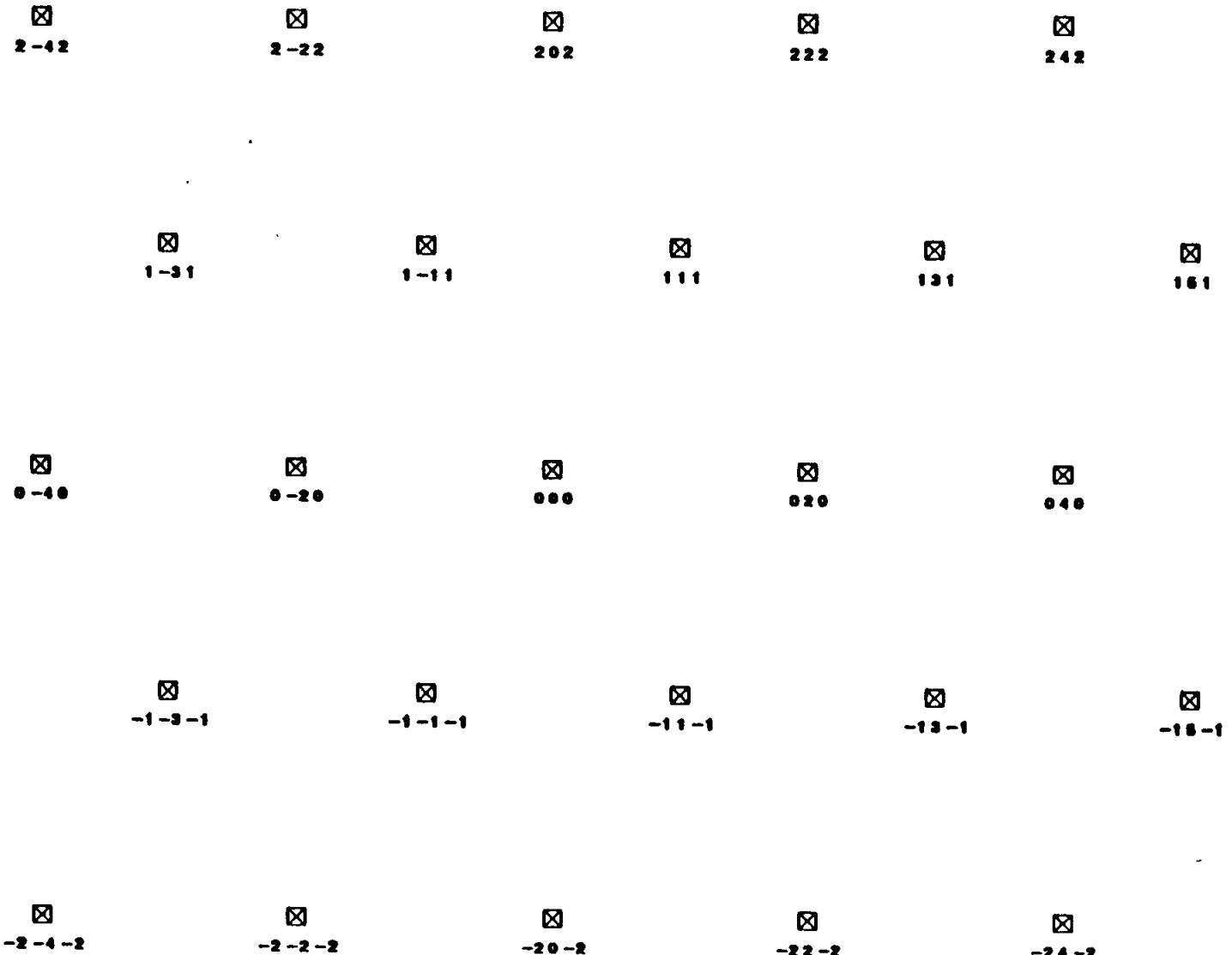

Squares are non–extinct. Diamonds are extinct. Camera Constant = 180.0 mm–Å

Figure 6.2

"Ortho–Talc" 1 1 1 ZONE AXIS

a = 5.287 Å b = 9.171 Å c = 18.698 Å ß = 90.00° Space Group = C mmm

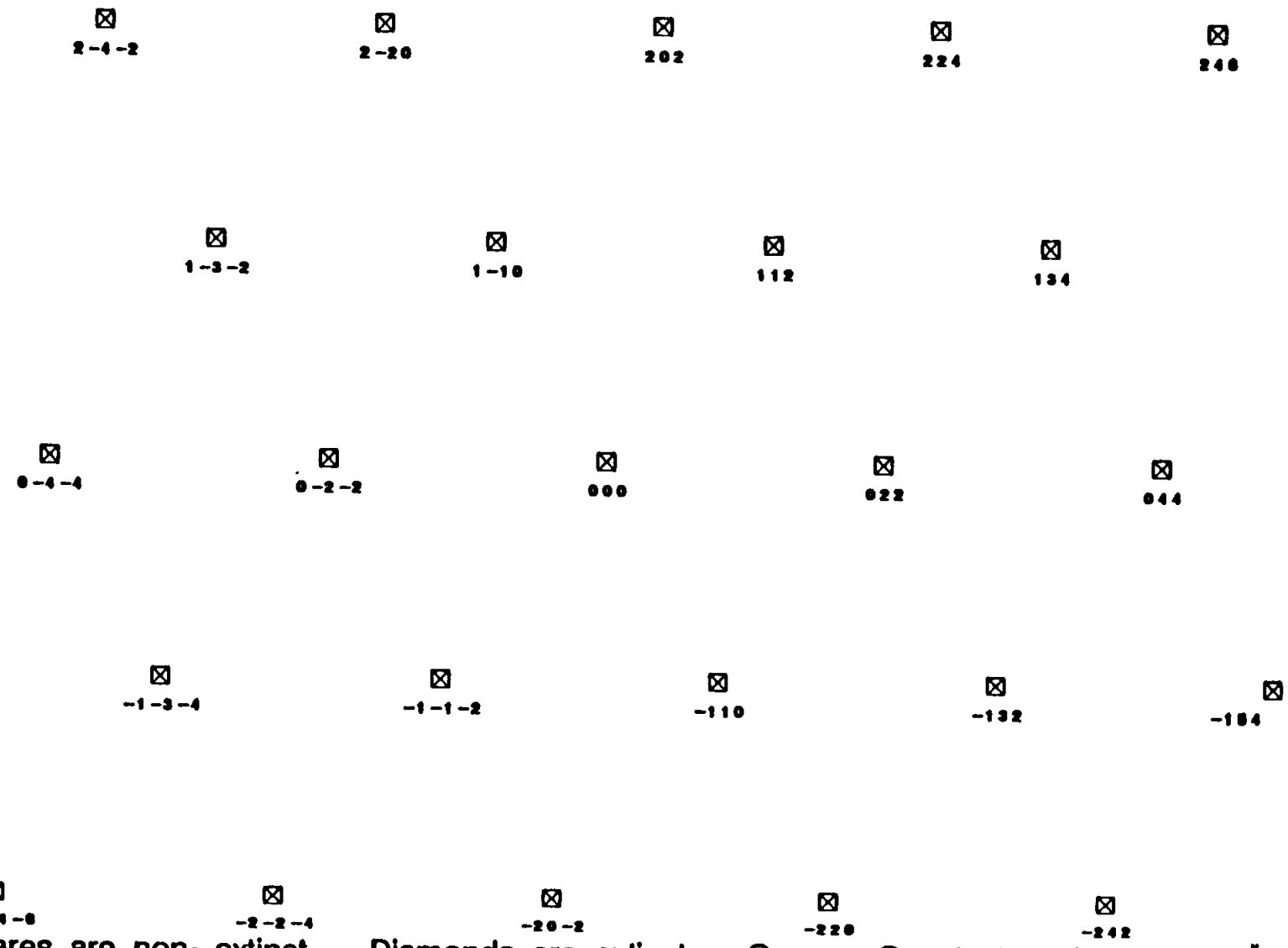

Squares are non–extinct. Diamonds are extinct. Camera Constant = 180.0 mm–Å

Figure 6.3

Figure 7. Magnesium Atoms vs. Silicon Atoms for Common Magnesium Silicates

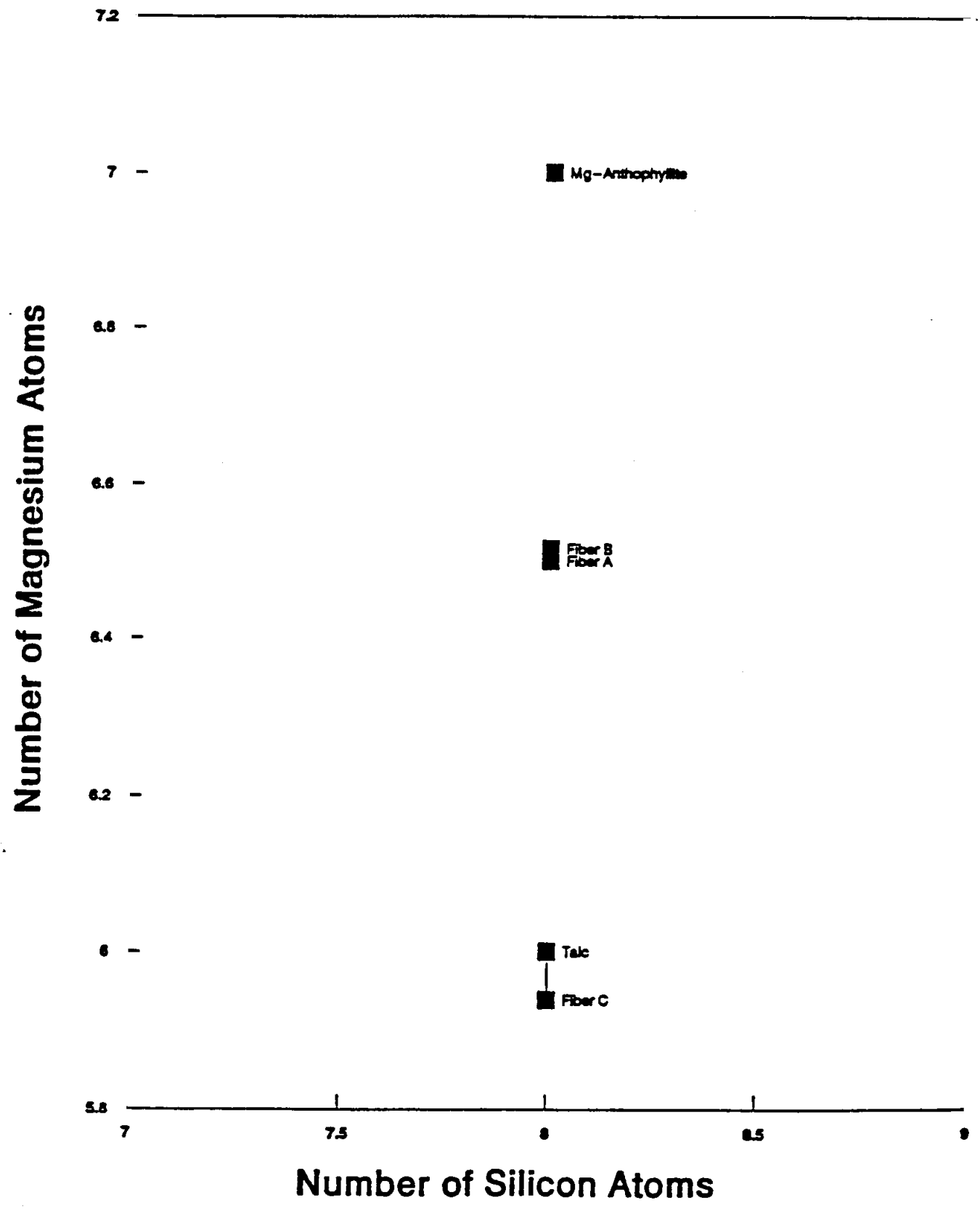

Figure 8. Unit Cell Relationships for Oriented Intergrowths of Talc, Ortho–Talc, and Magnesio–Anthophyllite

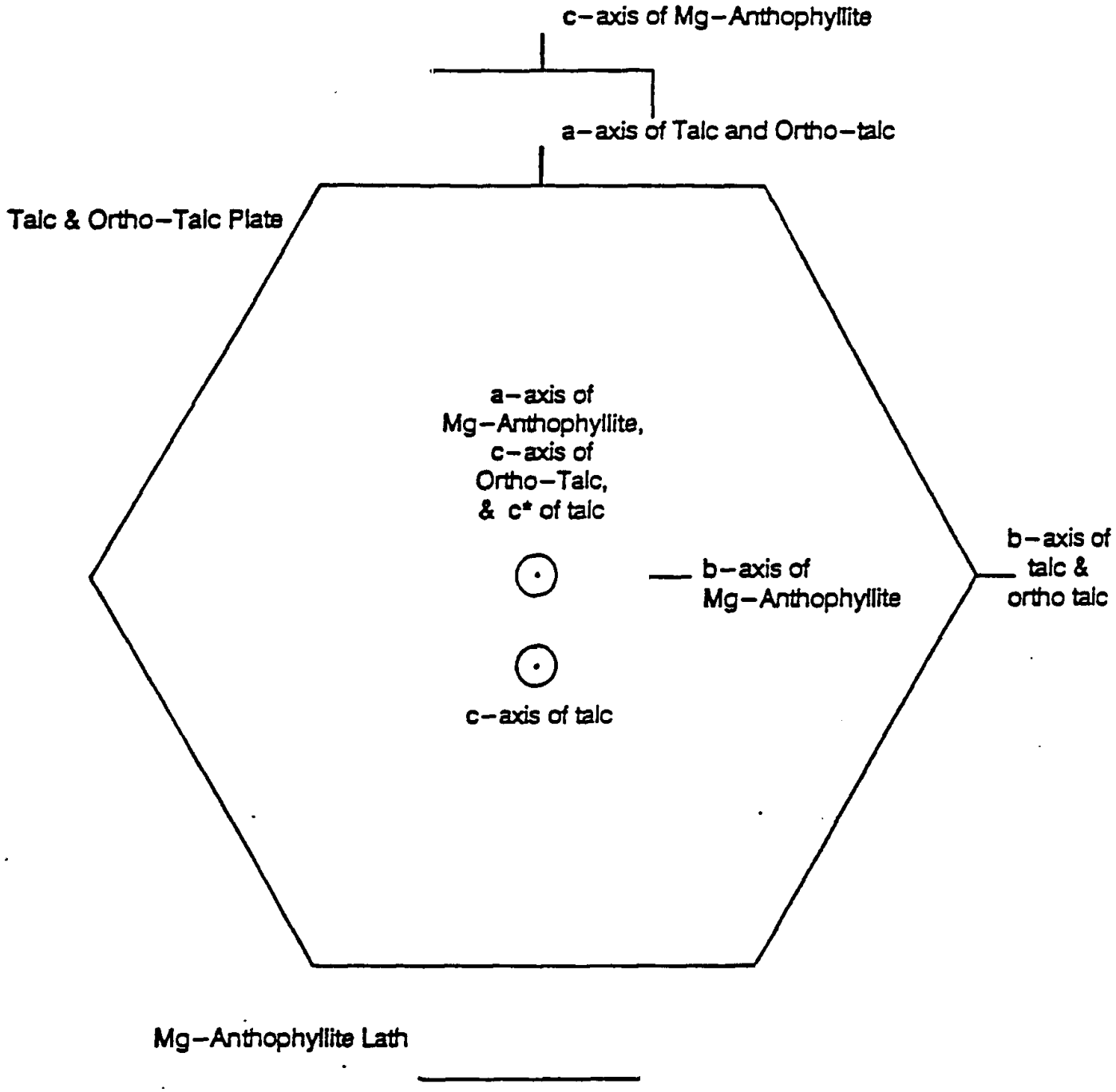

Note: The particle shapes used in these illustrations were chosen because of their easily recognized morphology. In the actual transitional talc fibers described herein, both the talc/ortho–talc and magnesio–anthophyllite components of the fibers may be lath–like or irregular in shape.

REPORT ON THE ANALYSIS OF [redacted] PAINT CLS-5067-1

AND

[redacted] MINERAL FILLER CLS-N-439-1

Submitted to:

[redacted]

23 September 1992

McCrone Associates-Atlanta
1412 Oakbrook Drive
Suite 100
Norcross, Georgia 30093

MA60597

TABLE OF CONTENTS

INTRODUCTION

McCrone Associates-Atlanta was retained by [redacted] Company and R.T. Vanderbilt Company, Inc., on 21 Aug 92. Two samples from the [redacted] Company were sent to the our laboratory in Norcross, GA, and were then split with our laboratory in Westmont, IL. The [redacted] paint sample (CLS-5067-1) was received on 22 Aug 92; the chain-of-custody which accompanied this sample is retained in the permanent project file in our Westmont laboratory. The [redacted] mineral filler sample (CLS-N-439-1) was received 26 Aug 92. We were requested to use all reasonable analytical methods to determine whether either sample contained asbestos as defined under the Environmental Protection Agency (EPA) Asbestos Hazard Emergency Response Act (AHERA) standard. We were also requested to compare the mineral assemblage in the mineral filler (talc) sample and in the paint sample.

The PLM and TEM analytical procedures used by our laboratories are traceable to EPA documents. The PLM analysis is the: USEPA, The Interim Method for the Determination of Asbestos in Bulk Insulation Samples, EPA 600/M4-82-020, December, 1982.

The TEM procedure for analyzing bulk asbestos utilizes the determinative mineralogical criteria listed in the AHERA (Asbestos Hazard Emergency Response Act, Federal Register, Vol. 52, Friday, October 30, 1987, or 40 CFR Part 763) NIOSH Method 7402, NIOSH Manual of Analytical Methods, 08/15/87, and Yamate, G., et al 1984, Methodology for the Measurement of Airborne Asbestos Concentrations by Electron Microscopy. Draft Report. Washington, D.C.: Office Research and Development, U.S. Environmental Protection Agency. Contract No. 68-02-3266.

Two XRD procedures were used for the analysis. Powder XRD follows standard diffraction procedures which are detailed in

the Cosmetic, Toiletry, and Fragrance Association (CTFA) method J4-1, and in generally available references such as: Elements of X-Ray Diffraction, B.D. Cullity, Addison-Wesley Publishing Company, Inc., 1978, or X-Ray Diffraction Procedures, H.P. Klug and L.E. Alexander, Wiley & Sons, 1974. Powder camera XRD was used on aggregates of isolated fibers. This analysis is referable to the Debye-Scherrer technique. The diffraction spacings obtained from the analysis are compared to standard Joint Committee on Powder Diffraction Standards (JCPDS) cards for authentication versus published standards.

EXECUTIVE SUMMARY

The mineral filler (solid residue) was isolated from the paint by washing with organic solvents. This solid residue (CLS-5067-1) and the mineral filler (CLS-N-439-1) were analyzed by polarized light microscopy (PLM), x-ray diffraction (XRD), and transmission electron microscopy (TEM) for suspected asbestos mineral fiber content. Two XRD methods were used. These methods were powder x-ray diffraction of bulk mineral powder and powder camera diffraction of selected fibers by the Debye-Scherrer method. Asbestos is defined by EPA and OSHA to include the asbestiform habit of anthopyllite, tremolite, and actinolite from the amphibole class of minerals. Analytical results were either inconsistent with or clearly negative for the presence of chrysotile and/or asbestos amphibole minerals.

The highest refractive index determined by PLM for the fibrous minerals in the samples was $\leq$1.60 (gamma direction). This refractive index is consistent with talc fibers. The lowest reported refractive index for any amphibole is 1.61 (gamma direction). By PLM the optical properties of the fibrous minerals are not consistent with anthophyllite or any other amphibole.

The powder XRD analyses of paint residue and mineral filler did not match published diffraction data for the mineral anthophyllite. However, tremolite was present (non-asbestiform by PLM analysis). Suspect fibers were isolated and collected by PLM for analysis using powder camera XRD. These selected suspect fibers produced powder diffraction lines which matched talc and an amphibole. The fibers may be a mineral transitional between talc and an amphibole or (intimate) intergrowths of talc and an amphibole. They do not match published data for anthophyllite.

Analysis by TEM is inconclusive for several reasons, which will be detailed in (this) report. A number of the "fibers" are clearly cleavage fragments and not asbestos.

Some fibers show the pseudohexagonal (SAED) diffraction pattern typical of talc, not amphiboles. Many fibers show a constant diffraction pattern, which does not vary through 20 degrees of rotation. These characteristics are similar to talc, but unlike a typical amphibole mineral.

The precise mineralogy of the fibers from the two [redacted] samples awaits further analysis. However, these results are clearly negative in the sense that anthophyllite asbestos cannot be demonstrated to occur in the samples (Executive Summary section submitted as our "Preliminary Report" dated 28 Aug 92).

In summary, we could not confirm the presence of asbestos at any level in either sample.

PLM ANALYSES

Sample CLS-5067-1 ([redacted] paint) was treated with xylene to remove organic components. The sample was centrifuged,

decanted, and washed. This procedure was repeated six times. The xylene insoluble residue was examined by optical microscopy (PLM), and compared to mineral filler CLS-N-439-1. The optical properties of the minerals identified in the samples are presented in Table I-A. Additional work was done on the samples by the method of point counting (Table I-B); asbestiform fibers were counted separately from non-asbestiform "Federal Fibers" ($\geq$5 μm and $\geq$3:1 aspect ratio).

Percentages are based on area/volume estimates from microscopical examinations. The fibrous talc and tremolite-actinolite insoluble mineral components of the paint are consistent with the fibrous talc and tremolite-actinolite components of the mineral filler. The paint residue contained titanium white, which was not found in the mineral filler and it contained a higher percentage of carbonates than the mineral filler.

Optical examination consisted of dispersion of random aliquots in refractive index liquids with n_D #1.550, 1.580, and 1.605. The second part of the optical examination involved particle picking about 25 fibers from the sample for detailed refractive index measurements, and other optical characterization. The results are summarized in Tables I and II. Several other fibers were picked, crushed, and mounted for powder camera x-ray diffraction analysis. The fibers are illustrated in the photomicrographs (Figure 1).

XRD ANALYSIS

Powder X-Ray Diffraction: Both the mineral filler (CLS-N-439-1) and the xylene insoluble residue from sample CLS-5067-1 were analyzed as bulk samples by the powder diffraction method using a Siemens D5000 Diffractometer. The diffraction patterns are included. The phases identified are indicated on the patterns (Figures 2 A-C). The diffraction results were consistent with the optical information (Table III).

Powder Camera X-Ray Diffraction: Selected fibers of high gamma refractive index (approximately 1.60) by PLM were isolated from each sample (Figure 1), ground with forceps, and analyzed by the Debye-Scherrer powder camera method. The samples were exposed for four hours to produce diffraction lines on a film. The lines were subsequently measured and recorded. The reduced data is presented as Tables IV - VI. The data shows that the fibers from each sample are essentially the same material. The diffraction lines indicate that the fibers have some d-lines that match tremolite or possibly anthophyllite and talc. Some d-lines are missing in the sample compared to either standard amphibole. Those are listed in Tables IV and VI. The few antigorite lines are probably some fines clinging to the fibers. The data indicates that the fibers are either: a) intergrowths of talc and tremolite, or b) possibly an unknown mineral phase (biopyribole?). Powder camera film strips are in Appendix A.

TEM ANALYSES

Small amounts of each sample were put in suspension and deposited on filters. The filters were prepared according to NIOSH 7402, and examined by a 120 kV JEOL 1200EX instrument. Only "fibers" (particles with substantially parallel sides, $\geq$5 μm and $\geq$3:1 aspect ratio) were examined for crystallographic information and EDS chemistry.

The results are qualitative. Several photomicrographs (Figures 3 and 4) illustrate the interfacial angle of a typical mineral fiber from these paint samples, as well as SAED (selected area electron diffraction) patterns of the larger fiber. Mineral fibers from the two samples yielded similar crystallographic and qualitative EDS chemical results.

By TEM examination many of these "fibers" are clearly cleavage fragments. According to the U.S. Department of Labor, OSHA (NEWS from the Office of Information dated Friday, May 29, 1992) non-asbestiform varieties of the regulated amphibole minerals have been removed from the 1986 revision of the 1972 asbestos standard.

Many fibers, especially the larger ones, showed pseudo-hexagonal SAED patterns typical of talc, not amphibole. The larger fibers examined represented most of the weight of the fibrous part of the mineral assemblage. Though some fibers have amphibole-like SAED patterns, they have only approximately 5% to 8% calcium content (of total cations only, oxygen is not detected by this system) by EDS analysis. TEM examination shows that most fibers are talc with a possible contaminating phase. Fibers which can clearly be called amphibole do not seem to be present in these samples. No amphibole was detected in individual mineral fibers.

CONCLUSIONS

These analytical data taken together indicate that no asbestos was detected in the two [redacted] samples. Talc is present in the fibrous portion of the samples. There is an amphibole-like component, which gives variable crystallographic characteristics for a high magnesium amphibole, or a magnesium calcium amphibole (tremolite), or some unknown phase resembling jimthompsonite perhaps or chesterite (biopyriboles). However, though powder camera XRD identifies the amphibole-like phase as being similar to tremolite, there is very low calcium sufficient for only about 10% amphibole domains in the talc fibers. Anthophyllite may be selected as a match for the amphibole-like phase, but some significant d-lines are absent from the sample which are present in the standard.

It must be clearly stated that PLM is the only official method for the determination of asbestos in bulk school building materials. By PLM analysis this material contains fibers of talc and talc-like phases only. The refractive indices precludes inferring detectable amphibole minerals are present. They are not.

Analysis of minerals by TEM (120 kV) excludes all but the finest particles from the sample analysis. Fibers of about $\leq$50 μm in length and $\leq$1-2 μm thickness can be studied crystallographically and chemically (EDS). It should be noted that this population of fibers may or may not be representative of the mineralogy of the bulk material being analyzed. TEM may detect phases which seem prominent, but which represent less than 0.1% or a trace amount, of the composition of the bulk material. However, no dominantly amphibole fibers were detected in these samples.

Analysis of minerals by PLM and powder XRD offer significantly better statistical representation of the bulk composition of materials than does TEM. XRD is a widely accepted technique in the mineralogic and chemical sciences. XRD yields much the same information as TEM, but the results are integrated over a more representative sample. XRD can be used on about 100 mcg to 20 mg sample sizes. TEM is restricted to 10 to 1000 ng sample size per analysis.

It was possible for the McCrone Associates laboratories to analyze a small well characterized and hand-picked (by PLM) set of suspect fibers using powder camera XRD. The fibers show crystallography of talc and amphibole. But the crystallographic data (tremolite) by matching with JCPDS cards conflicts with the EDS chemistry (very low calcium).

XRD indicates the presence of amphibole domains (small areas of that mineral phase intergrown with the dominant mineral

phase-talc) in the fibers. But crushing and grinding of the fibers (which are very resistant to physical breakdown) does not create or release detectable asbestos fibers. The domains of the amphibole-like mineral seem to be very small perhaps on the scale of nanometers.

Respectfully submitted,

Joseph M. Sprague

for E. Kent Sprague
Research Scientist

McCrone Associates-Atlanta

TABLE I-A

SUMMARY OF PLM EXAMINATION BY EPA INTERIM PROTOCOLS

SAMPLE	FIBROUS TALC*	TITANIUM WHITE	ANTIGORITE	NON-ASBESTIFORM TREMOLITE-ACTINOLITE	CARBONATES CALCITE & DOLOMITE
CLS-5067-1	40%	10%	10%	20%	20%
CLS-N-439-1	50%	ND	10%	30%	10%

ND = None Detected.

TABLE I-B

POINT COUNTING DATA

SAMPLE	TALC FIBERS ASBESTIFORM HABIT[a]	FIBROUS TALC*	NON-ASBESTIFORM TREMOLITE-ACTINOLITE	OTHER
CLS-5067-1	1.78	10.55	5.42	82.25
CLS-N-439-1	2.13	12.93	6.12	78.77

*Using Federal Fiber definition ($\geq$5 μm and $\geq$3:1 aspect ratio. Expressed in volume percent.

[a]High aspect ratio, show curvature or flexability, have splayed ends, occur in bundles, exhibits one or more of the properties.

McCrone Associates-Atlanta

TABLE II.

OPTICAL PROPERTIES OF TALC FIBERS

SAMPLE	REFRACTIVE INDEX PARALLEL TO FIBER LENGTH*	REFRACTIVE INDEX PERPENDICULAR TO FIBER LENGTH**	ASPECT RATIOS	MORPHOLOGY	EXTINCTION ANGLE
CLS-5067-1	1.600	1.548	5:1 TO 50:1	acicular fibers	parallel and incomplete
CLS-N-439-1	1.596	1.560	5:1 TO 40:1	acicular fibers	parallel and incomplete

*GAMMA MAXIMUM
**ALPHA MAXIMUM

McCrone Associates-Atlanta

TABLE III.

SUMMARY OF POWDER XRD-SIEMENS

SAMPLE	PHASES
CLS-5067-1 paint	tremolite, rutile, talc, dolomite, antigorite, titanium white
CLS-N-439-1 HCl treated	tremolite, rutile, talc, dolomite, antigorite, titanium white
CLS-N-439-1 raw material	tremolite, talc, dolomite, antigorite,

McCrone Associates-Atlanta

TABLE IV.

SUMMARY OF POWDER CAMERA X-RAY DIFFRACTION COMPARED TO TREMOLITE

FIBERS FROM PAINT CLS-5067-1		TALC 13-558		TREMOLITE 13-437		ANTIGORITE 9-444	
d	I/I^O	d	I/I^O	d	I/I^O	d	I/I^O
9.35	100	9.35	100				
8.40	50			8.38	100		
7.38	<10					7.33	100
4.88	<10			4.87	10		
4.65	60	4.60	100				
4.52	30	4.55	30	4.51	20		
3.85	20			3.87	16		
3.62	20					3.66	100
3.42	<10	3.43	1				
3.35	30			3.38	40		
3.25	20			3.27	75		
3.10	100	3.12	100	3.12	100		
2.92	60			2.938	40		
2.79	<10						
2.70	100			2.705	90		
2.58	20	2.595	30				
2.52	40			2.529	40		
2.476	20	2.476	65				
2.38	20			2.380	40		
2.33	20	2.335	16	2.335	30		
2.216	20	2.212	20				
2.15	50			2.163	35		
2.00	<10			2.015	45		
1.88	<10	1.870	40				
1.85	<10			1.864	16		
1.73	<10			1.746	6		
1.68	20	1.682	20	1.686	10		
1.64	<10			1.649	40	1.636	40
1.599	<10						
1.540	<10					1.535	80
1.527	20	1.527	40				
1.509	10	1.509	10				

Fibers from paint sample CLS-5067-1. 13-558, 13-437, and 9-444 are JCPDS Reference Standard card numbers.

Tremolite peaks missing in sample: 8.98, 5.07, 4.76, 4.20, 3.03, 2.805, 2.730, 2.592, 2.298, 2.273, 2.042.

McCrone Associates-Atlanta

TABLE V.

X-5477		TALC 13-558		TREMOLITE 13-437		ANTIGORITE 9-444	
d	I/I^O	d	I/I^O	d	I/I^O	d	I/I^O
9.35	100	9.35	100				
8.40	50			8.38	100		
7.30	<10					7.33	100
4.88	<10			4.87	10		
4.65	60	4.66	100				
4.52	30	4.55	30	4.51	20		
3.85	20			3.87	16		
3.65	<10					3.66	100
3.42	<10	3.43	1				
3.35	30			3.38	40		
3.25	20			3.27	25		
3.10	100	3.12	100	3.12	100		
2.92	40			2.938	40		
2.79	<10					2.720	5
2.70	100			2.705	90		
2.54	20	2.595	30	2.529	40		
2.476	70	2.476	65				
2.52	40			2.529	40		
2.38	20			2.380	40		
2.33	20	2.335	16	2.335	30		
2.15	50			2.163	35		
2.216	20	2.212	20				
2.00	<10			2.015	45		
1.88	<10	1.870	40				
1.73	<10			1.746	6		

Fibers from raw material (mineral fiber) CLS-N-439-1. 13-558, 13-437, and 9-444 are JCPDS Reference Standard card numbers.

McCrone Associates-Atlanta

TABLE VI.

SUMMARY OF POWDER CAMERA X-RAY DIFFRACTION COMPARED TO ANTHOPHYLLITE

FIBERS FROM PAINT CLS-5067-1		TALC 13-558		TREMOLITE 13-437		ANTIGORITE 9-444	
d	I/I^O	d	I/I^O	d	I/I^O	d	I/I^O
9.35	100	9.35	100	9.3	25		
8.40	50			8.26	55		
7.38	<10			7.48	<10	7.33	100
4.88	<10			4.90	10		
4.65	60	4.60	100	4.62	14		
4.52	30	4.55	30	4.50	25		
3.85	20			3.90	14		
3.62	20			3.65	35	3.66	100
3.42	<10	3.43	1				
3.35	30			3.36	30		
3.25	20			5.24	60		
3.10	100	3.12	100	3.05	100		
2.92	60			2.87	20, 40		
				2.84			
2.79	<10			2.74	20		
2.70	100			2.68	30		
2.58	20	2.595	30	2.59	30		
				2.54			
2.52	40			2.54	20		
2.476	20	2.476	65	2.43	13		
2.38	20						
2.33	20	2.335	16	2.318	20		
2.216	20	2.212	20				
2.15	50			2.142	30		
2.00	<10			1.991	16		
1.88	<10	1.870	40	1.875	12		
1.85	<10			1.839	20		
1.73	<10			1.734	30		
1.68	20	1.682	20	1.693	14		
1.64	<10			1.639	10	1.636	40
1.599	<10			1.618	30		
1.540	<10					1.535	80
1.527	20	1.527	40				
1.509	10	1.509	10				

Fibers from paint sample CLS-5067-1. 13-558, 13-437, and 9-444 are JCPDS Reference Standard card numbers.

Tremolite peaks missing in sample: 8.9, 5.04, 4.13, 2.252, 2.216, 2.174, 2.074, 2.060, 1.583.

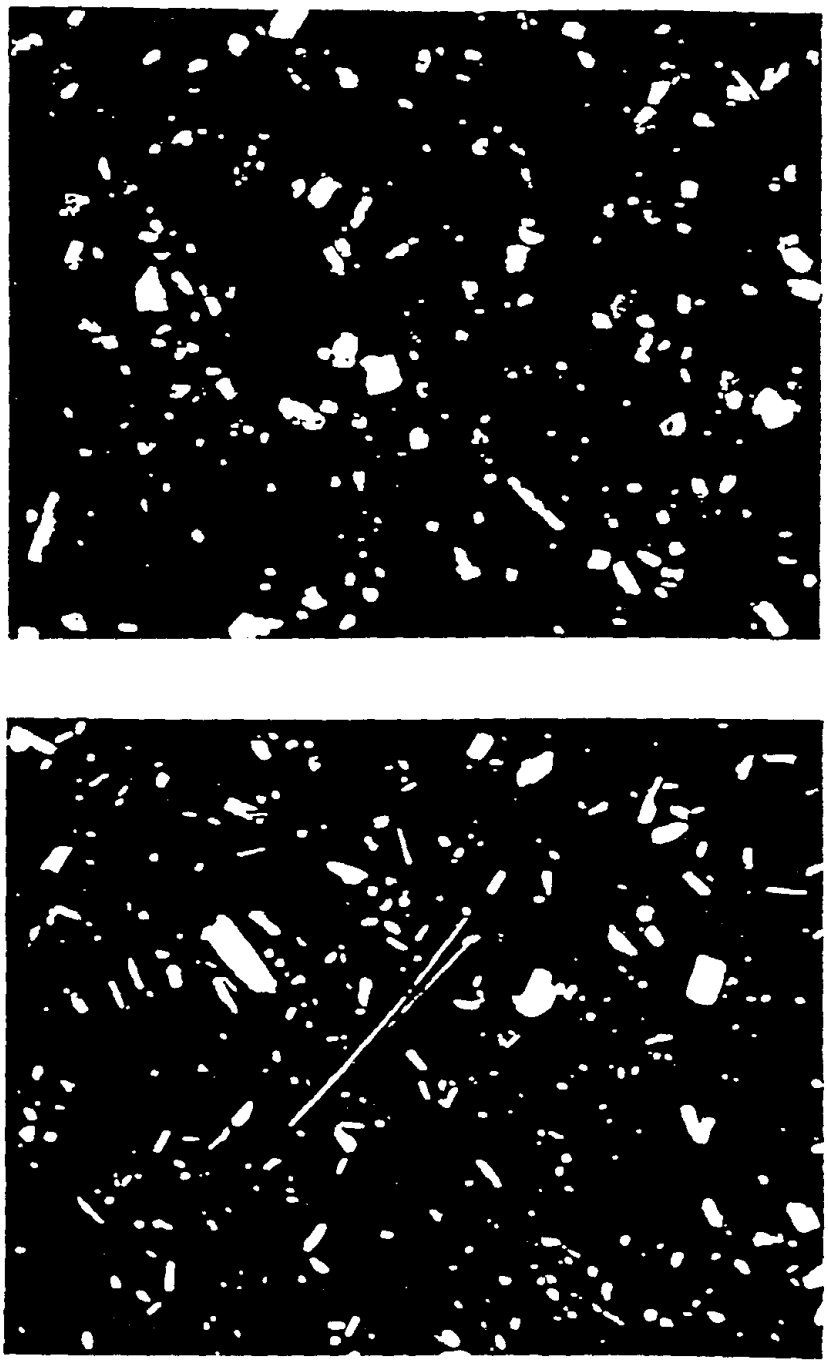

Figure 1.

Photomicrographs of xylene washed paint residue (CLS-5067-1, upper) and mineral filler (CLS-N-439-1, lower).
Mag. = 200X

Figure 2. Powder XRD diffraction patterns. Vertical lines are search/match program standard locations of peaks for the minerals listed.

2a) [redacted] paint CLS-5067-1 xylene residue.

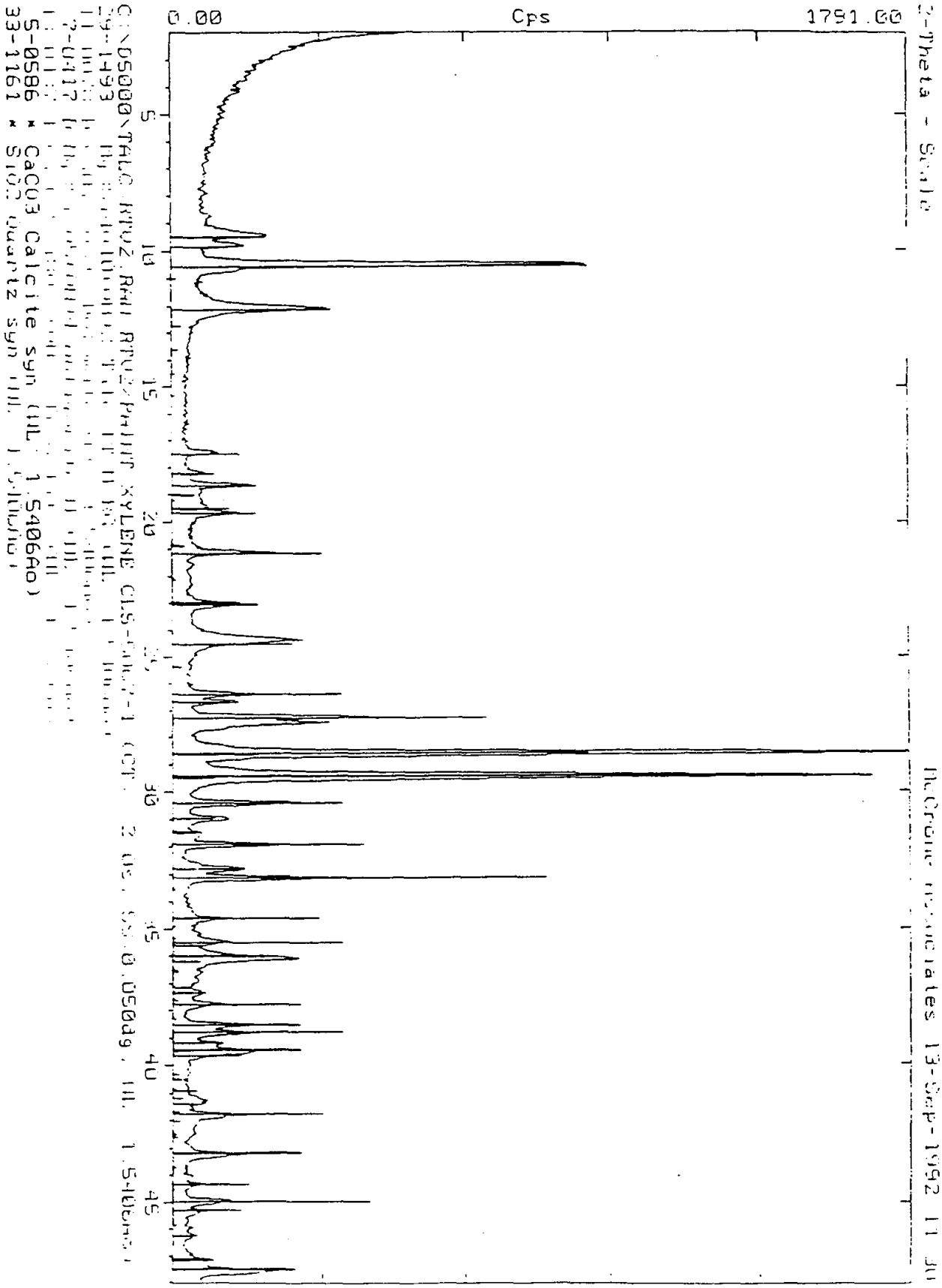

Figure 2b) [redacted] paint CLS-5067-1 xylene residue - HCl treated.

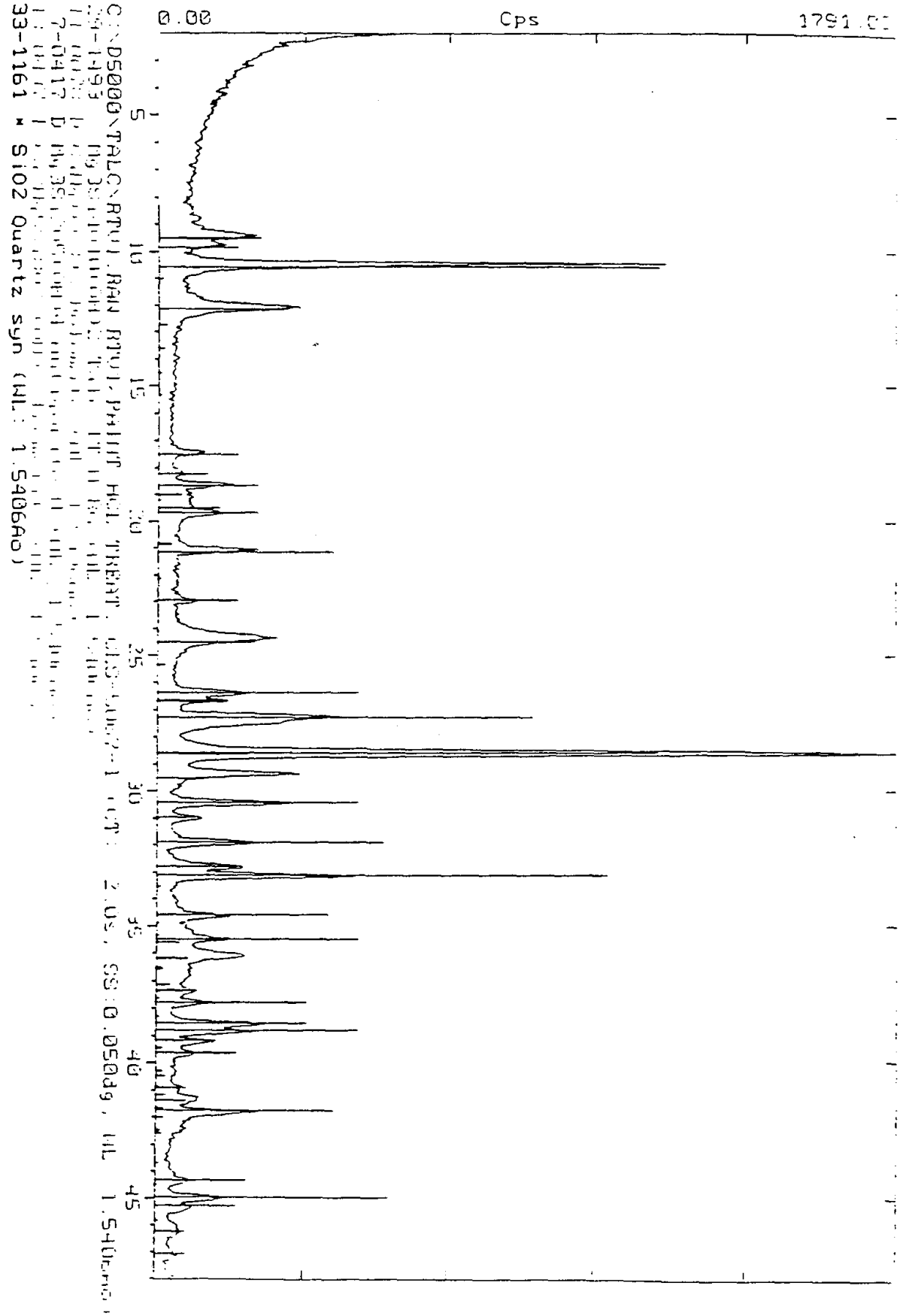

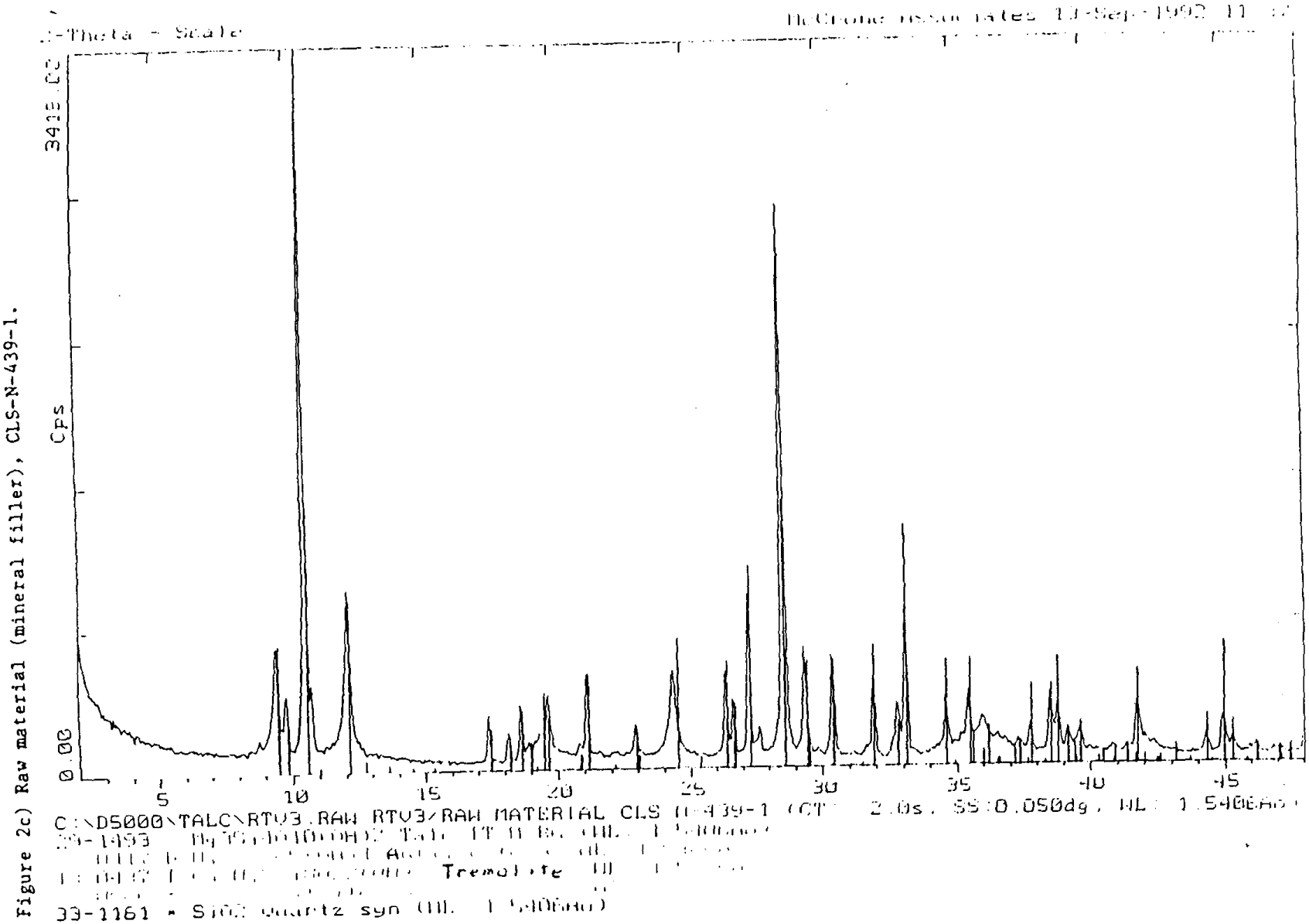

Figure 2c) Raw material (mineral filler), CLS-N-439-1.

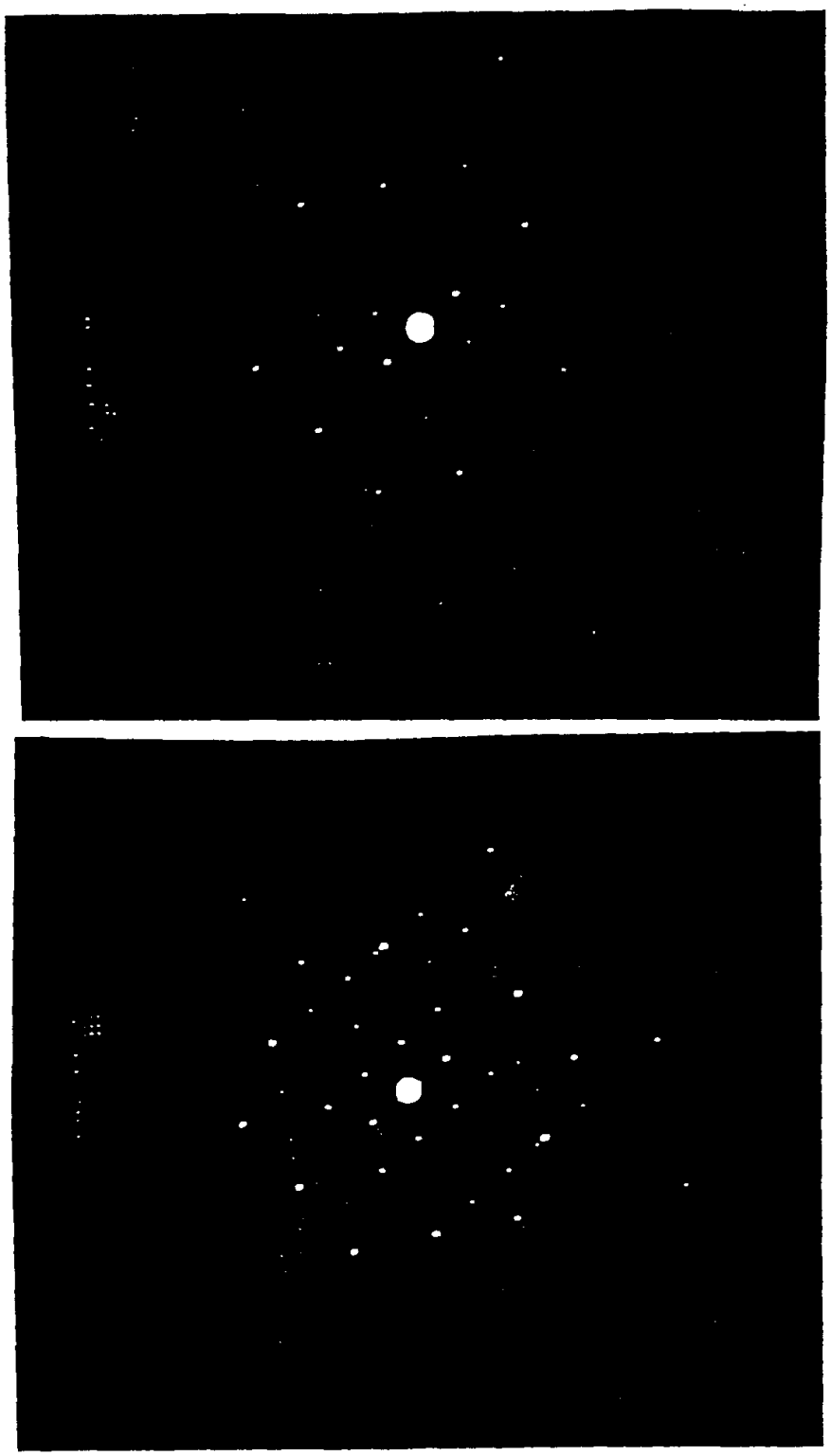

Figure 3. TEM photomicrographs of typical SAED patterns of representative paint (CLS-5067-1) fibers at 0° tilt. The patterns are dominantly pseudohexagonal, typical of talc.

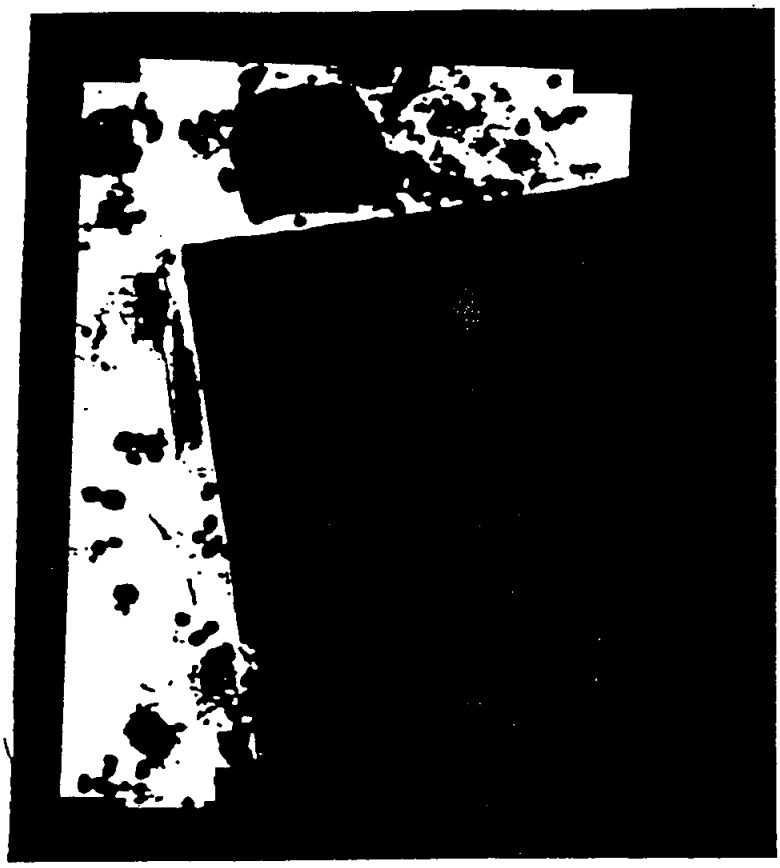

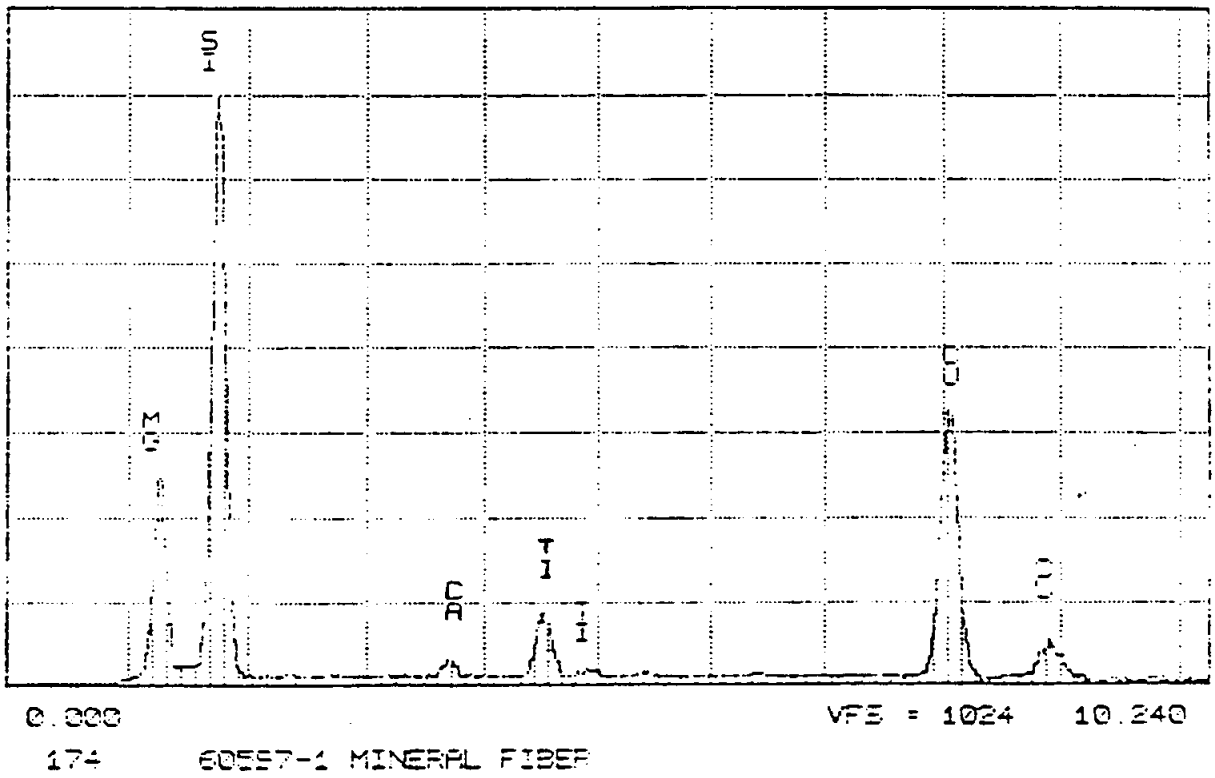

Figure 4. Top - TEM photomicrograph of talc fibers (10,000X). Fiber is 50 um X 7 um. The interfacial angle is 90° 15". Bottom - EDS spectrum of part of the fiber (Cu is from the support grid and not the fiber).